Drought responses of selected C_4 photosynthetic NADP-Me and NAD-Me Panicoideae and Aristidoideae grasses

A thesis submitted in fulfilment of the
requirements for the degree of

MASTER OF SCIENCE

of

RHODES UNIVERSITY

by

Nicolaas Venter

April 2015

Abstract

Grass species within South Africa show a photosynthetic subtype and phylogenetic response to rainfall gradients, with Panicoideae species (NADP-Me and NAD-Me) inhabiting mesic environments, while Aristidoideae species (NADP-Me) inhabit more arid environments. It is predicted that climate change will alter rainfall patterns within southern Africa, which could have implications for grassland distributions and functional composition. Globally, and in South Africa, species distributions indicates that NAD-Me species have a preference for more arid environments, but this may be complicated by phylogeny as most NAD-Me species belong to the Chloridoideae subfamily. Additionally, differences in the metabolism and energetic requirements of different carboxylation types are expected to confer different ecological advantages, such as drought tolerance, but the role of these different pathways is not well understood. Based on natural distribution and photosynthetic subtype differences, it was hypothesised that Panicoideae NADP-Me species would be less drought tolerant than Panicoideae NAD-Me and Aristidoideae NADP-Me species and that subtypes and lineages would show different drought recovery rates. Furthermore, drought sensitivity would be of a metabolic and not a stomatal origin and plants that maintained favourable leaf water status would be more drought tolerant and recover faster. This was tested experimentally by comparing Panicoideae species (NADP-Me and NAD-Me) and NADP-Me species (Panicoideae and Aristidoideae). Plants were subjected to a progressive 58 day drought period and a recovery phase where gas exchange, chlorophyll fluorescence and leaf water relations were measured at select intervals. In conjunction with this, a rapid drought experiment was performed on *Zea mays* (NADP-Me: Panicoideae) plants where similar parameters were measured.

Photosynthetic drought and recovery responses showed both a subtype and phylogenetic response. Panicoideae species were less drought tolerant than Aristidoideae species, although Panicoideae NAD-Me showed better recovery rates than Panicoideae NADP-Me species, while Aristidoideae species recovered the quickest. Panicoideae NAD-Me and Aristidoideae species maintained higher leaf water status during drought which contributed to the maintenance of *PSII* integrity and thus

facilitated rapid photosynthetic recovery. During drought Panicoideae species showed greater metabolic limitations over Aristidoideae species and for the first time, lower metabolic limitations were associated with osmotic adjustment. This is a novel finding whereby osmotic adjustment and the subsequent maintenance of leaf water are key to preventing metabolic limitations of photosynthesis in C_4 grasses. Results from the *Z. mays* rapid drought study showed the limitations to photosynthesis were exclusively metabolic and unlikely to be a direct consequence of turgor loss. It was apparent that the response to drought was stronger amongst lineages, as NADP-Me species from different subfamilies showed a significant difference in drought tolerances. Aristidoideae species' exceptional drought tolerance and predicted increased aridification could favour these species over Panicoideae species under future climates.

Acknowledgements

- First and foremost thanks to Brad Ripley for the opportunity to do this project which allowed me to gain invaluable knowledge and experience in the field of ecophysiology. I would also like to thank Brad for his patience and understanding during the past few years it took me to complete this thesis.
- Thank you to Matthew Janks, Göetz Neef and Gareth Coombs for helping with field collections, watering of the plants and keeping me company in the lab.
- Thank you to Kendall Hauptfleisch for help with the final formatting of this thesis.
- Thank you to Riaan Strauss for all your general help and guidance with most aspects regarding to this research.
- Thank you to the Botany Department support staff but specifically William Ntleki for all your help with the soil preparation, potting and general tasks.
- Last but not least Carol Venter for the patience and support you provided to me during the many years that this Masters took to complete.

Table of Contents

Chapter Contents

List of Figures

Figure 2.4: Dry-down (a-c) photosynthetic rates (*A*), (f-h) stomatal conductance (g_{ST}), (k-m) water use efficiency (A/g_{st}), and (p-r) C_i/C_a for Panicoideae NAD-Me, Panicoideae NADP-Me and Aristidoideae NADP-Me subfamilies. Control minus drought *A,* g_{ST}*,* A/g_{ST} *and* C_i/C_a (d,i,n,s) for "subtype comparison within Panicoideae" and (e,j,o,t) for "subfamily comparison within NADP-Me". Asterisk symbol (*) indicates significant differences between treatments and controls at the corresponding days (a-c, f-h, k-m, p-r) and between treatments at the corresponding days (d-e, i-j, n-o, s-t). n= 16–18 for each data point (mean ± SE).

Figure 2.5: Dry-down (a-c) *PSII* maximum efficiency (F_v'/F_m'), (f-h) *PSII* operating efficiency (*ΦPSII*), (k-m) photochemical quenching (q_P) and (p-r) electron transport rate (*ETR*) for Panicoideae NAD-Me, Panicoideae NADP-Me and Aristidoideae NADP-Me species. Control minus drought F_v'/F_m', Φ*PSII*, q_P and *ETR* (d,i,n,s) for "subtype comparison within Panicoideae" and (e,j,o,t) for "subfamily within comparison within NADP-Me". Asterisk symbol (*) indicates significant differences between treatments and controls at the corresponding days (a-c, f-h, k-m, p-r) and between treatments at the corresponding days (d-e, i-j, n-o, s-t). n= 16–18 for each data point (mean ± SE).

Figure 2.6: Recovery (a-c) photosynthetic rates (*A*), (f-h) stomatal conductance (g_{ST}), (k-m) water use efficiency (A/g_{st}), and (p-r) C_i/C_a for Panicoideae NAD-Me, Panicoideae NADP-Me and Aristidoideae NADP-Me subfamilies. Control minus drought *A,* g_{ST}*,* A/g_{ST} *and* C_i/C_a (d,i,n,s) for "subtype comparison within Panicoideae" and (e,j,o,t) for "subfamily within comparison within NADP-Me". (*) symbol indicates significant differences between treatments and controls at the corresponding days (a-c, f-h, k-m, p-r) and between treatments at the corresponding days (d-e, i-j, n-o, s-t). n= 12–18 for each data point (mean ± SE).

Figure 2.7: Recovery (a-c) *PSII* maximum efficiency (F_v'/F_m'), (f-h) *PSII* operating efficiency (*ΦPSII*), (k-m) photochemical quenching (q_P) and (p-r) electron transport rate (*ETR*) for Panicoideae NAD-ME, Panicoideae NADP-ME and Aristidoideae NADP-ME species. Control minus drought F_v'/F_m', Φ*PSII*, q_P and *ETR* (d,i,n,s) for "subtype comparison within Panicoideae" and (e,j,o,t) for "subfamily within comparison within NADP-Me". (*) symbol indicates significant differences between treatments and controls at the corresponding days (a-c, f-h, k-m, p-r) and between treatments at the corresponding days (d-e, i-j, n-o, s-t). n= 12–18 for each data point (mean ± SE).

Figure 2.8: (a-i) Leaf water potential (Ψ_{leaf}) and (j-r) relative leaf water content (*RLWC*) for the dry-down and recovery phase of the experiment for all the species. n= 4–6 for each data point (mean ± SE) and asterisks symbol (*) indicates significant differences between treatments and controls at the corresponding days. All treatments at day 56 were compared to the controls at day 61 and are significantly different. Plants were re-watered at day 58.

Figure 2.9: Gas exchange dry-down and recovery parameters *A*, g_{ST}, A/g_{ST} and C_i/C_a for species grouped by subtype/subfamily. n= 4–6 for each data point (mean ± SE) and asterisks symbol (*) indicates significant differences between treatments and controls at the corresponding days. All treatments at day 56 were compared to the controls at day 61 and are significantly different. Plants were re-watered at day 58.

Figure 2.10: Chlorophyll fluorescence dry-down and recovery parameters F_v'/F_m', *ΦPSII,* q_P *and ETR* for species grouped by subtype/subfamily. n= 4–6 for each data point (mean ± SE) and asterisks symbol (*) indicates significant differences between treatments and controls at the corresponding days. All treatments at day 56 were compared to the controls at day 61 and are significantly different. Plants were re-watered at day 58.

Figure 2.11: Recovery of photosynthesis (*A*) after three days of re-watering related to (a) the relative leaf water content (*RLWC*) and (b) *PSII* maximum efficiency (F_v'/F_m') after 56 days of drought (~3.5% *SWC*). Regression stats (a); (R^2= 0.126, p= 0.3496), excluding *P. virgatum* (R^2= 0.906, p= 0.0003) and (b); (R^2= 0.26, p= 0.16), excluding *Panicum virgatum* (R^2= 0.73, p= 0.0067) Species are grouped by subfamily and subtype and *P. virgatum* is indicated by (□) symbol.

Figure 2.12: *PSII* maximum efficiency (F_v'/F_m') after 56 days of drought (~3.5% *SWC*) related to the *RLWC* on the same day. Regression stats; (R^2= 0.57, p= 0.0187), excluding *P. virgatum* (R^2= 0.558, p= 0.0331). Species are grouped by subfamily and subtype and *Panicum virgatum* is indicated by the open square symbol. Abbreviation: Relative leaf water content (*RLWC*).

Figure 3.1: Control *Z. mays* pressure-volume curve (——) with SE bars plotted using the equations of Schulte and Hinckley (1985). The curvilinear portion indicates the effect of osmotic (Ψ_π) and turgor (Ψ_P) potential and the straight line (– – and ——) represents the osmotic potential (Ψ_π). The turgor loss point (*TLP*) is denoted by the open circle (O) and this is where Ψ_P = 0 MPa. Turgor potential (Ψ_P) is calculated by subtracting Ψ_π from Ψ_{leaf}. Abbreviation: relative leaf water content (*RLWC*).

Figure 3.2: Calculation of stomatal limitation (S_L) and relative metabolic limitation (R_{ML}). The two lines represent hypothetical CO_2 response curves ($A:C_i$) for well-watered and drought stressed leaves. For the well-watered leaf S_L = [((A - B) / A) x 100] where A is the photosynthetic rate corresponding to a C_i of 400 μmol m^{-2} s^{-1} CO_2 (infinite g_{st}) and B is the photosynthetic rate corresponding to a C_i at finite g_{st} (ambient CO_2). For the drought treatment S_L = [((C - D) / C) x 100]. The R_{ML} for the well-watered leaf is by definition = 0. For the drought stressed leaf R_{ML} = [(A – C) / A) x 100]. The shaded areas indicate stomatal limitations for each curve (Ripley *et al.*, 2007). Abbreviations: intercellular CO_2 concentration (C_i), photosynthetic rate (*A*).

Figure 3.3: Pressure-volume curve (——) constructed for *Z. mays* (n= 11) with SE bars using the equations of Schulte and Hinckley (1985). The curvilinear portion indicates the effect of osmotic (Ψ_π) and turgor (Ψ_P) potential and the straight line (– – and ——) represents the osmotic potential (Ψ_π). Turgor loss point (*TLP*) is denoted by the open circle (O) and this is where Ψ_P = 0 MPa. Turgor potential (Ψ_P) is calculated by subtracting Ψ_π from Ψ_{leaf}. Abbreviation: relative leaf water content (*RLWC*).

Figure 3.4: Response of *Z. mays* (a) *RLWC* and (b) Ψ_{leaf} to decreasing *SWC*. Lines fitted to all the data including the controls using the following best fit model y=a/(1+b*exp(-cx)). *RLWC* R^2= 0.91; Ψ_{leaf} R^2= 0.94. Each point represents an individual leaf from a separate plant. Abbreviations: Relative leaf water content (*RLWC*), leaf water potential (Ψ_{leaf}), soil water content (*SWC*), turgor loss point (*TLP*).

Figure 3.5: (a-c) *Z. mays* photosynthesis (*A*) and (d-f) stomatal conductance (g_{ST}) with decreasing *SWC*, *RLWC* and Ψ_{leaf} measured at ambient CO_2 concentrations (400 μmol mol^{-1}). The vertical dashed line (- - -) represents the *TLP* of *Z. mays* leaves for each independent variable. Drought treatment (■) and control leaves (○) while each point represents an individual leaf from a separate plant. Abbreviations: Soil water content (*SWC*), relative leaf water content (*RLWC*), leaf water potential (Ψ_{leaf}), turgor loss point (*TLP*).

Figure 3.6: *Z. mays* relative metabolic (a-c) and stomatal limitations (d-e) with decreasing *RLWC* and Ψ_{leaf}. The vertical dashed line (- - -) represents the *TLP* and the dotted line (⋯) represents the *TLP* SE of *Z. mays* leaves for each independent variable. Drought treatment (■) and control leaves (○) and each point represents an individual plant. Linear lines fitted to (a-d) and non-linear (2^{nd} order polynomial) lines fitted to (a-b). Non-linear lines are not displayed on (c-d) as they did not differ to the linear fits. Lines fitted to treatment data only. All R^2 values are presented on Table 3.1.

Figure 3.7: Relative metabolic limitation (R_{ML}) for individual *Z. mays* leaves against SWC. Line fitted to all the data including the controls using the following best fit model y=a/(1+b*exp(-cx)) (R^2=0.91). Abbreviations: soil water content (*SWC*), turgor loss point (*TLP*).

Figure 4.1: The two lines represent hypothetical CO_2 response curves (A:C_i) for well-watered and drought stressed leaves. For the well-watered leaf the stomatal limitation (S_L) = [((A - B) / A) x 100] where *A* is the rate equal to 400 μmol mol^{-1} (infinite g_{st}) and B is the rate corresponding to C_i at finite g_{st} (ambient CO_2). For the drought treatment the S_L = [((C - D) / C) x 100]. Relative stomatal limitation (RL_S) for the well-watered leaf is the same as S_L but for the water stressed leaf R_{SL} = [(C - D) / B) x 100]. Relative metabolic limitation (R_{ML}) for the well-watered leaf is by definition = 0 and

for the drought stressed leaf R_{ML} = [(A – C) / A) x 100]. The shaded areas indicate the S_L for each curve (Ripley *et al.*, 2007). Abbreviation: photosynthetic rate (*A*), intercellular CO_2 concentration (C_i).

Figure 4.2: Pressure-volume curve (——) constructed for *Aristida junciformis* well-watered leaves (n= 3) with SE bars using the equations of Schulte and Hinckley (1985). The short dashed line (– –) represents the osmotic potential (Ψ_π) of well-watered leaves while the long dashed line (— —) represents the Ψ_π of the *A. junciformis* water stressed leaves. Diamonds (◊) represents mean data at two sampling intervals for *A. junciformis* (n= 4 plants). The difference between the y-intercept of the two lines was calculated as osmotic adjustment (*OA*). Turgor loss point (*TLP*) is denoted by the open circle (O) and this is where Ψ_P= 0 MPa. Abbreviations: leaf water potential (Ψ_{leaf}), relative leaf water content (*RLWC*).

Figure 4.3: Average $A:C_i$ responses of (a) Panicoideae NAD-Me, (b) Panicoideae NADP-Me and (c) Aristidoideae NADP-Me species in response to drought. The solid line (—) indicates the well-watered (control) curve at day 10 (15% *SWC*), the dashed line (— —) indicates day 30 (~10% *SWC*) and the dotted line indicates (⋯) day 45 (~6.5% *SWC*). The curves at day 30 and 45 were adjusted according to the control values of the gas exchange measurements at the corresponding days. The vertical solid line (—) represents *A* at ambient CO_2 concentration (400 μmol mol^{-1}) assuming no stomatal limitations for all curves. The three diagonal lines (—, – –, ·····) which correspond to the respective CO_2 response curves at the well watered and drought treatments represent the limitation on *A* imposed by CO_2 diffusion through the stomata. The plotted curves represent mean ± SE, n= 9-12.

Figure 4.4: $A:C_i$ responses of (a-c) Panicoideae NAD-Me, (d-f) Panicoideae NADP-Me and (g-i) Aristidoideae NADP-Me species. The solid line (—) indicates the well-watered (control) curve at day 10 (~15% *SWC*), the dashed line (— —) indicates day 30 (~10% *SWC*) and the dotted line indicates (⋯) day 45 (~6.5% *SWC*). The curves at day 30 and 45 were adjusted according to the control values of the gas exchange measurements at the corresponding days. The inset on *A. diffusa* graph (h) indicates the full $A:C_i$ curves as the *A* rates were too high to be included in the scale of the other species. The vertical solid line (—) represents *A* at ambient CO_2 concentration (400 μmol mol^{-1}) assuming no stomatal limitations for all curves. The three diagonal lines (—, – –, ·····) which correspond to the respective CO_2 response curves at the well watered and drought treatments represent the limitation on *A* imposed by CO_2 diffusion through the stomata. The plotted curves represent mean ± SE and n= 2-5 per curve.

Figure 4.5: (a-e) Mitochondrial respiration rates (R_d), (f-j) initial slope (*k*) and (k-o) maximum Rubisco activity (V_{max}) for Panicoideae NAD-Me species, Panicoideae NADP-Me species, Aristidoideae NADP-Me species and average Panicoideae (NAD-Me vs. NADP-Me) and average

NADP-Me (Panicoideae vs. Aristidoideae). Day 10 indicates the control. The plotted data points represent mean ± SE, n= 2-5 per species and n= 9-12 for subtype/subfamily. Small case letters signify homogenous groups.

Figure 4.6: Relative metabolic limitations (R_{ML}) and relative stomatal limitations (R_{SL}) and their contribution to the reduction in the photosynthetic rate (A) measured at an ambient CO_2 concentration of 400 μmol mol^{-1} for drought stressed (a) Panicoideae NAD-Me, (b) Panicoideae NADP-Me and (c) Aristidoideae NADP-Me species. Values for R_{ML} and R_{SL} were calculated by deducting the control value (Day 10: well watered) from the final value (Day 45: 6.5% *SWC*). R_{ML} control values were zero. The bars represent mean ± SE, n= 9-12. Abbreviation: Photosynthetic rate (A).

Figure 4.7: (a-e) Stomatal limitations (S_L), (f-j), relative stomatal limitations (R_{SL}) and (k-o) relative metabolic limitations (R_{ML}) for Panicoideae NAD-Me species, Panicoideae NADP-Me species, Aristidoideae NADP-Me species and average Panicoideae (NAD-Me vs. NADP-Me) and average NADP-Me (Panicoideae vs. Aristidoideae). Day 10 for S_L and R_{SL} (same value for both) indicates the controls whereas the R_{ML} could only be calculated from day 30 onwards. The plotted data points represent mean ± SE, n= 2-4 per species and n= 9-12 for subtype/subfamily averages. Small case letters signify homogenous groups.

Figure 4.8: (a) Relative metabolic limitations (R_{ML}), (b) mitochondrial respiration (R_d), (c) maximum Rubisco activity (V_{max}), (d) *PSII* maximum efficiency (F_v'/F_m') and stomatal conductance (g_{ST}) at day 42 (~6.5% *SWC*) related to the relative osmotic adjustment (*OA*) of leaves during the drought experiment. Regression stats (a); (R^2= 0.5, p= 0.035), excluding *H. contortus* (R^2= 0.75, p= 0.0057), (b); (R^2= 0.17; p= 0.26), excluding *H. contortus* (R^2= 0.61, p= 0.022), (c) (R^2= 0.51, p= 0.03), excluding *H. contortus* (R^2= 0.66, p= 0.014;), (d); (R^2= 0.67, p= 0.047), excluding *H. contortus* (R^2= 0.76, p= 0.027) and (e); (R^2= 0.46; p= 0.046). Data points represent individual species means (n= 2-4). Species are grouped by subfamily and subtype and *H. contortus*, indicated by (□) symbol.

Figure 4.9: (a) Relative metabolic imitations (R_{ML}) and (b) maximum Rubisco activity (V_{max}) at day 42 (~6.5% *SWC*) related to the *PSII* maximum efficiency (F_v'/F_m') on the same day. Regression stats (a); (R^2= 0.61, p= 0.013) and (b); (R^2= 0.6, p=0.01). Data points represent individual species means (n= 2-4). Species are grouped by subfamily and subtype.

Figure 4.10: Relative metabolic limitations (R_{ML}) at day 42 (~6.5% *SWC*) related to (a) the percentage leaf water loss required to decrease turgor to zero and (b) stomatal conductance (g_{ST}) on the same day . Regression stats (a); (R^2= 0.17; p= 0.27) and excluding *P. coloratum* outlier (R^2= 0.52, p= 0.044) and (b); (R^2= 0.6; p= 0.014) and excluding *A. junicformis* outlier (R^2= 0.96; p= 0.00002). Data points

represent an individual species (n= 2-4). Species are grouped by subfamily and subtype and (a) *P. coloratum* and (b) *A. junciformis* indicated by (□) and (◊) symbols respectively.

List of Tables

drought (recovery). To account for the time effects of the controls in the GLM results, treatments were deducted from the mean of the controls at corresponding days. n.s. (not significant), *= $p < 0.05$, **= $p < 0.01$ and ***= $p < 0.001$.

Table 2.7: General Linear Model (GLM) results of a comparison of *PSII* maximum efficiency (F_v'/F_m'), *PSII* operating efficiency ($\Phi PSII$), photochemical quenching (q_P) and electron transport rate (*ETR*) between photosynthetic subtypes (represented as species nested in photosynthetic subtype) in response to decreasing *SWC* (dry-down) and re-watering after drought (recovery). To account for the time effects of the controls in the GLM results, treatments were deducted from the mean of the controls at corresponding days. n.s. (not significant), *= $p < 0.05$, **= $p < 0.01$ and ***= $p < 0.001$.

Table 2.8: General Linear Model (GLM) results of a comparison of *PSII* maximum efficiency (F_v'/F_m'), *PSII* operating efficiency ($\Phi PSII$), photochemical quenching (q_P) and electron transport rate (*ETR*) between subfamilies (represented as species nested in subfamily) in response to decreasing *SWC* (dry-down) and re-watering after drought (recovery). To account for the time effects of the controls in the GLM results, treatments were deducted from the mean of the controls at corresponding days. n.s. (not significant), *= $p < 0.05$, **= $p < 0.01$ and ***= $p < 0.001$.

Table 3.1: Average values (± SE) for soil water content (*SWC*), soil water potential (Ψ_{soil}), relative leaf water content (*RLWC*), leaf water potential (Ψ_{leaf}), leaf osmotic potential (Ψ_π) and leaf turgor potential (Ψ_P) of plants group according to their leaf turgor status. Pre-*TLP* refers to parameters measured before leaf turgor is lost, while post-*TLP* refers to parameters measured after leaf turgor is lost. Abbreviation: turgor loss point (*TLP*).

Table 3.2: Average C_i (μmol mol^{-1}) (± SE) for plants according to their leaf turgor status at saturating CO_2 for the well-watered and drought plants photosynthetic measurements.

Table 3.3: Linear and non-linear coefficient of determination (R^2) values and level of significance for relative metabolic (R_{ML}) and stomatal (S_L) limitations in response to decreasing *RLWC* and Ψ_{leaf} (MPa) for control and drought plants pre- and post-turgor loss.

Table 4.1: General Linear Model (GLM) results for mitochondrial respiration (R_d), the initial slope (k) and maximum Rubisco activity (V_{max}) between Panicoideae photosynthetic subtypes exposed to drought treatments. n.s. (not significant), *= $p < 0.05$, **= $p < 0.01$ and ***= $p < 0.001$.

Table 4.2: General Linear Model (GLM) results for mitochondrial respiration (R_d), the initial slope (k) and maximum Rubisco activity (V_{max}) between Panicoideae and Aristoideae NADP-Me

photosynthetic subtypes exposed to drought treatments. n.s. (not significant), *= $p < 0.05$, **= $p < 0.01$ and ***= $p < 0.001$.

Table 4.3: General Linear Model (GLM) results for stomatal limitations, relative stomatal limitations and relative metabolic limitations between Panicoideae photosynthetic subtypes exposed to drought treatments. * = $p < 0.05$, ** = $p < 0.01$ and *** = $p < 0.001$.

Table 4.4: General Linear Model (GLM) results for stomatal limitations, relative stomatal limitations and relative metabolic limitations between Panicoideae and Aristidoideae NADP-Me photosynthetic subtypes exposed to drought treatments. * = $p < 0.05$, ** = $p < 0.01$ and *** = $p < 0.001$.

Table 4.5: Average osmotic adjustment (*OA*) in MPa and the relative *OA* (%) for species (grouped by subfamily/subtype) used the drought experiment. n.s. (not significant), *= $p < 0.05$, **= $p < 0.01$ and ***= $p < 0.001$. n= 2-4 per species.

Table 4.6: Species (grouped by subfamily/subtype) average turgor loss point (*TLP*) calculated from PV Curves represented as *RLWC* and the average *RLWC* of the control plants throughout the drought and recovery experiment. *TLP* and control *RLWC* were compared within each subfamily/subtype group using a *t*-test

Chapter 1

Introduction: C_4 grasses and drought

1.1 C_4 grasses overview

C_4 photosynthetic grasses represent approximately 4500 species of the 7500 C_4 angiosperm species (60%), but only 1.8% of the total (~250,000) land plant species (Sage, 2012). In contrast to the low number of species, C_4 grasses produce about 18% of the world's primary production (Ehrlinger *et al.*, 1997) and 11 out of the 12 most productive crop plants are C_4 (Furbank, 1998). Humans consume a large portion of this directly as plant material or indirectly from animal products derived from pasture grasses and C_4 crop plants (Lloyd & Farquhar, 1994; Brown, 1999). As a result of the evolution of the carbon concentration mechanism (CCM), C_4 grasses are most productive and widespread in tropical and subtropical environments which are hot, frequently dry with high evaporative demand and nutrient poor (Sage, 1999). Globally, C_4 grasses dominate warm-climate grassland and savannas biomes. As a result of this distribution, rainfall and associated drought play a major role in C_4 functional type composition and distribution (Ellis *et al.*, 1980; Taub, 2000). Paradoxically C_4 grasses show susceptibility under severe drought conditions and susceptibility or drought tolerance appears to differ between subtypes and phylogenetic lineages. Drought tolerance refers to the ability of the plant to maintain metabolic and physiological processes, such as photosynthesis, under conditions of increasing soil water deficits (drought). Mechanisms that may infer this drought tolerance are the preservation of cellular water content (slowing water loss), turgor, decreasing osmotic potential and protective/regulatory processes. Drought tolerance also refers to the rate at which the plant's metabolic and physiological processes recover to that of pre-drought plants, upon re-watering (Lawlor, 2013). The purpose of this study was to therefore determine how functional types differ, and the physiological mechanisms responsible for drought in/tolerance.

1.2 C_4 grasses importance in South Africa

Understanding the drought response of C_4 grasses in South Africa is important since the grassy and savanna ecosystems occupy 27.9 and 32.5% of the land surface area respectively (Mucina and Rutherford, 2009). The Grassland biome in South Africa supports significant economies, such as livestock grazing, agriculture, coal mining, forestry and ecotourism where biodiversity is only second to that of the Fynbos biome. Some of the ecosystem services include water provision and materials that sustain rural subsistence populations (Grasslands Programme, SANBI). Despite its significance,

this biome is threatened by rapid urban, coal mining and forestry expansion, most of which are not sustainable and this biome has already been reduced by over 30% (Fairbanks, 2000). However a potentially worse threat to the grasslands could be the effects of climate change.

It is predicted that by 2070 global climate will be altered significantly due to a doubling in CO_2 concentrations and average global temperature increases of 3ºC (IPCC, 2001). Christinson *et al.,* (2007) predicted that southern African grasslands will be subjected to increased drought events (duration and severity), monsoonal type climate and increased fire frequencies. Climate models predict possible desertification expanding west to east as a result of decreased summer precipitation and increasing temperatures (Shongwe *et al.,* 2009; IPCC, 2013). These ecosystems are particularly susceptible to climate change as their life histories are short and this allows species composition to change rapidly from altered selective pressures (Smith and Donoghue, 2008). As the major component of these ecosystems are C_4 grasses, it is imperative to understand their responses at a leaf level to altered climate and importantly drought. This knowledge can then be scaled up to a landscape level where further inferences regarding distribution and functional type compositions can be made.

1.3 Present C_4 grassy ecosystem distribution – The role of rainfall and temperature

C_4 savanna ecosystems cover about 20% of the Earths vegetated surface and lie between ~30º N and S of the equator. These C_4 ecosystems include the tropics, subtropics and warm temperate zones (Long, 1999; Still *et al.,* 2003; Bond, 2008). All these ecosystems experience seasonal precipitation with significant dry seasons and mean annual precipitation (MAP) that ranges from 200 to 3000 mm (Sarmiento 1992, Scholes and Archer, 1997). In addition to precipitation, different studies have shown that various climatic and environmental factors such as temperature, altitude, light and fire also determine the distribution and composition of C_4 grasslands.

For various regions of North America Teeri and Stowe (1976) showed that high minimum temperatures during the growing season showed the best relationship for C_4 grass distribution. Low temperatures during the growing season favoured C_3 grasses and excluded the C_4 grasses. There was however no strong relationship for C_4 distribution and precipitation variables. A similar trend was observed in Egypt (Batanouny *et al.,* 1988). In Australia, Hattersley (1983) found that C_4 distributions were linked to temperature and precipitation. The number of C_4 species correlated with spring (October) average minimum temperatures and median mid-summer (February) rainfall. The percentage of C_4 species correlated to summer (January) average minimum temperature.

Surveys by Tieszen *et al.*, (1979), Boutton *et al.*, (1980) and Cabido *et al*., (1997) in Kenya, Wyoming (USA) and Central Argentina respectively showed significant correlations of altitude to C_4 grass species distributions. In Kenya C_4 grasses occurred exclusively below 2000m in the open grasslands while C_3 species occurred exclusively above 3000m with a mosaic of C_3 and C_4 species in between. In Wyoming and Central Argentina C_4 species abundance increased with decreasing altitude. In Kenya the altitudinal range was between 350 and 2100 m with the crossover point of C_3 and C_4 species at 1500 m. The lower altitudes favoured by the C_4 species are however linked to high temperatures, high levels of solar irradiances and increased aridity.

In South Africa, C_4 grasses are dominant in most summer rainfall grasslands and savannas. Vogel *et al.*, (1978) hypothesized that mean daily temperatures below a maximum of 25°C during the rainy season was the selection criteria that favoured C_3 grasses over C_4 grasses. C_3 and C_4 grasses co-occurred in areas that experienced MAP of between 100 – 1000 mm. Exclusion of C_4 grasses only occurred in the Western Cape winter rainfall region, summits of the Drakensburg and some Eastern Cape mountain ranges. Ellis *et al.*, (1980) later proceeded to investigate the ecological requirements that determine C_4 distribution in Namibia (South West Africa) as the climate is less complex than that of South Africa. Temperatures are mostly uniform with average summer maximums of 30ºC, except a narrow strip of coastal land which average summer maximum is 20ºC. MAP shows the most variability ranging from 50 mm (southwest along the coast) to 500 mm (extreme northeast). C_4 grasses accounted for 95% of the species in all regions except the southwest and northeast where C_3 species accounted for 18 and 5% respectively.

1.4 C_4 attributes that infer aridity tolerance

The C_4 pathway increases the CO_2 partial pressure around the site of Rubisco, and CO_2 concentrations in the bundle sheath cells (BSC) can be ten times that of ambient CO_2 concentrations (Furbank and Hatch, 1987). Even with reduced stomatal apertures, the site of Rubisco is saturated with CO_2 and photorespiration remains almost negligible. The result is increased photosynthetic efficiency, higher water use efficiency (*WUE*) and higher photosynthetic nitrogen use efficiency (*PNUE*). The consequence of this is that is that C_4 grasses have a competitive edge over C_3 grasses in environments that experience water deficits, high temperatures and low nutrients.

1.4.1 Photorespiration

Arid conditions promote increased photorespiratory rates in C_3 plants, but C_4 plants have almost eliminated the negative effects of this energy-dependent process (Sage, 2004). The C_4 pathway

achieves this by concentrating CO_2 at the site of Rubisco which increases the $[CO_2]$:$[O_2]$ ratio, which helps to minimises this oxygenation reactions (Kanai and Edwards 1999). For both C_3 and C_4 plants, stomatal apertures reduce in response to dry conditions (increased soil water deficits, low humidity) which affects CO_2 diffusion and leaf temperature. Under these conditions C_4 plants can still maintain high $[CO_2]$:$[O_2]$ ratios in the BSC, however in C_3 plant this $[CO_2]$:$[O_2]$ ratio decreases, which in turn increases the likelihood of photorespiration. High temperatures are also a major contributor to photorespiration, which can be an environmental affect and/or increased leaf temperature from decreased stomatal conductance. As Rubisco's affinity for O_2 increases at higher temperatures, C_3 plants become more susceptible to photorespiration than C_4 plants. At 25ºC, photorespiration in C_3 leaves runs at approximately 20 - 30% of photosynthesis (Sage, 2001, 2004) while this value is about 3.5 – 6% in C_4 plants (Lacuesta *et al.,* 1997; Carmo-Silva *et al.,* 2008). C_4 grasses have an optimal temperature of approximately 28 - 35ºC (Ward, 1987; Massad *et al.,* 2007). This is achieved by maintaining high $[CO_2]$:$[O_2]$ ratios in the BSC which allows C_4 plants to be more competitive in environments that experience water deficits and high temperatures (Osborne and Freckleton, 2009; Edwards and Smith, 2010), environmental factors that would promote photorespiration in C_3 plants.

1.4.2 Water use efficiency (*WUE*)

Being better suited to operate at higher temperatures has allowed C_4 plants to colonize drier subtropical and tropical environments (Osborne and Freckleton, 2009; Edwards and Smith, 2010). By concentrating atmospheric CO_2 within the BSC, C_4 plants can reduce their stomatal apertures while retaining high photosynthetic rates, thereby reducing leaf transpiration and consequently operating at higher *WUE*. *WUE* discussed here refers to either instantaneous *WUE* (A/E) or intrinsic *WUE* (A/g_{ST}), which are calculated from gas exchange parameters, photosynthesis (A), transpiration (E) and stomatal conductance (g_{ST}). Increased *WUE* (between plants with the same unit leaf area), reduces the demand on soil moisture and thereby conserves water, which is beneficial in drier habitats where the evaporative demand is higher (Pearcy and Ehleringer, 1984; Samarakoon and Gifford, 1996; Seneweera *et al.,* 1998, 2001; Wall *et al.,* 2001; LeCain *et al.,* 2003; Leakey *et al.,* 2006). At comparatively lower stomatal apertures, C_4 plants can fix CO_2 at rates equal to or higher than C_3 plants (Pearcy and Ehleringer, 1984).

1.4.3 Photosynthetic nitrogen use efficiency (*PNUE*)

On average, per unit leaf area, the photosynthetic rate of C_4 plants is higher than C_3 plants per unit N. As a consequence of the high CO_2 concentration at the CO_2 assimilating site of Rubisco, less of this enzyme is required to attain high photosynthetic rates resulting in improved *PNUE* (Sage and Pearcy, 1987). This allows C_4 plants to exploit nutrient poor environments more effectively than C_3 plants and

thus to potentially outcompete C_3 plants, which require greater availability of N (Ehleringer, 1993). Two alternate strategies have been proposed by Long (1999) whereby C_4 plants exploit their PNUE by 1) outcompeting C_3 species by an equal N investment in leaves but with a greater leaf area and 2) produce an equal leaf area as the C_3 competitor and apportion the saved N to root growth, which would increase their ability to forage for resources, such as nutrients and water. The latter strategy can be advantageous in seasonal drought environments whereby *PNUE* allows resource flexibility and plants can allocate greater resource to root growth (Ripley *et al.*, 2008).

1.5 What is C_4 photosynthesis?

C_4 plants are derived from ancestors with C_3 photosynthesis. C_4 photosynthesis involves changes to both leaf anatomy and biochemistry where the basic C_3 structure is modified with C_4 leaves having two morphologically distinct cells that are arranged concentrically around the vascular system, termed Kranz anatomy (Kanai and Edwards, 1999). It is the coordinated functioning of the mesophyll cells (MC) and the bundle sheath cells (BSC) that allows C_4 photosynthesis to function. These cells are situated adjacent to one another with the MC in direct contact with the intercellular airspaces whilst the BSC lies closer to the vascular tissue (Sage, 2004). Atmospheric CO_2 that diffuses through the stomata and into the intercellular airspaces come into contact with the MC where the CO_2 is converted to bicarbonate (HCO_3^-). HCO_3^- reacts with the primary inorganic carbon acceptor phosphoenolpyruvate (PEP), catalysed by phosphoenolpyruvate carboxylase (PEPcase) to form oxaloacetate (OAA), which is then converted to C_4 dicarboxylic acids (malate or aspartate). These C_4 acids are then shuttled through the plasmodesmata to the BSC where they are decarboxylated. The CO_2 that is released is then refixed in the photosynthetic carbon reduction (PCR) cycle, in reaction with ribulose-1,5-bisphosphate (RuBP) by ribulose-1,5-bisphosphate carboxylase (Rubisco). The product of the reaction is phosphoglyceric acid which is then assimilated to regenerate RuBP and also used to form sucrose and starch, which are exported (Kanaai and Edwards, 1999). These steps are common to the three variations of C_4 biochemistry and they are named according to the most abundant decarboxylation enzyme found in the BSC.

Morphologically, NADP-Me and PCK subtypes have suberised lamellae layer/s within the BSC wall, adjacent to the MC, which functions to limit gaseous exchange (von Caemmerer and Furbank, 2003). NAD-Me species do not possess a suberised lamellae but instead have striated structures in the cell walls which may act as a diffusion barrier (Wilson and Hattersley, 1983). At a species level there is morphological variation amongst subtypes. Aristideae NADP-Me species and *Alloteropsis semialata subp. semialata* (Panicoideae NADP-Me) contain three chlorenchymous cell layers which consists of an inner and outer BSC layer, and a MC layer surrounding these two layers. Along with a starch

storage function, the outer BSC layer is believed to re-fix CO_2 leaked from the inner BSC layer, as it contains low levels of Rubisco and PEPcase (Hattersley 1984; Voznesenskaya *et al.*, 1996). Below the details of the three subtypes, NADP-Me, NAD-Me and PCK are discussed, highlighting their intrinsic properties.

1.5.1 NADP-Me subtype

In the MC chloroplast, OAA is reduced to malate by nicotinamide adenine dinucleotide phosphate-malate dehydrogenase (NADP-MDH) after which malate is shuttled to the BSC via plasmodesmata (Fig. 1.1 a). In the BSC chloroplast malate is decarboxylated by NADP malic enzyme (NADP-Me). This releases CO_2 and reduced NADP for the PCR cycle and the by-product pyruvate is transported back to the MC chloroplast, where it is phosphorylated by pyruvate-phosphate dikinase (PPDK) to form PEP (Kanai and Edwards, 1999; Furbank, 2011).

Chloroplasts are arranged centrifugally within the BSC (Hatch et al., 1975). These chloroplast have reduced grana which suggests low Photosystem II (*PSII*) activity. The consequence of this is reduced ATP production, with ATP instead being produced by cyclic photophosphorylation in Photosystem I (*PSI*) (Lawlor, 2001; Furbank, 2011). The advantage of this process is that electrons are cycled from *PSI* to the electron transport chain and therefore water is not split and no O_2 is evolved which in turn helps maintain the higher $[CO_2]$:$[O_2]$ ratio within the BSC. It is however argued that there is considerable variation amongst NADP-Me species in terms of functional *PSII* levels, with up to 50% whole chain electron transport capacity of C_3 thylakoids (Furbank, 2011).

1.5.2 NAD-Me subtype

OAA is converted to aspartate in the MC cytosol by asparate aminotrasnferase (AspAT), after which aspartate is transferred to the BSC mitochondria to be converted back to OAA by AspAT (Fig. 1.1 b). OAA is then reduced to malate by nicotinamide adenine dinucleotide-malate dehydrogenase (NAD-MDH) which is decarboxylated by NAD-malic enzyme (NAD-Me), releasing CO_2 for the PCR cycle and reduced NAD for the reduction of OAA to malate. The product pyruvate is then converted to alanine, by alanine aminotransferase (AlaAT) in the cytosol, which is transported to the MC cytosol where it is converted back to aspartate by AlaAT. Pyruvate is phosphorylated by PPDK in the chloroplast to form PEP (Kanai and Edwards, 1999; Furbank, 2011).

BSC chloroplasts and mitochondria are grouped together and form a prominent centripetal distribution towards vascular tissue. There is a higher ratio of mitochondria to chloroplasts, however respiratory rates are not dissimilar to NADP-Me and PCK subtypes (Hatch, 1975). Structurally the

mitochondria have a well developed cristae system which is thought to provide a larger surface area to increase metabolite fluxes between the mitochondria and cytoplasm, as mitochondria play a significant role in decarboxylation (Hatch, 1975). Within the BSC cholorplasts, additional ATP is produced for the C_4 cycle by pseudocyclic photophosphorylation, using both *PSII* and *PSI*. Ultimately this process evolves O_2, which results in a higher O_2 uptake rate than the NADP-Me subtypes (Lawlor, 2001).

1.5.3 PCK subtype

The PCK pathway has two decarboxylation steps utilising the two enzymes phosphoenol pyruvate carboxykinase (PEPCK) and NAD-Me (Fig. 1.1 c). Within the MC cytosol the majority of OAA is converted to aspartate, by asparate aminotransferase (AspAT), which is transported to the BSC cytosol where it is converted back to OAA by AspAT. OAA is then decarboxylated by PEPCK in the cytosol where CO_2 is released for the PCR cycle and the product PEP (phosphoenol pyruvate) is transported back to the MC cytosol for re-use. The remaining OAA in the MC is reduced to malate by nicotinamide adenine dinucleotide-malate dehydrogenase (NAD-MDH), transported to the BSC, where it is decarboxylated by NAD-malic enzyme (NAD-Me), releasing additional CO_2 for the PCR cycle and NADH. The by-product pyruvate is then converted to alanine by alanine aminotransferase (AlaAT) in the cytosol and transported to the MC cytosol where it is converted back to aspartate by AlaAT. (Kanai and Edwards, 1999; Furbank, 2011). It is suggested that the NADH generated by NAD-Me is used for the oxidative phosphorylation which generates ATP which in turn provides energy to drive PEPCK (Furbank, 2011). Furthermore NAD-Me could serve to balance amino groups between cells by shuttling the metabolite alanine to the MC (Hatch, 1975).

BSC chloroplasts and mitochondria are more evenly distributed around the cell periphery in this C_4 subtype than in others. Mitochondrial cristae development varies among species (Hatch, 1975). *PSII* activities within the BSC are similar to C_3 plants (Kanai and Edwards, 1999). The O_2 uptake rate is higher in this subtype than the NADP-Me subtype, as ATP required for the C_4 cycle is produced by BSC mitochondrial respiration (Kanai and Edwards, 1999).

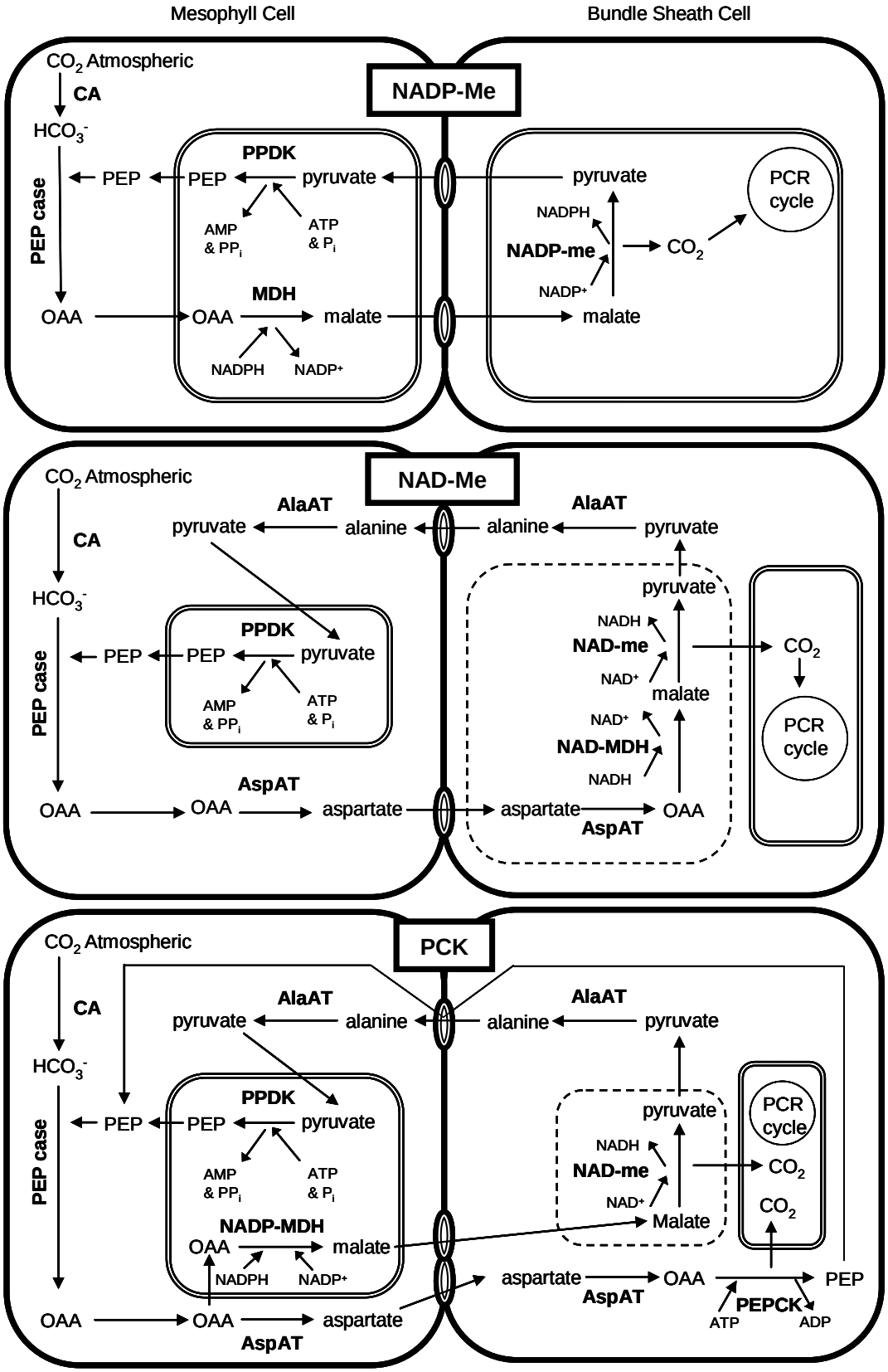

Figure 1.1: The three variations of C_4 photosynthesis, namely NADP-Me, NAD-Me and PCK, showing the various steps of the biochemistry. These subtypes are named according to the enzymes catalysing the decarboxylation of C_4 acids in the bundle sheath cells (BSC). Legend: Chloroplasts ═══ Mitochondria - - - - Plasmodesmata ═══. Redrawn from Kanaai and Edwards (1999) and Furbank (2011).

1.6 Evolution of C_4 photosynthesis and the links to drought

Declining atmospheric CO_2 concentrations during the Oligocene epoch, 24 - 35 million years ago (Mya), is hypothesised as the pre-condition for the evolution of C_4 photosynthesis (Christin *et al.*, 2008; Sage, 2006, 2012). Notable effects of reduced atmospheric CO_2 concentrations are increased stomatal conductance, which significantly affect plant water relations. By concentrating atmospheric CO_2 in the BSC, C_4 plants could increase their *WUE*, which gave them an advantage under the arid and less humid conditions which became more prevalent during Earth's historical climate shifts. Furthermore photorespiration rates, which increase with decreasing stomatal conductance in response to arid conditions, were negated by the ability of C_4 plants to concentrate CO_2, thereby promoting their widespread past expansion (Sage, 2004, 2012).

During the last 50 million years (Myr), CO_2 concentrations have declined from about 1000 to 200 μmol mol^{-1}. During this period there was an abrupt change 25 – 32 Mya when CO_2 concentrations declined from 1000 to 500 μmol mol^{-1}, which was coupled with a change in the Earth's climate. During this period, the Earth shifted from warm, moist (humid) with temperate poles to cold, relatively dry, polar ice caps, extreme deserts and widespread C_3 dominated grasslands (Zachos *et al.*, 2008; Huber and Caballero, 2011; Sage *et al.*, 2012). C_4 dominated ecosystems only started to appear about 10 Mya, being linked to further increased aridity, seasonality, fire frequency and also a decline in CO_2 to 300 μmol mol^{-1} (Sage *et al.*, 2012). Also prior to the Oligocene epoch (24 - 35 Mya), ratios of atmospheric $[CO_2]$:$[O_2]$ were high and RuBP oxygenation (photorespiration) was negligible. Historically atmospheric conditions have only favoured photorespiration during the Carboniferous period (280 - 340 Mya) and the past 35 Myr (Berner and Kothavala, 2001; Sage, 2006). Thus during the Oligocene the interaction of drought or salinity, higher temperatures and low CO_2 concentrations promoted high photorespiration rates, and C_4 photosynthesis evolved independently into various lineages in response to these conditions that promoted higher incidents of photorespiration over the last 35 Myr (Sage, 2012).

It has been suggested by Edwards and Smith (2010) that changes to precipitation patterns (drought) during the last 35 Myr (Oligocene) and the direct effects on forest canopy cover may have indirectly co-contributed to C_4 evolution. Changes in rainfall may have limited canopy growth in tropical forest environments which would have exposed leaves to high light and subsequently high temperatures. High light would have been necessary to drive the CCM and subsequently limiting photorespiration that would be encountered at elevated temperatures (Edwards and Smith, 2010). This suggests that drought was not a selection pressure that favoured the high *WUE* of C_4 plants, but in fact it was

drought that indirectly exposed ancestors of C_4 plants to the environmental conditions necessary to facilitate the evolution of C_4 photosynthesis.

Current studies indicate that C_4 photosynthesis has evolved into 66 independent lineages (Edwards *et al.,* 2012; Sage *et al.,* 2011; 2012) which include the eudicots and monocots. Even though the evolution from C_3 to C_4 photosynthesis requires many complicated modifications (Hibberd and Covshoff, 2010), it is a significant convergent trait shared amongst the C_4 lineages (Sage *et al.,* 2011). Evolution from C_3 to C_4 photosynthesis would have required several evolutionary steps (Rawsthorne, 1992), and these steps are explained in a five phase model (Sage, 2004; **S**age *et al.,* 2012). The first phase is preconditioning, which essentially requires high vein density (closely spaced veins). The second phase is the evolution of the Proto-Kranz anatomy, which is the enlargement of the BSC, an increased number of BSC organelles and in most cases centripetally located BSC mitochondria. The third phase is the evolution of C_2 photosynthesis, which is a C_3-C_4 intermediate that also concentrates CO_2 in the BSC. The fourth phase is the establishment of the C_4 metabolic cycle, showing enhanced PEPcase activity in the MC and restriction of the C_3 metabolic cycle to the BSC. The final phase is the optimisation of the C_4 cycle, where modification of the Kranz anatomy and biochemistry improve C_4 photosynthetic efficiency. All five evolutionary phases proposed are represented in extant species of *Flaveria* and *Heliotropium.*

Grasses represent 22-24 independent lineages with one likely reversal from C_4 to C_3 (*Alloteropsis*) (Edwards *et al.,* 2012). Chloridoideae represents the oldest C_4 photosynthetic lineage which dates between 25 (± 4) and 32 (± 4.5) Mya. This coincides with the Oligocene origin of C_4 photosynthesis, however most C_4 grass lineages evolved from about 30 Mya until more recent (Kellogg, 1997; Christin *et al.,* 2008).

1.7 What is known about C_4 drought responses?

The carbon concentration mechanism allows C_4 grasses to maintain high *WUE*, a trait that has been used to explain their preference for semi-arid habitats (Pearcy and Ehleringer, 1984). However, paradoxically C_4 grasses, specifically NADP-Me subtypes, are more sensitive to drought than C_3 grasses (Ibrahim *et al.,* 2008; Ripley *et al.,* 2007, 2010; Taylor *et al.,* 2011). Like C_3 grasses, C_4 grasses respond to decreases in relative leaf water content (*RLWC*) and leaf water potential (Ψ_{leaf}) with declining photosynthetic rates (Lawlor, 2002). This reduction in photosynthesis is a result of reduced stomatal conductance which limits CO_2 diffusion into the leaf, thereby reducing the intercellular CO_2 concentration (C_i) at Rubisco (stomatal limitation) and metabolic impairment (metabolic limitation). For C_3 and C_4 plants alike, declining leaf water status reduces stomatal conductance similarly which

invariably reduces the photosynthetic rates (e.g. Kalapos *et al.*, 1996; Maroco *et al.*, 2000; Ghannoum *et al.*, 2003; Carmo-Silva *et al.*, 2008). Under conditions of mild water stress (*RLWC* < 70%), the decline in photosynthesis in C_3 and C_4 grasses is associated with decreased stomatal conductance, but as drought becomes more severe, metabolic limitations become more important, especially in the C_4 grasses (Ghannoum, 2009).

1.7.1 Stomatal versus non-stomatal limitations

1.7.1.1 C_4 response to mild water stress

Decreasing stomatal conductance (g_{ST}) limits photosynthesis (A) as a result of reduced C_i at the site of Rubisco. This is particularly evident in water stressed C_3 plants where it is generally accepted that as g_{ST} decreases, the C_i and A decrease in response. However, amongst C_4 grasses, studies show the response of C_i to changes in g_{ST} is variable. Several studies show that C_i decreases at the early stages of drought, and then at the later stages of drought C_i increases, while A decreases (Becker and Fock, 1986; Du *et al.*, 1996; Kalapos *et al.*, 1996; Williams *et al.*, 2001; Leakey *et al.*, 2004; Marques da Silva and Arrabaça, 2004). Contrasting studies show that C_i remains unchanged during increasing drought, and only at the end of the drying cycle (severe drought) does the C_i increase with a decline in A (Kalapos *et al.*, 1996; Saliendra *et al.*, 1996; Ripley *et al.*, 2007).

If stomatal limitation is the only factor limiting photosynthesis, then elevating CO_2 concentrations to overcome the reduced g_{ST} will restore A to pre-water stress values by saturating Rubisco. However a study on water stressed sugar cane showed that maintenance of C_i only restored A to control values at very mild drought. Under conditions of increasing drought A could not be restored to control values (Du *et al.*, 1996). This could indicate a non-stomatal effect such as an increase in mesophyll conductance (Cornic, 2000) or some other metabolic impairment.

In C_3 plants, water stress and the resultant decreased C_i alters the $[CO_2]$:$[O_2]$ at the site of Rubisco, thereby increasing the rate and proportion of photorespiration. However this is not apparent in C_4 plants and under drought conditions photorespiration does not increase or shows only a slight increase and has no significant effect on A (Lawlor and Fock, 1978; Ripley *et al.*, 2007; Carmo-Silva *et al.*, 2008). It is also argued that if Rubisco activity decreases independently to C_i, then the oxygenation and carboxylation reactions will decrease in the same proportions. Carmo-Silva *et al.*, (2008) showed this proportional decline in C_4 grasses subject to severe water stress resulted in a decrease in both photosynthesis and photorespiration, thus indicating a non-stomatal limitation.

If the limitation of *A* is purely stomatal, then on re-watering and rehydration of the leaf, *A* should recover to that of the control values. Ripley *et al.*, 2010 showed that for C_3 grasses, *A* recovery from severe drought was rapid whereas the C_4 grasses showed a much slower *A* recovery, indicating additional mechanisms of photosynthetic inhibition. There are however very few studies that measure the *A* recovery of C_4 grasses after exposure to severe water stress at the plant level.

1.7.1.2 C_4 response to severe water stress

The metabolic limitations to photosynthesis become more significant than stomatal limitations during prolonged or extreme leaf water stress (Lawlor, 2002; Ghannoum *et al.*, 2003; Flexas *et al.*, 2006). For C_3 and C_4 plants the effects of severe water stress can elicit a multitude of responses that inhibit photosynthesis. These include, but is not limited to, loss of turgor potential, reduced photosynthetic enzyme activity, nitrate assimilation inhibition, initiation of premature senescence, changes to leaf anatomy and cellular ultrastructure and reduced RuBP regeneration (Tezara *et al.*, 1999; Flexas and Medrano, 2002; Lawlor, 2002; Flexas *et al.*, 2004).

Loss of cellular turgor potential from severe water stress has direct negative effects on plant physiological functions, metabolism, growth and morphological processes such as leaf enlargement, stomatal functions and associated photosynthesis (Jones and Turner, 1986; Decosta, 2006). Osmotic adjustment (*OA*) is a physiological mechanism which is related to maintenance of positive cell turgor, thus sustaining leaves at favourable water contents to continue physiological and morphological processes (Hare *et al.*, 1998; Decosta 2006). *OA* in the dehydrated cells is achieved by the accumulation of osmolytes, such as amino acids, ammonium compounds, sugars, polyols, organic acids and inorganic ions (Hare *et al.*, 1998; Decosta 2006). It is argued that *OA* can either contribute to drought tolerance by maintaining important plants processes at lower leaf water potentials or drought avoidance, by increased soil-water extraction and improved root growth. Various grass species do however show a positive correlation of *OA* and drought tolerance (Decosta, 2006). This is evident in C_4 NADP-Me species such as *Sorghum bicolour* (Jones and Turner, 1978) and *Hyparrhenia rufa* (Baruch and Fernandez, 1993) which exhibit improved drought tolerance over phylogenetically similar species which demonstrated less *OA*.

Although there is limited data regarding C_3 and C_4 cycle enzymes, the majority of studies indicate a down-regulation or inhibition of the C_3 (Rubisco) cycle as opposed to the C_4 (PEPcase) cycle. This leads to a decrease in the C_3/C_4 activity ratio, resulting in an increase in the BSC CO_2 concentration. While carboxylation activity decreases comparatively to the decarboxylation activity, the CO_2 concentration gradient between BSC walls increases and CO_2 leakage occurs (Hatch *et al.*, 1996; Fravolini *et al.*, 2002). Other studies indicate an increase in PEPcase activity relative to Rubisco

activity, which resulted in BS leakiness (Saliendra *et al.*, 1996). Bowman *et al.*, (1989) showed that leakiness followed a diurnal pattern indicating biochemical responses (not anatomical), and secondly leakiness showed a linear response to photosynthetic inhibition in response to water stress. This data suggest the C_3 cycle is more sensitive to water stress than the C_4 cycle.

Other metabolic factors that may affect C_4 plants under water stress are the uptake and assimilation of nitrates (Becker and Fock, 1986; Foyer *et al.*, 1998). This may affect chlorophyll and protein content but could also be due to protein degradation from induced senescence (Becker and Fock, 1986). It has also been shown that there are ultrastructure distortions in C_4 leaves during severe water stress which can affect CO_2 diffusion and light penetration (Flexas *et al.*, 2004).

Lawlor, (2002) suggested that decreased photosynthetic potential is due to impairment of the C_3 cycle. This is most likely due to RuBP regeneration, which is affected by the reduction of ATP synthase (Lawlor and Tezara, 2009). Water stress increases Mg^{2+} concentrations, which result in the progressive loss or inactivation of the Coupling Factor (ATP synthase) which reduces the amount of ATP synthesised (Tezara *et al.*, 1999; Lawlor, 2002). Electron transport, generation of NADPH and the thylakoid proton gradient show little or no correlation to water stress (Lawlor, 2002).

In C_3 plants it has been suggested that photorespiration can act as an alternative electron sink in stressed plants. This is achieved by reducing the over reduction of the electron transport chain, allowing C_3 plants to recover more quickly from water stress by protecting the photosynthetic metabolism. However in C_4 plants photorespiration is suppressed under most environmental conditions, and if it indeed protects the photosynthetic metabolism, it is doubtful that it may act as in alternative electron sink. The Mehler reaction is another alternative electron sink which involves the direct reduction of molecular O_2 to superoxide radicals at *PSI* (Cornic and Fresneau 2002; Ghannoum, 2009). The Mehler reaction has a slightly greater capacity in C_4 plants (18% of total O_2 uptake in light dependent reactions) as opposed to C_3 plants (Siebke *et al.*, 2003). The Mehler reaction seems to remain unaltered or even suppressed under conditions of water stress (Brown *et al.*, 1995; Badger *et al.*, 2000) except in C_4 *Alloteropsis semialata*, where Ripley *et al*., (2007) found that it increased under water stress. The lack of photorespiration and the largely unaltered Mehler reaction under different environmental conditions could partially explain why severe drought has a negative effect on C_4 metabolism and the subsequent recovery upon re-watering. It would seem that the C_3 cycle within C_4 plants is the site of probable metabolic limitation, and the coupling of the two cycles seems to augment water stress sensitivity.

1.8 What is known about C_4 subtypes drought responses?

There are intrinsic differences between the three C_4 biochemical pathways, and their assumed advantages under drought conditions are based on distribution and limited experimental data. Subtype distribution is complicated by phylogeny, as phylogenies tend to show stronger relationships to rainfall gradients compared to subtypes (Tieszen, 1979; Schulze *et al.,* 1996; Taub, 2000; Visser *et al.,* 2012), however experimental data does show some differences between subtypes when exposed to water deficits.

Using an 18 species comparison Ghannoum *et al.,* (2002) showed that relative to NADP-Me species, NAD-Me grasses increased their *WUE* during drought by decreasing water loss and hence their sensitivity to drought. Carmo-Silva *et al*., (2007) subjected single grass species, belonging to NADP-Me, NAD-Me and PCK subtypes to a rapidly induced drought using PEG-4000. The leaf water content of the NAD-Me grass was most sensitive to drought, however it maintained higher photosynthetic rates, stomatal conductance and instantaneous *WUE* under drought, compared to the other subtypes. The NADP-Me was most sensitive to drought, but this was not thought to be related to Rubisco and PEPcase activity, which was the mechanism responsible for the decline of photosynthesis in the NAD-Me and PCK subtypes. Using one grass species of each C_4 subtype, Carmo-Silva *et al.,* (2010) suggested that a decrease in RuBP in NAD-Me and PCK contributed to the drought induced decrease in photosynthesis, which is in line with what Lawlor, (2002) hypothesised.

All these experiments however did not fully account for lineage effects. Of the nine NAD-Me grasses used by Ghannoum *et al.,* (2002), seven were from the Chloridoideae subfamily and two were in the Panicoideae subfamily, which adds a strong phylogenetic bias towards a clade that is drought tolerant. Taub (2000) and Cabido *et al*., (2008) showed strong phylogenetic relationships of increasing numbers of species of Chloridoideae (mainly NAD-Me and PCK) grasses to increasing aridity. Carmo-Silva *et al.,* (2007; 2010) only used three grass species, two belonging to Chloridoideae and the third to Panicoideae. By not fully accounting for phylogeny, interpretation of the results for direct subtype comparisons is further complicated.

Martin (2008) suggested that drought sensitivity, or more notably the recovery from drought of NADP-Me grasses, could be related to their fundamental biochemistry. In the NADP-Me subtype, reduced malate is transported to the BSC chloroplast where it is decarboxylated, producing CO_2, pyruvate and an electron which is used to reduce $NADP^+$ to NADPH (Fig. 1.1 a). However in the NAD-Me subtype, NADPH is produced in the BSC chloroplast by non-cyclic photophosphorylation and is not fully dependent on electrons transported from the MC (Fig. 1.1 b). This has implications

under conditions of water stress where turgor loss can occur. Efficient transport of the intermediates between the MC and BSC may be negatively affected, due to impaired plasmodesmata and plasmolysis which are symptoms of turgor loss. The effects of this may be exacerbated for NADP-Me subtypes as less NADPH is likely to be transported to the BSC, where NADPH is used in the PCR step where 3-phosphoglycerate is reduced to glyceraldehyde-3-phosphate (G3P). Unlike the NAD-Me BSC chloroplast, NADP-Me have reduced grana in the BSC chloroplast, indicating low *PSII* activity and resulting in ATP being produced mainly by *PSI* cyclic photophosphorylation. A disadvantage of cyclic photophosphorylation is that NADPH is not produced (Lawlor, 2001), demonstrating a further reliance on the transport of reduced malate to the BSC from the MC. Coupled with reduced ATP synthase (Lawlor, 2002), the C_3 cycle of NADP-Me may be more vulnerable than that of the NAD-Me subtypes. This implies that the proposed breakdown of the C_4 cycle from water stress has a direct effect on the C_3 cycle. For PCK subtypes the situation is slightly more complicated as both aspartate and malate are transported from the MC to the BSC as part of the C_4 cycle.

1.9 Quantum yield in C_4 grasses

Quantum yield and the associated energetic requirements, BSC CO_2 leakage and interveinal distances may offer some explanations as to why C_4 species are susceptible to severe drought, and specifically the differences in vulnerability between the C_4 photosynthetic subtypes. There is however limited ecological data that indicates the advantage of more efficient quantum yields between C_4 subtypes during drought (Ghannoum *et al.*, 2001, Furbank, 2011).

Quantum yield (quantum efficiency) is the initial slope of the photosynthetic light response curve and is measured as the moles of CO_2 fixed per moles of absorbed photons at the leaf level (Ehleringer, 1978). Quantum efficiency of C_4 plants remains constant over a range of temperatures whereas C_3 plants have a higher quantum efficiency at low temperatures, which decreases with increasing temperature. Ehleringer and Bjorkman (1977) showed for grasses that C_3 quantum efficiency is maintained above that of the C_4 grasses up to approximately 30ºC, where a crossover point is reached and the C_3 photosynthesis becomes less efficient. The decrease in quantum efficiency with increasing temperature for C_3 grasses is directly attributed to photorespiration. In contrast C_4 quantum yield remains constant due to photorespiratory inhibition across a range of temperatures. The higher quantum efficiency at low temperatures (minimal photorespiration) for the C_3 pathway, reflects the inherently lower cost of this pathway (Ehleringer, 1978), while the C_4 pathway requires an additional 2 to 2.25 ATP per CO_2 fixed as a result of the C_4 cycle (Hatch, 1970).

Within C_4 grasses, quantum efficiency varies significantly according to photosynthetic subtype. NADP-Me and PCK subtypes have similar quantum efficiencies and both are significantly higher than NAD-Me subtypes (Ehleringer and Pearcy, 1983). Reasons for variability between subtypes are 1) different intrinsic energy requirements; 2) differential rates of CO_2 leakage from BS cells and 3) leaf interveinal distances.

Both NADP-Me and NAD-Me subtypes have the same energy requirements of 5 ATP and 2 NADPH per CO_2 fixed. The stoichiometries for PCK subtypes are less certain as the enzymes PEPcase and NAD-Me function collectively in the decarboxylation step. Estimates are 3.5 ATP and 2.25 NADPH per CO_2 fixed (Kanai and Edwards, 1999). It is suggested that there is a degree of flexibility between the three subtype's energetics which may be environmentally and developmentally controlled (Furbank, 2011).

CO_2 that is released from the decarboxylation of the C_4 acid into the BSC is not always re-fixed by Rubisco. The CO_2 that is not fixed can diffuse back into the mesophyll cells which reduces the quantum efficiency, as 2 ATP are consumed by PPDK to produce one molecule of the primary carbon acceptor (PEP) (Hatch, 1996). Ehleringer and Pearcy (1983) attributed the higher quantum yield of NADP-Me subtypes to the presence of suberized lamella in the BS cell walls, which reduced the leakage of CO_2 to the MC. Studies have shown that genotypes/species of different subtypes (sugarcane – NADP-Me and *Eragrostis lehmanniana* – NAD-Me), which exhibited less of an increase in BSC leakiness rates during water stress, demonstrated greater drought tolerance (Saliendra *et al.*, 1996; Fravolini *et al.*, 2002).

Decreasing interveinal distance (IVD) in grasses increases the [BSC]:[MC] ratio (Griffiths *et al.*, 2012), which can affect photosynthesis as photon capture and the PCR cycle are largely restricted to the BS cells (Ogle, 2003). C_4 and C_3 grasses have IVD's of approximately 118 μm (1 - 4 mesophyll cells) and 267 μm (>5 mesophyll cells) respectively, which correlates well with the higher quantum yields of C_4 grasses (Dengler *et al.*, 1994; Ehleringer *et al.*, 1997; Ogle, 2003). Within C_4 grasses this relationship extends to the different photosynthetic subtypes where NADP-Me grasses (IVD ± 89 μm) have on average significantly higher quantum yields than NAD-Me grasses (IVD ± 142 μm). From a C_4 perspective, shorter interveinal distances are attributed to higher quantum yield, shade intolerance (Ehleringer, 1978; Ogle, 2003) and improved leaf hydraulic conductance (Grifiths *et al.*, 2012). Improved leaf hydraulic conductance can be beneficial in arid environments where low leaf water potentials can potentially cause the water column within the xylem to cavitate (Kocacinar and Sage, 2003). On the whole, the implications for drought tolerance arising from different quantum yields for C_4 subtypes are not fully understood.

1.10 Why propose differences in drought responses between lineages and subtypes?

1.10.1 Lineage and subtype associations with rainfall gradients

Factors that determine C_4 grass distributions have been well documented, however the interaction response between C_4 photosynthetic subtype and phylogeny is more complex, in particularly their responses to rainfall gradients. Sage and Monson (1999) suggested that the three C_4 carboxylation types have physiological traits that favour particular ecological conditions. This is evident from studies where the number of NADP-Me species increases with increased precipitation while the number of NAD-Me species shows the reciprocal response (Fig. 1.2) (Ellis *et al*., 1980; Vogel *et al.,* 1986; Taub, 2000; Cabido *et al.,* 2008). PCK species show an intermediate distribution to rainfall gradients thus possibly indicating physiological traits that favour widespread ecological or environmental conditions.

Data from Taub (2000) indicated that the association to rainfall gradients was stronger amongst C_4 subfamilies compared to the C_4 subtypes, thus suggesting that the interaction of phylogeny and possibly unknown physiological traits, and not photosynthetic subtype, determine these distributions. However the majority of these studies focused on Arundinoideae and Panicoideae species consisting predominantly of NADP-Me, and Chloridoideae, which are either NAD-Me or PCK subtypes. Virtually no emphasis has been placed on C_4 species from the Aristidoideae subfamily, which possess the NADP-Me subtype biochemistry. Unlike the NADP-Me species from these studies (previous paragraph), the Aristidoideae shows an increase in species numbers with aridity (Tieszen, 1979; Schulze *et al.,* 1996; Visser *et al.,* 2012). In South Africa, species from Andropogoneae and Paniceae tribes (mainly NADP-Me, but also NAD-Me and PCK) are found in mesic habitats. Chloridoideae species (NAD-Me and PCK) show a relatively constant distribution (distributions not separated by subtypes) and species from Aristidoideae (NADP-Me) are most abundant in arid regions (Visser *et al.*, 2012). This conforms to the notion of phylogenetic conservatism of environmental niches (Webb, 2000; Donoghue, 2008), despite NADP-Me Panicoideae and Aristidoideae utilising the same C_4 subtype pathway. Selective pressures that prompted the evolution of the C_4 pathway as a whole are reasonably well understood, however the roles of different C_4 carboxylation subtypes in plant fitness (e.g. drought tolerance) are not fully understood (Furbank, 2011).

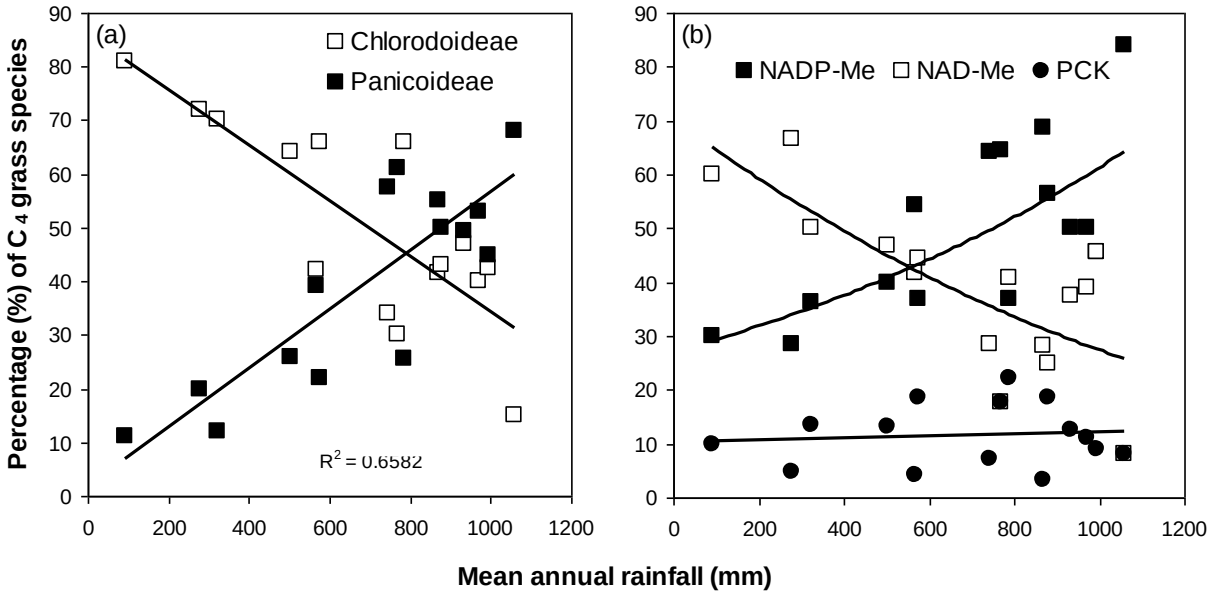

Figure 1.2: Percentage of C_4 grass species along a rainfall gradient for a) subfamilies and b) photosynthetic subtypes. Trend lines fitted using best fit R^2 .Graphs redrawn from Cabido *et al.,* (2008).

1.11 Rationale for phylogenetic and photosynthetic subtype experiments

To experimentally determine the drought responses of different grasses, species were selected from the PACMAD phylogeny (Fig. 1.3) (Edwards *et al.,* 2012). Comparisons between photosynthetic subtypes (NADP-Me and NAD-Me) were made within the Panicoideae subfamily. Panicoideae is the only subfamily that includes all three subtypes thus differences in phylogenetic effects are mostly eliminated and the effects of subtype are shown.

A second comparison controlled for photosynthetic subtype and tested the effects of phylogeny. NADP-Me subtypes from Panicoideae and Aristidoideae were compared, as both are major PACMAD clades and are ecologically important in southern Africa (Christin *et al.,* 2009; Visser *et al.,* 2012). A second major attribute of Aristidoideae is that globally the majority of species are distributed in arid regions, in contrast to most other NADP-Me species, which have a preference for more mesic environments (Visser *et al.,* 2012).

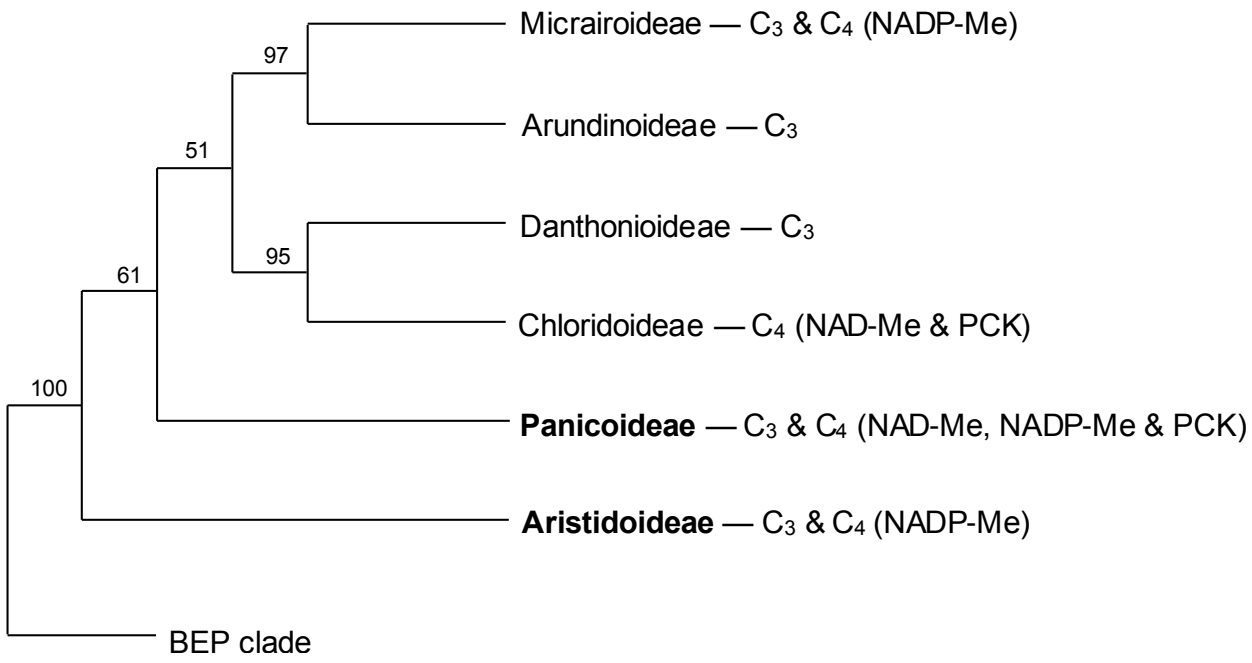

Figure 1.3: PACMAD phylogeny inferred from Bayesian analysis of three chloroplast markers. Values at the nodes are bootstrap support values (redrawn from Edwards *et al.*, 2012). Photosynthetic type is indicated for each lineage.

1.12 Aims

The main aims of this study were to determine if Panicoideae NAD-Me and Aristidoideae NADP-Me grass species were more drought tolerant than Panicoideae NADP-Me grass species. This was based on the observed natural distributions of C_4 photosynthetic subtypes and subfamilies in response to rainfall. An additional basis for the differential drought sensitivity arises from subtype differences in metabolism and requirements for energy and intermediate transfer between the MC and BSC. The underlying mechanisms investigated between subtypes and subfamilies were:

- Differences in metabolic and stomatal limitations.
- The avoidance of limitations by the maintenance of plant water status, positive turgor and osmotic adjustment.
- The relationship between turgor loss and metabolic limitations.
- The relationship between recovery from drought and metabolic limitations.

Chapter 2

General responses to drought and recovery

2.1 Introduction

Research has shown that C_4 grasses are more susceptible to severe drought than C_3 grasses, despite being physiologically adapted for hot arid environments. This susceptibility to drought is also evident from research that shows C_4 grasses require a longer period to recover from drought as opposed to C_3 grasses from the same clade (Ibrahim *et al.,* 2008; Ripley *et al.,* 2010). This severe drought susceptibility is mainly a biochemical (metabolic) limitation, and not a limitation imposed by stomata, as is the case under less severe drought (Lawlor 2002; Ghannoum *et al.,* 2003; Marques da Silva and Arrabaca, 2004; Ripley *et al.,* 2007, 2010).

The susceptibility of C_4 grasses to drought varies both with photosynthetic subtype and phylogenetic group. Within subtypes, NAD-Me species have been shown to be less susceptible to drought than NADP-ME species and have increasing water use efficiency (*WUE*) at the leaf level (Ghannoum *et al.,* 2002). This allows NAD-Me species to conserve plant water status, for a comparative leaf area, and possibly endure longer periods of drought and the larger *WUE* will be important to offset the required smaller stomatal conductance and leaf area in very dry habitats. This mechanism might explain the biogeography of NAD-Me species, which increases in frequency with increasing aridity, while the converse response is true for NADP-Me species (Ellis *et al.,* 1980; Vogel *et al.,* 1986; Taub, 2000; Cabido *et al.,* 2008). This trend is however complicated, as most NAD-Me species belong to the Chloridoideae subfamily, while most NADP-Me species belong to the Panicoideae subfamily, and hence the distribution in response to aridity may be due to phylogenetic differences un-associated with photosynthetic subtype. Furthermore, C_4 species from the *Aristida* genus (Aristidoideae subfamily) belong to the NADP-Me photosynthetic subtype, but their biogeography globally and in South Africa indicates a preference for hot arid habitats (Christin *et al.,* 2009; Cerros-Tlatilpa, 2011; Visser *et al.,* 2012). This conflicts with the notion that NADP-Me species exist in more mesic habitats (Vogel *et al.,* 1986; Cabido *et al.,* 2008) and demonstrates a phylogenetic basis to the response.

In addition to the susceptibility to drought, the rate of recovery from drought may be an important determinant for life in arid environments. Within South Africa, Aristidoideae species richness is well correlated to hot arid environments that show frequent levels of disturbance, environmental conditions that would require fast photosynthetic recovery rates. Conversely, Panicoideae species richness is high in more mesic environments with low to high grazing intensity (Visser *et al.,* 2012), environmental conditions that would require fast re-growth of removed biomass as opposed to rapid

photosynthetic recovery at the leaf level. This would imply that C_4 grasses within each subfamily show phylogenetic conservatism in the ecological habitats they occupy, and traits such as photosynthetic carboxylation type are of lesser importance (Taub, 2000; Webb, 2000; Donoghue, 2008; Visser *et al.*, 2012). Sage and Monson (1999) suggested that the different C_4 carboxylation types have traits suited for particular environmental conditions, however there is to date little evidence to show how photosynthetic subtypes confer advantage to particular environments. Furbank (2011) suggested that there may be flexibility between the three pathways which could be developmentally and environmentally controlled. Ratios of aspartate to malate within NADP-Me species can vary substantially and this is thought to be governed by seasonal changes in irradiance or some other environmental condition, and not a mechanism that is genetically predetermined (Kanai and Edwards, 1999; Furbank, 2011).

The mechanisms whereby photosynthetic productivity of C_4 grasses is decreased by drought have not been fully elucidated, nor have potential differences between subtypes. What is known is that after an initial period of reduced stomatal conductance, intercellular CO_2 supply is decreased, resulting in decreased carbon transport and assimilation, and thus affecting the rate of ATP and NADPH consumption. However as drought becomes more severe, metabolic limitations become more significant (Lawlor, 2002; Ghannoum *et al.*, 2003). These are correlated to declining concentrations (per unit leaf area) of C_3 and C_4 intermediates, decreases in enzyme activity and concentrations, and decreases in ATP concentrations (Bowman *et al.*, 1989; Lawlor, 2002). There are also direct and indirect effects on the light reactions. Drought increases the production of reactive oxygen species (ROS) (Asada, 2006; Sharma *et al.*, 2012), and these decrease the repair-cycle of *PSII* turnover, resulting in symptoms characteristic of photoinhibition (Melis, 1999; Sharma *et al.*, 2012; Tikkanen *et al.*, 2014). Subsequently, as a result of metabolic limitations and photoinhibition, the decline in the efficiency of the light reactions become evident from decreases in the maximum (F_v'/F_m') and operating efficiency ($\Phi PSII$) of *PSII* (Baker, 2008).

PSII maximum efficiency (F_v'/F_m') which is calculated in a light adapted state, is a measure of the potential operating efficiency ($\Phi PSII$) if all the *PSII* centres are open (quinine electron acceptor – Q_A "oxidised"), and therefore capable of photochemistry (Baker, 2008). Alternatively *PSII* maximum quantum efficiency (F_v/F_m) can be measured in the dark adapted state where Q_A becomes maximally oxidised (open), and therefore indicating the maximum ability to perform photochemical reactions. Saccardy *et al.*, (1998) showed that in *Z. mays* (NADP-Me) leaves, F_v/F_m values only declined when relative leaf water content (*RLWC)* dropped below 60%. This was mainly attributed to a decrease in F_m (maximal fluorescence) and an increase in F_o (initial or minimal fluorescence). F_m and F_m' is the fluorescence signal when Q_A is maximally reduced (*PSII* centres "closed") and therefore unable to perform photochemistry while F_o and F_o' is the fluorescence signal when Q_A is maximally oxidised

(*PSII* centres "open"). A decrease in F_m' is associated with photosynthetic down-regulation (decreased consumption rate of ATP and NADPH) and the concomitant increase in heat dissipation (non-photochemical quenching processes) from *PSII* reaction centres. Changes in F_o' are associated with photoinhibition (non-photochemical quenching processes) where excitation energy is dissipated as heat rather than photochemistry, and this includes *PSII* degradation (ROS) and photoprotective processes such as provided by the xanthophyll cycle (Maxwell and Johnson, 2000; Rong-hua *et al.*, 2006; Baker, 2008).

The xanthophyll cycle is a mechanism utilized by plants to protect *PSII* from damage caused through photoinhibition, by the de-epoxidation of the carotenoid pigment violaxanthin to antheraxanthin (intermediate) and then zeaxanthin. The reverse process is the epoxidation. Saccardy *et al.*, (1998) showed that these changes in F_m and F_o were correlated to an increases in violaxanthin de-epoxidation (increase in antheraxanthin and zeaxanthin pigments). Compared to C_3 plants, C_4 plants (*Z. mays* and *Sorghum bicolour*) have a comparatively smaller xanthophyll cycle pool and less convertible violaxanthin (Brugnoli *et al.*, 1995).

The aims of this chapter was to determine; (1) if Aristidoideae NADP-Me and Panicoideae NAD-Me species showed a greater tolerance to progressive drought than Panicoideae NADP-Me species; (2) if each subtype/subfamily group showed different rates of recovery from severe drought; and (3) if there was a correlation between drought and recovery responses. Drought responses were determined from gas exchange and chlorophyll fluorescence, highlighting differences in stomatal and metabolic limitations during drought and recovery.

2.2 Methods

2.2.1 Plant collection, growth conditions and experimental set-up

Plants collected from the Grahamstown area (Eastern Cape, South Africa) included *Tristachya leucothrix*, *Heteropogon contortus*, *Aristida diffusa* and *Aristida congesta*, while *Aristida junciformis* was collected at Port Alfred (Eastern Cape, South Africa). Whole plants were dug up in the field, trimmed and potted such that each pot represented an individual plant. *Panicum coloratum*, *P. stapfianum* and *Alloteropsis semialata* were grown from existing potted plants that were trimmed and re-potted. *Panicum virgatum* was grown from seed. All plants were potted in 10 litre pots containing 6.7 kg of a homogenous soil mixture made from locally obtained top-soil, similar to the soil the grasses grow in naturally. Plants were kept in a clear polythene tunnel at the Department of Botany,

Rhodes University. Plants were well watered (using field capacity of the soil as a guide) and hydroponic fertilizer (Chemicult - 1g $1L^{-1}$) was added twice in the month leading up to the experiments. Six treatment and six control replicates (except *P. coloratum* and *A. diffusa* which had five due to mortality) of each species were used in all the experiments. Table 2.1 gives a summary of the species used in the experiment.

Table 2.1: Details on the nine perennial C_4 grass species used in the progressive drought and recovery experiment. *Z. mays* was included as a tenth species which was used in the rapid drought experiment (Chapter 3).

Species name	Subtype	Subfamily	Tribe	Growth form	Description	Distribution
Panicum coloratum L. var. coloratum	NAD-me	Panicoideae	Paniceae	Perennial tufted erect grass	Maximum height 1000 mm, leaves 5 – 10 mm wide and up to 300 mm long	Occurs in the eastern half of South Africa in the Nama-Karoo, Grassland and Savanna biomes. It also occurs in tropical and sub-tropical Africa
Panicum stapfianum Fourc.	NAD-me	Panicoideae	Paniceae	Perennial tufted, sometimes prostate grass	Maximum height 900 mm, leaves up to 5 mm wide and no longer than 400 mm	Occurs in the eastern and south western parts of South Africa in the Fynbos, Grassland, Savanna and Nama-Karoo biomes. It is endemic to South Africa
Panicum virgatum L.	NAD-me	Panicoideae	Paniceae	Perennial tall grass	Maximum height 1800 mm	Occurs throughout most of North America
Heteropogon contortus (L.) Roem. & Schult.	NADP-me	Panicoideae	Andropogoneae	Perennial rhizomatous grass	Maximum height 1000 mm, leaves 3-8 mm wide and 30-300 mm long	Occurs almost throughout the whole of South Africa in the Fynbos, Savanna, Grassland and Nama-Karoo biomes
Tristachya leucothrix Nees	NADP-me	Panicoideae	Arundinelleae	Perennial tufted grass	Maximum height 900 mm, leaves 2–6 mm wide, 50–400 mm long and sparsely hairy	Occurs in the eastern to south eastern halves of South Africa in the Fynbos, Savanna and Grassland biomes. It also occurs in tropical Africa
Alloteropsis semialata (R. Br.) Hitchc. subsp. semialata	NADP-me	Panicoideae	Paniceae	Perennial short-rhizomatous tufted grass	Maximum height 1300 mm, leaves 3-6 mm wide and sparsely hairy	Occurs in the eastern half of South Africa in the Savanna and Grasslands biomes
Aristida congesta Roem. & Schult. subsp. barbicolis	NADP-me	Aristidoideae	Aristideae	Perennial or annual slender tufted grass	Maximum height 750 mm, leaves 3 mm wide and up to 200 mm long. Very low leaf yield	Occurs in the eastern half of South Africa in the Savanna and Grassland biomes. It also occurs northwards to East Africa
Aristida diffusa Trin. Subsp. burkei (Stapf) Meld.	NADP-me	Aristidoideae	Aristideae	Perennial slender densely tufted grass	Maximum height 1000 mm, leaves 2-4 mm wide and up to 300 mm long	Occurs throughout most of South Africa in the Savanna, Grassland and Nama-Karoo biomes. It also occurs in Zimbabwe

Continued from Table 2.1

Aristida junciformis Trin. & Rupr. Subsp. junciformis	NADP-me	Aristidoideae	Aristideae	Perennial, stoutly rhizomatous tufted and densely erect grass	Maximum height of 900 mm, leaves are 2-3 mm wide and 300 mm long	Occurs throughout the eastern and southern halves of South Africa in the Fynbos, Savanna and Grassland biomes. It also occurs northwards to East Africa
Zea mays L. Kalahari early pearl	NADP-me	Panicoideae	Andropogoneae	Annual erect, fast growing	Young plants used, 4-6 weeks. Height 350 mm, leaves up to 25 mm	*Zea mays* grown worldwide for agriculture

2.2.2 Drought treatments

Progressive drought was imposed by starting experiments with potted plants watered to field capacity (±20% *SWC*), and then allowing them to decrease soil water content (*SWC*) by ±0.3% each day over the subsequent 58 days. On day 58 plants were re-watered and maintained at field capacity over the remaining 11 days (recovery phase). During the dehydration phase of the experiment potted plants were weighed every second day, and supplementary water added where necessary to ensure that all plants dehydrated at similar rates.

Field capacity of the soil was determined by soaking pots in water for 24 hours and then allowing the soil to drain to constant mass under gravity. During this period the evaporation from the soil surface was minimised by covering the pots with plastic lids. To estimate *SWC* it was necessary to determine the dry weight of the soil added to each pot and to estimate the weight of the plants. Soil dry weights were determined by oven drying soil at 70ºC for 72 hours and representative plants weights were determined by harvesting a subset of plants from each species.

During the experiment evaporation from the soil was minimised by adding 1 kg of fine stone (< 1 cm diameter) to the soil surface. Hence as plant, soil, pot and stone weights were accounted for, the percentage *SWC* for the potted plants could be calculated as follows:

$$SWC = \frac{soil\ wet\ mass - soil\ dry\ mass}{soil\ dry\ mass} \times 100$$

2.2.3 Leaf gas exchange, chlorophyll fluorescence and plant water relations during drought and recovery

Gas exchange (GE), chlorophyll fluorescence (CF), leaf water relations (Ψ_{leaf} and *RLWC*) and photosynthetic response to intercellular CO_2 concentrations ($A:C_i$) (Chapter 4), were measured on various occasions during the dehydration and re-watering phase of the experiment (Fig. 2.2).

2.2.3.1 Leaf gas exchange and chlorophyll fluorescence

To obtain net CO_2 assimilation rates (A), stomatal conductance (g_{ST}), intrinsic water-use efficiency (A/g_{ST}) and the ratio of intercellular to ambient CO_2 concentration (C_i/C_a), leaf gas exchange was measured on the youngest fully-expanded leaf (first down from the apical bud) of the control and treatment plants. These parameters were measured on the days indicated in Fig 2.2 with the exception of the Aristidoideae which were not measured on day 10. Measurements were made using a Licor 6400-40 LCF photosynthesis system (Li-Cor Inc., Lincoln, NE, USA) between 10:30 am and 3:30pm under laboratory conditions. Plants were acclimated under a sodium vapour light at a photosynthetic photon flux density (PPFD) similar to that used in the leaf chamber. Cuvette conditions were maintained as follows: a PPFD of 1200 μmol m^{-2} s^{-1} was supplied by a blue-red led light source, leaf temperature was set at 29°C, vapour pressure deficits (VPD) ranged between 1 – 2.5 kPa. To ensure a consistent gas exchange reading was obtained per leaf, five spot measurements were taken at ten second intervals and averaged. Leaf areas were measured manually and gas exchange parameters were calculated according to the equations of von Caemmerer and Farquhar (1981).

To ensure that instantaneous measurements were conducted at near saturating light intensities, photosynthetic response to incident light intensity was measured on control plants according to Long and Bernacchi (2003).

Chlorophyll fluorescence measurements were made immediately following each instantaneous gas exchange measurement as not to disrupt the steady state photosynthesis. Leaves were acclimated until steady state fluorescence (F_s) was achieved. A multiphase flash (MPF) protocol was used to ensure maximum reduction of Q_A. The following MPF settings were used: 30% ramp, 250ms for phase 1 and 3 and 500ms for phase 2. The light intensity required to ensure Q_A reduction was experimentally determined (data not shown). Chlorophyll fluorescence parameters measured are defined (Baker, 2008) and where necessary their calculations and units are shown. *PSII* maximum efficiency, $F_v'/F_m' = (F_m' - F_o') / F_m'$. At a given photosynthetic photon flux density (PPFD), this estimates the maximum *PSII* photochemistry (efficiency of oxidised (Q_A) *PSII* reaction centers). F_m' is the maximal fluorescence during the saturating light phase (PPFD > 7000 μmol m^{-2} s^{-1}) (Q_A maximally reduced)

and F_o' is the minimal fluorescence of a briefly darkened (6 seconds at 740nm), light adapted leaf (Q_A maximally oxidised). *PSII* operating efficiency, $\Phi PSII = (F_m' - F_s) / F_m'$. At a give PPFD, this estimates the efficiency at which light absorbed by *PSII* is used for Q_A reduction, (steady state photosynthesis). Photochemical quenching, $q_P = (F_m' - F_s) / (F_m' - F_o')$. At a given PPFD, this estimates the *PSII* reaction centers (Q_A) that are oxidised. This includes photosynthesis and photorespiration. Electron transport rate, $ETR = \Phi PSII \times f \times I \times \alpha_{leaf}$ (µmol electrons m^{-2} s^{-1}). Flux of photons driving *PSII*. *f* is the fraction of absorbed quanta used by *PSII* (0.5), *I* is the incident photon flux density (µmol m^{-2} s^{-1}) and α_{leaf} is the leaf absorptance.

2.2.3.2 Leaf water potential (Ψ_{leaf}) and relative leaf water content (*RLWC*)

The leaves used for gas exchange measurements were either excised on the same day as the gas exchange measurements or the following day (midday). The excised leaves were immediately weighed and the leaf water potential (Ψ_{leaf}) was measured using a Schőlander pressure chamber. Following Ψ_{leaf} measurements, the leaves were placed upright in a glass vial which contained enough water to cover the first 10mm of the excised end of the leaf. The leaves were left in the dark overnight to regain full turgor pressure. The following morning the leaves were blotted and weighed and then placed in a drier at 70ºC for 48 hours, after which they were weighed again. This method allowed the Ψ_{leaf} and relative leaf water content (*RLWC*) to be obtained for the same leaf. Trial experiments were conducted to determine if the measurement of Ψ_{leaf} with a pressure chamber affected the rehydration of leaves and it was found to have no significant effect (data not shown).

$$RLWC = \frac{leaf\ wet\ mass - leaf\ dry\ mass}{leaf\ turgid\ mass - leaf\ dry\ mass} \times 100$$

Leaf water potential (Ψ_{leaf}) could not easily be measured at day 56 (±3.5% *SWC*) as a result of the extreme leaf dehydration. Ghannoum *et al.*, (2003) showed that the relationship of Ψ_{leaf} to *RLWC* was mostly linear. Models were fitted to the mean Ψ_{leaf} and corresponding *RLWC* data for each species (control and treatment plants) during the drought and recovery phase. All the species showed a strong linear relationship of Ψ_{leaf} to *RLWC*, thus a straight line function (y = mx – c) was used to describe Ψ_{leaf} at day 56.

2.2.4 Statistics

Nested General Linear Models (GLM) were used to detect the effects of drought and recovery on species, date, photosynthetic subtype/subfamily and their interactions with *A*, g_{ST}, A/g_{ST}, C_i/C_a,

F_v'/F_m', ΦPSII, q_P, ETR, Ψ_{leaf} and RLWC. Comparisons were made between photosynthetic subtypes (NAD-Me and NADP-Me) but confined to species within the Panicoideae (Panicoid), and is hereafter referred to as the "subtype" comparison. A second comparison was made between Aristidoideae (Aristoid) and Panicoid subfamilies and confined to the NADP-Me photosynthetic subtype. This is referred to the as the "subfamily" comparison. Species were nested in photosynthetic subtype/subfamily as appropriate and separate analyses were done on the dry-down (days 0-56) and the recovery phases (days 56-70) of the experiment. Two separate GLM analyses were performed. Firstly within individual groups, GLM analyses compared controls and drought treated plants and their interaction over time. This was performed to determine at which stage of the drought and recovery, treatments differed from the controls. Secondly for subtype and subfamily comparisons, to account for the time effect on the controls in the GLM analyses, treatments were deducted from the mean of the controls at corresponding days. Average data is presented for each individual group (Panicoid NAD-Me, Panicoid NADP-Me and Aristoid NAD-Me) and the comparison made between subtype (restricted to Panicoideae) and subfamily (restricted to NADP-Me subtype). GLM analyses results are presented for subtype and subfamily comparisons. Data was tested for homogeneity of variance using Levene's test, and statistical differences between means were determined by Tukeys HSD *post-hoc* test (at $P < 0.05$) if the GLM effect was significant. The linear relationship of relative photosynthetic recovery to *RLWC* and F_v'/F_m' to *RLWC* was tested for significance by fitting linear regressions. Statistics were performed using Statistica© (Version 12, StatSoft, Inc).

2.3 Results

2.3.1 Growth conditions

Average min/max temperatures (± SD) of the tunnel for the duration of the experiment were 17.6 ± 1.2 and 34.1 ± 4.6°C respectively (Fig. 2.1) and the average tunnel temperature was 25.1 ± 8.8°C.

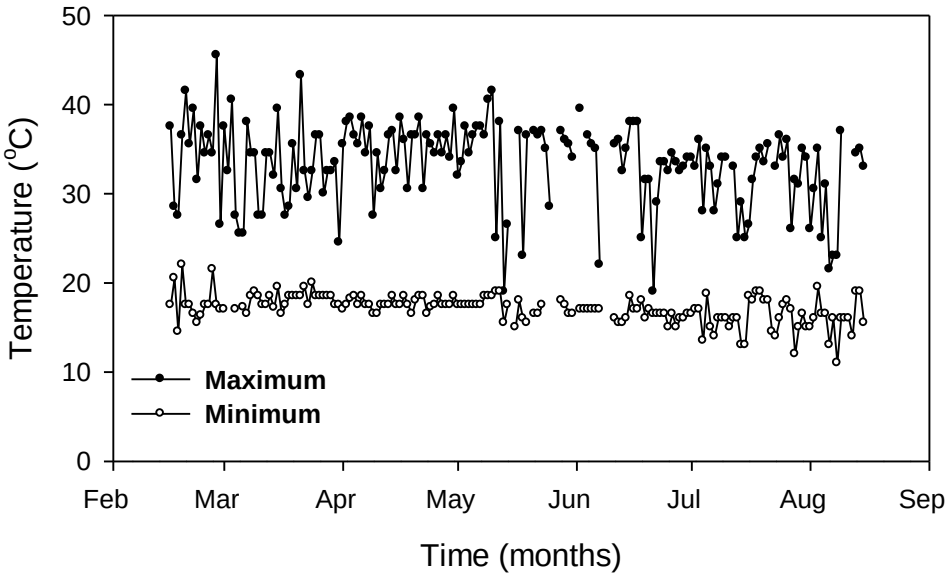

Figure 2.1: Minimum and maximum temperatures recorded in the poly-tunnel where the plants were housed during the drought and recovery experiment.

2.3.2 Progressive drought and recovery procedure

Figure 2.2 shows the mean dry-down rate (± SE) for the progressive drought from day 0 to day 58 for the nine species in the drought experiment. Control plants had a *SWC* of ~20% for the duration of the experiment. Pants were re-watered to field capacity on day 58 and *SWC* returned to ~20% rapidly and was maintained at this level for the next 11 days. The time course of changes in *SWC* was not statistically different between species and replicates (data not shown).

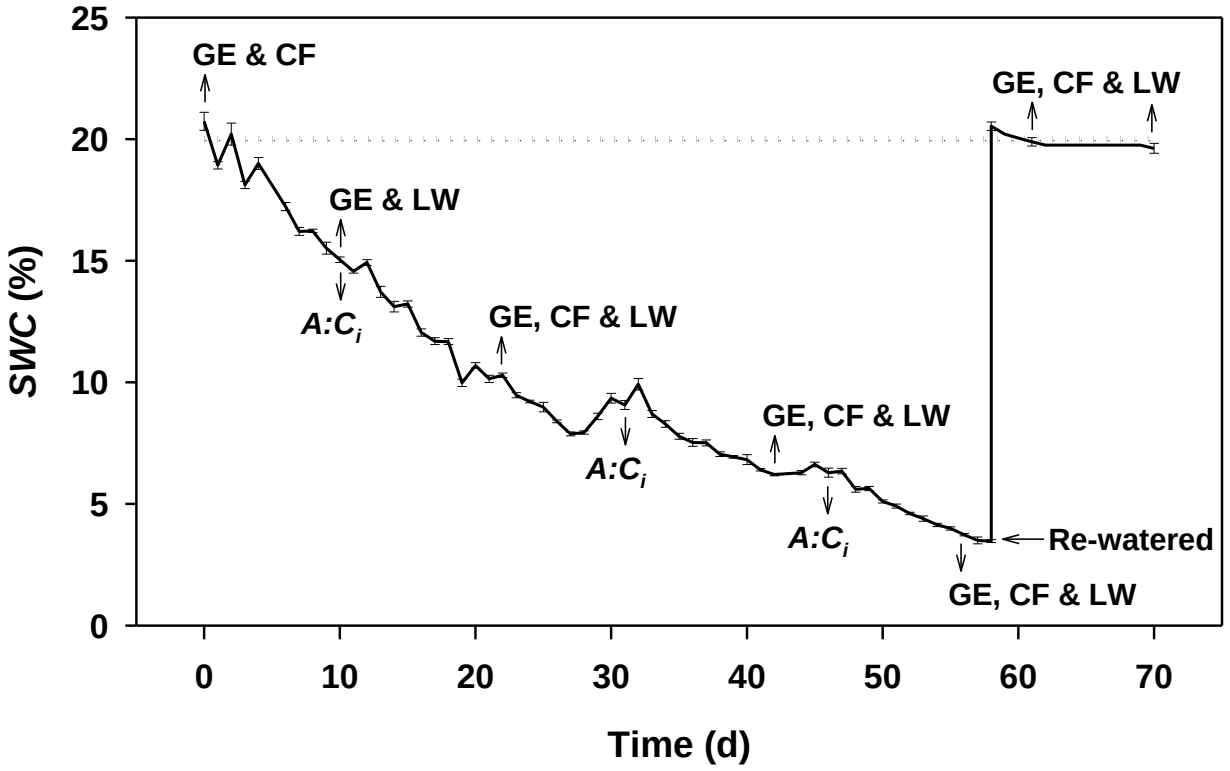

Figure 2.2: Soil water content (*SWC*) for the treatment (▬) and control plants (····) during the pot dry-down and re-watering phases of the experiment averaged across all nine species and replicates (n= 106). The occasions on which experimental measurements were conducted are superimposed: GE= Gas exchange, CF= Chlorophyll fluorescence, LW= Leaf water relations (Ψ_{leaf} and *RLWC*) and *A:C*$_i$= CO_2 Response Curves. Control measurements (not shown) were performed on the same days that treatments were measured, except for Aristidoideae species where gas exchange and leaf water relations measurements were not done on days 10 and 70. For all the plants, day 61 control data was used as the control for days 56 and 61 treatments.

2.3.3 Light responses

During instantaneous gas exchange measures an incident light intensity (*PPFD*) of 1200 μmol m^{-2} s^{-1} was used. When compared to *A:PPFD* responses it was evident that for all species these instantaneous measures were within 10% of being light saturated, except for *P. virgatum* and *A. congesta* which operated within 15.6 and 12% of light saturation respectively (Table 2.2).

Table 2.2: Percentage difference between photosynthesis (*A*) at saturating light intensity and at measurement *PPFD* of 1200 μmol m^{-2} s^{-1} for the control species used in the drought experiment including *Z. mays* (Chapter 3). n= 3 per species. Values are means and SE is given in brackets.

Subfamily (Subtype)	Species	*A* % within *PPFD* saturation (mean ± SE)	Average *A* % within *PPFD* saturation (mean ± SE)
Panicoideae (NAD-Me)	*P. coloratum*	3.3 (1.7)	7.2 (1.5)
	P. stapfianum	2.6 (1.2)	
	P. virgatum	15.6 (1.6)	
Panicoideae (NADP-Me)	*A. semialata*	3.5 (0.6)	4 (0.8)
	H. contortus	2.5 (1.2)	
	T. leucothrix	5.9 (0.6)	
Aristidoideae (NADP-Me)	*A. congesta*	12 (1.6)	7.3 (1.5)
	A. diffusa	7.6 (1.8)	
	A. junciformis	5.1 (1.1)	
Panicoideae (NADP-Me)	*Z. mays*	2.6 (0.3)	

2.3.4 Plant water relations compared between Panicoid subtypes

With the manipulated soil dehydration, leaf water potential (Ψ_{leaf}) and relative leaf water content (*RLWC*) declined exponentially during the course of the experiment (Fig. 2.3 a,b,d & f,g,i). However the rates of decline in both parameters were different between subtypes (subtype x day interaction - Table 2.3), and by day 56 the Ψ_{leaf} of the NAD-Me species had declined to -3.33 MPa, while the corresponding value for NADP-Me species was -4.7 MPa. At the same point *RLWC* had declined to 62.3% for the NAD-Me and 39.5% for the NADP-Me subtypes.

Both NAD-Me and NADP-Me species showed full Ψ_{leaf} recovery relative to their controls after 3 days of re-watering, and Ψ_{leaf} values were not different between subtypes on day 61 and 70 (Fig. 2.3 a,b,d; Table 2.3).

2.3.5 Plant water relations compared between subfamilies

Rates of Ψ_{leaf} declined exponentially and did not vary between subfamilies (subfamily x day interaction – Table 2.4). However the exponential rate of the *RLWC* decline did vary by subfamily (subfamily x day interaction – Table 2.4) and *RLWC* at day 56 for Panicoid species was 39.5% while the corresponding Aristoid value *RLWC* was 68% (Fig. 2.3. g,h,j).

Unlike Panicoid NADP-Me species, the Ψ_{leaf} of Aristoid species did not show full recovery after three days of re-watering, while *RLWC* showed a full recovery within this period (Fig. 2.5 e,j; Table 2.4).

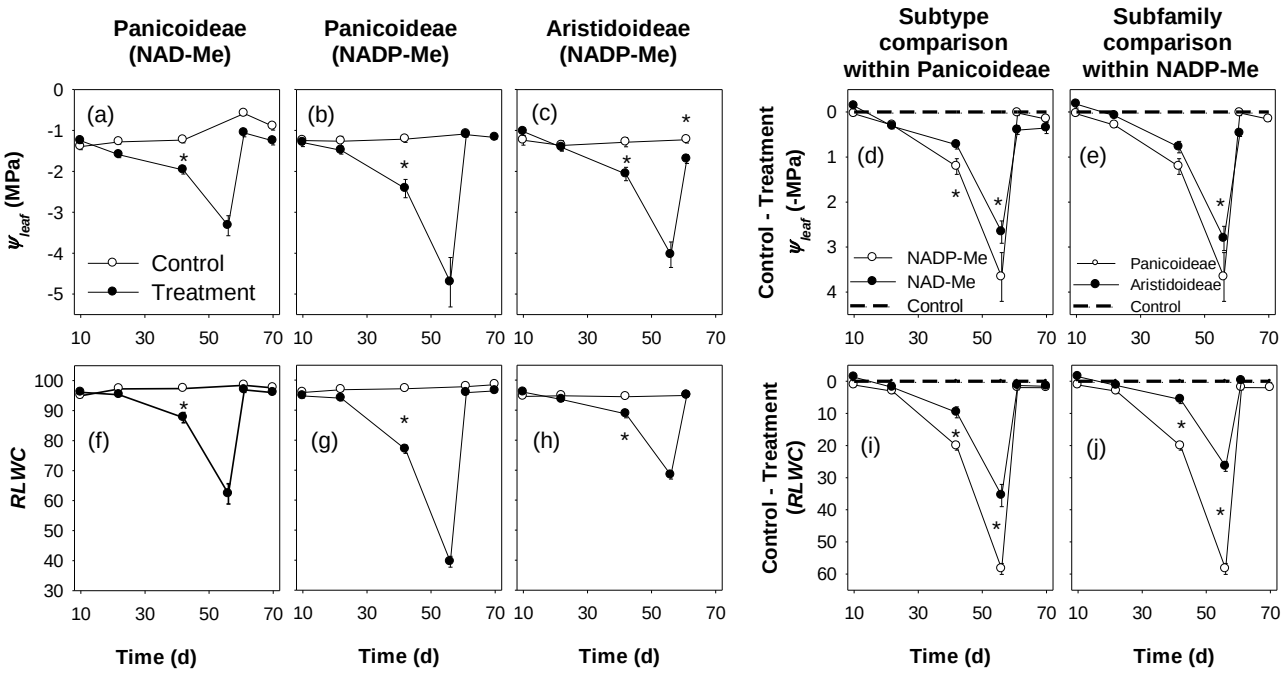

Figure 2.3: (a-c) Leaf water potential (Ψ_{leaf}) and (f-h) relative leaf water content (*RLWC*) for Panicoideae NAD-Me, Panicoideae NADP-Me and Aristidoideae NADP-Me species. Control minus treatment (d-e) Ψ_{leaf} and (i-j) *RLWC* for subtype and subfamily comparisons. Asterisk symbol (*) indicates significant differences between treatments and controls at the corresponding days (a-c & f-h) and between treatments at the corresponding days (d-e & i-j). n= 9-15 for each data point (mean ± SE). Plants were re-watered at day 58. All treatments at day 56 were compared to the controls at day 61 and are significantly different.

Table 2.3: General Linear Model (GLM) results of a comparison leaf water potential (Ψ_{leaf}) and *RLWC* between photosynthetic subtypes (represented as species nested in photosynthetic subtype) in response to decreasing *SWC* (dry-down) and re-watering after drought (recovery). To account for the time effects of the controls in the GLM results, treatments were deducted from the mean of the controls at corresponding days. n.s. (not significant), *= $p < 0.05$, **= $p < 0.01$ and ***= $p < 0.001$.

Parameter	Phase	Species	Species x Day	Species (Subtype)	Subtype	Day	Subtype x Day
Leaf Water Potential (Ψ_{leaf})	Dry-down	** $F_{5,89}= 3.8$	*** $F_{10,89}= 3.4$	*n.s.* $F_{4,89}= 1.9$	** $F_{1,89}= 8.2$	*** $F_{2,89}= 66$	* $F_{2,89}= 4$
	Recovery	*** $F_{4,48}= 6.1$	* $F_{4,48}= 2.7$	*n.s.* $F_{3,48}= 2.4$	*** $F_{1,48}= 14$	*n.s.* $F_{1,48}= 0.44$	*n.s.* $F_{1,48}= 1.5$
Relative Leaf Water Content (*RLWC*)	Dry-down	*** $F_{5,118}= 31$	*** $F_{15,118}= 12.8$	** $F_{4,118}= 4.4$	*** $F_{1,118}= 79$	*** $F_{3,118}= 427$	*** $F_{3,118}= 22$
	Recovery	*** $F_{4,72}= 10.3$	*** $F_{8,72}= 11.8$	*n.s.* $F_{3,72}= 0.6$	*** $F_{1,72}= 26.7$	*** $F_{2,72}= 984$	*** $F_{2,72}= 21$

Table 2.4: General Linear Model (GLM) results of a comparison leaf water potential (Ψ_{leaf}) and *RLWC* between subfamilies (represented as species nested in subfamily) in response to decreasing *SWC* (dry-down) and re-watering after drought (recovery). To account for the time effects of the controls in the GLM results, treatments were deducted from the mean of the controls at corresponding days. n.s. (not significant), *= $p < 0.05$, **= $p < 0.01$ and ***= $p < 0.001$. [a] Only two Ψ_{leaf} data points after recovery so not tested.

Parameter	Phase	Species	Species x Day	Species (Subfamily)	Subfamily	Day	Subfamily x Day
Leaf Water Potential (Ψ_{leaf})	Dry-down	*** $F_{5,64}= 13.5$	*n.s.* $F_{10,64}= 1.1$	*** $F_{4,64}= 6.4$	*** $F_{1,64}= 50.4$	** $F_{2,64}= 5.3$	*n.s.* $F_{2,64}= 2.2$
	Recovery [a]						
Relative Leaf Water Content (*RLWC*)	Dry-down	*** $F_{5,117}= 71.6$	*** $F_{15,117}= 23.6$	* $F_{4,117}= 3$	*** $F_{1,117}= 274$	** $F_{3,117}= 661$	*** $F_{3,117}= 85$
	Recovery	*** $F_{5,59}= 79$	*** $F_{5,64}= 65.5$	* $F_{4,59}= 2.9$	*** $F_{1,59}= 219$	*** $F_{1,59}= 1307$	*** $F_{1,59}= 167$

2.3.6 Leaf gas exchange and chlorophyll fluorescence compared between Panicoid subtypes

Leaf gas exchange (*A*, g_{ST}) and chlorophyll fluorescence parameters (F_v'/F_m', *ΦPSII,* q_P and *ETR*) for subtypes declined exponentially in response to the manipulated soil dehydration, while A/g_{ST} and C_i/C_a showed no decline until a *SWC* threshold of approximately 6.5% (day 42) was reached (Fig. 2.4 & 2.5).

The rates of decline for *A* and g_{ST} were not different between subtypes, with the effect of the progressive drought becoming significant from day 42 onwards, and by day 56 *A* and g_{ST} were essentially zero (Fig. 2.4 a,b,d & f,g,i; Table 2.5 - subtype x day interaction). The threshold at which both subtypes A/g_{ST} and C_i/C_a declined occurred at day 42 (Fig. 2.4 k,l,n & p,q,s; Table 2.5 - subtype x day interaction). The C_i/C_a values at day 56 equated to a C_i of 380 and 364 μmol mol^{-1} CO_2 for NAD-Me and NADP-Me species respectively.

The rate of decline of F_v'/F_m' was different between subtypes and by day 56 the F_v'/F_m' value for NAD-Me species had declined by 38% compared to 56% for NADP-Me species (Fig. 2.5 a,b,d; Table 2.7 – subtype x day interaction). This decline in F_v'/F_m' for both subtypes was attributable to a decrease in F_m' and F_o' while NADP-Me species larger decline in F_v'/F_m' was attributable to less of a decline in F_o' and a 74% decrease in F_v' ($F_m' - F_o'$) relative to the controls. The rates of decline for *ΦPSII,* q_P and *ETR* were not different between subtypes and the effect of the progressive drought became significant from day 42 onwards (Fig. 2.5; Table 2.7 – subtype x day interaction).

All gas exchange parameters (*A*, g_{ST}, A/g_{ST}, and C_i/C_a) and chlorophyll parameters (F_v'/F_m', *ΦPSII,* q_P and *ETR*) showed full recovery from drought after 11 days (day 70) of re-watering, however the rates of recovery varied between subtypes (Fig. 2.6 & 2.7; Table 2.5 & 2.7 – subtype x day interaction). Photosynthesis (*A*), A/g_{ST} and C_i/C_a recovery rates for NAD-Me species were significantly faster than NADP-Me species, and after three days of re-watering (day 61), NAD-Me species values were significantly higher than the NADP-Me values. NAD-Me species A/g_{ST} and C_i/C_a showed full recovery to control values, whereas *A* had not fully recovered to control values (Fig. 2.6; Table 2.5 – subtype x day interaction), however this recovery in *A* was 65% compared to only 31% of the NADP-Me species. The C_i/C_a values after three days of re-watering equated to a C_i of 108 μmol mol^{-1} CO_2 for NAD-Me species, whereas the NADP-Me species had a corresponding C_i of 208 μmol mol^{-1} CO_2. Stomatal conductance (g_{ST}) recovery rates did not differ between subtypes, and neither had recovered to control values after three days of re-watering (Fig. 2.6 f,h,i; Table 2.5 – subtype x day interaction). This suggested that recovery differences originated from metabolic, not stomatal processes.

PSII operating efficiency (*ΦPSII*), q_P and *ETR* recovery rates were significantly faster for NAD-Me compared to NADP-Me (Fig. 2.7; Table 2.7 – subtype x day interaction). *PSII* maximum efficiency (F_v'/F_m') recovery rates between subtypes were not different, however the mean F_v'/F_m' values at day 61 between subtypes were different (Fig. 2.7 d; Table 2.7 – species nested in subtype).

2.3.7 Leaf gas exchange and chlorophyll fluorescence compared between subfamilies

As observed for the Panicoid subtypes the Aristoid leaf gas exchange parameters (A, g_{ST}) and chlorophyll fluorescence parameters (F_v'/F_m', *ΦPSII*, q_P and *ETR*) also declined exponentially in response to the manipulated soil dehydration, while A/g_{ST} and C_i/C_a showed no decline until a *SWC* threshold of approximately 6.5% (day 42) was reached (Fig.2.4 & 2.5).

The rate of decline for A and g_{ST} was different between subfamilies and the effect of the progressive drought on Aristoid species was only significant at day 56 unlike the Panicoid species which were affected by day 42 (Fig. 2.4 b,c,e & g,h,j; Table 2.6 – subfamily x day interaction). The threshold at which both subfamilies A/g_{ST} and C_i/C_a declined occurred at day 42 (Fig. 2.4 l,m,o & q,s,t; Table 2.6 - subfamily x day interaction). The C_i/C_a values at day 56 equated to a C_i of 364 and 316 μmol mol^{-1} CO_2 for Panicoid and Aristoid species, respectively.

The rate of decline for F_v'/F_m', *ΦPSII*, q_P and *ETR* was different between subfamilies and the effect of the progressive drought on Aristoid species was only significant at day 56 (Fig. 2.5, Table 2.8 – subfamily x day interaction). *PSII* maximum efficiency (F_v'/F_m') was the only parameter for Aristoid species that did not decline to the same value as the Panicoid species at full drought. The decline in F_v'/F_m' was attributable to a decrease in both F_m' and F_o', with Aristoid species showing more of a decline in F_o' at full drought. The less significant decline of Aristoid species F_v'/F_m' at full drought was mainly a result of a 59% decrease in F_v' ($F_m' - F_o'$) relative to the controls, whereas the Panicoid species F_v' decrease was 74%.

The rates of recovery for Aristoid species gas exchange parameters (A, g_{ST}, A/g_{ST}, and C_i/C_a) and chlorophyll fluorescence parameters (F_v'/F_m', *ΦPSII*, q_P and *ETR*) were significantly faster than the Panicoid species. All Aristoid species parameters showed full recovery after three days of re-watering whereas Panicoid species only recovered after 11 days (Fig. 2.6 & 2.7; Table 2.6 & 2.8). Recovery of g_{ST}, and A/g_{ST} were not different (Fig. 2.6, Table 2.6 - subfamily x day interaction), emphasising that photosynthetic recovery was not limited by stomatal recovery, but the metabolic processes of photosynthesis. As a consequence A and C_i/C_a parameters recovered faster in the Aristoid species compared to the Panicoid species (Fig. 2.6, Table 2.6 – subfamily x day interaction).

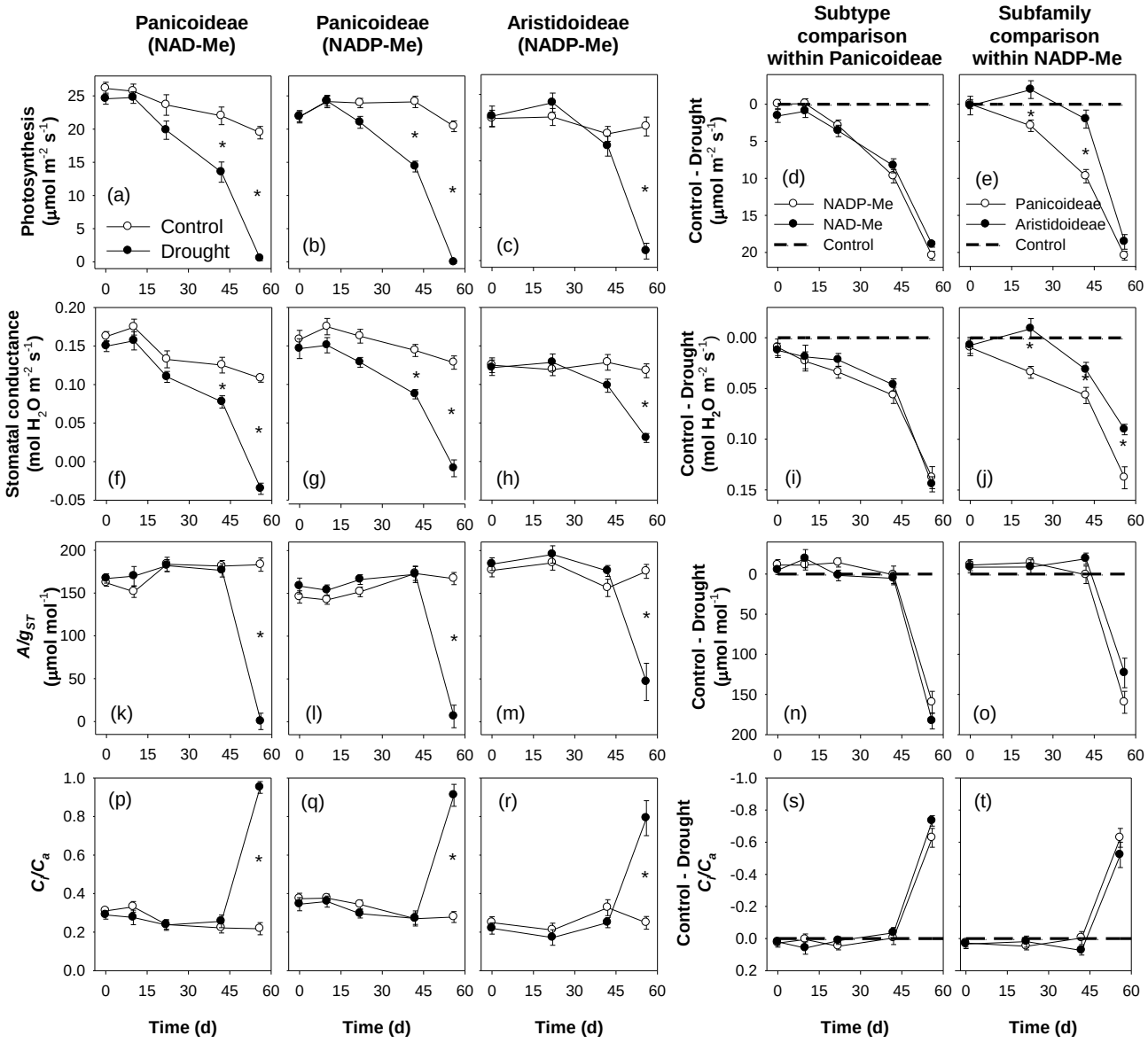

Figure 2.4: Dry-down (a-c) photosynthetic rates (*A*), (f-h) stomatal conductance (g_{ST}), (k-m) water use efficiency (A/g_{st}), and (p-r) C_i/C_a for Panicoideae NAD-Me, Panicoideae NADP-Me and Aristidoideae NADP-Me subfamilies. Control minus drought *A*, g_{ST}, A/g_{ST} *and* C_i/C_a (d,i,n,s) for "subtype comparison within Panicoideae" and (e,j,o,t) for "subfamily comparison within NADP-Me". Asterisk symbol (*) indicates significant differences between treatments and controls at the corresponding days (a-c, f-h, k-m, p-r) and between treatments at the corresponding days (d-e, i-j, n-o, s-t). n= 16–18 for each data point (mean ± SE).

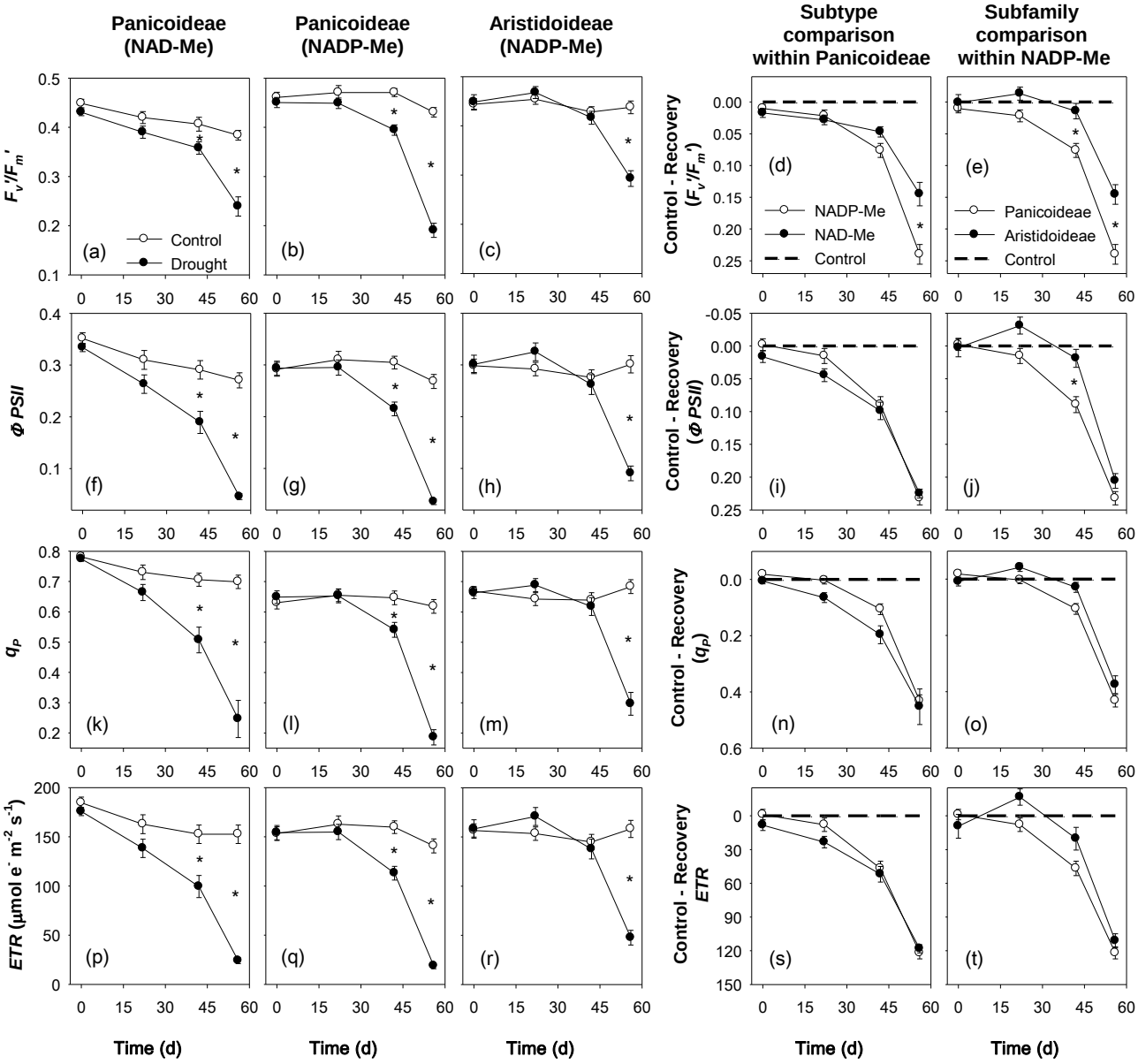

Figure 2.5: Dry-down (a-c) *PSII* maximum efficiency (F_v'/F_m'), (f-h) *PSII* operating efficiency ($\Phi PSII$), (k-m) photochemical quenching (q_P) and (p-r) electron transport rate (*ETR*) for Panicoideae NAD-Me, Panicoideae NADP-Me and Aristidoideae NADP-Me species. Control minus drought F_v'/F_m', $\Phi PSII$, q_P and *ETR* (d,i,n,s) for "subtype comparison within Panicoideae" and (e,j,o,t) for "subfamily within comparison within NADP-Me". Asterisk symbol (*) indicates significant differences between treatments and controls at the corresponding days (a-c, f-h, k-m, p-r) and between treatments at the corresponding days (d-e, i-j, n-o, s-t). n= 16–18 for each data point (mean ± SE).

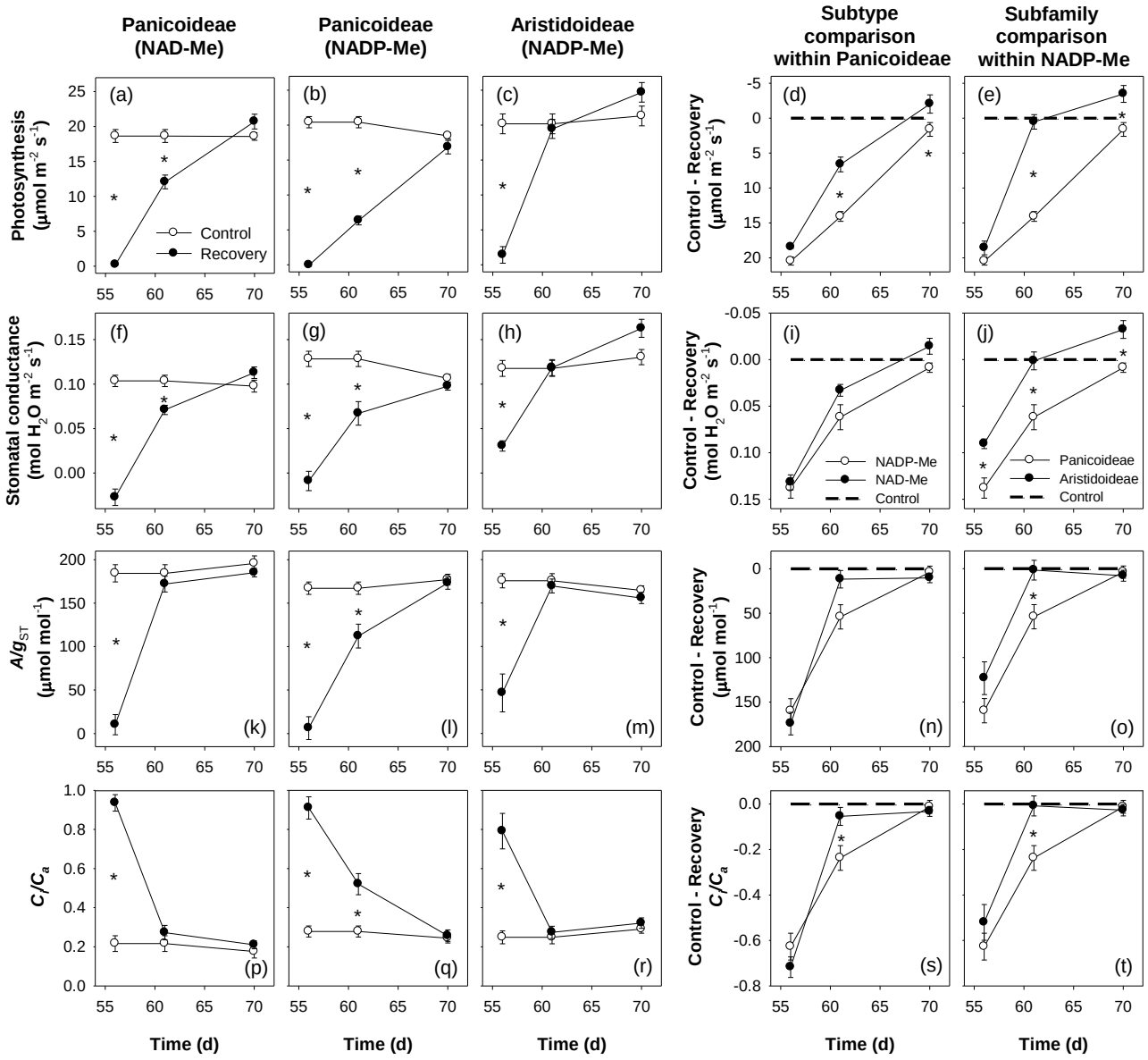

Figure 2.6: Recovery (a-c) photosynthetic rates (*A*), (f-h) stomatal conductance (g_{ST}), (k-m) water use efficiency (A/g_{st}), and (p-r) C_i/C_a for Panicoideae NAD-Me, Panicoideae NADP-Me and Aristidoideae NADP-Me subfamilies. Control minus drought *A*, g_{ST}, A/g_{ST} *and* C_i/C_a (d,i,n,s) for "subtype comparison within Panicoideae" and (e,j,o,t) for "subfamily within comparison within NADP-Me". (*) symbol indicates significant differences between treatments and controls at the corresponding days (a-c, f-h, k-m, p-r) and between treatments at the corresponding days (d-e, i-j, n-o, s-t). n= 12–18 for each data point (mean ± SE).

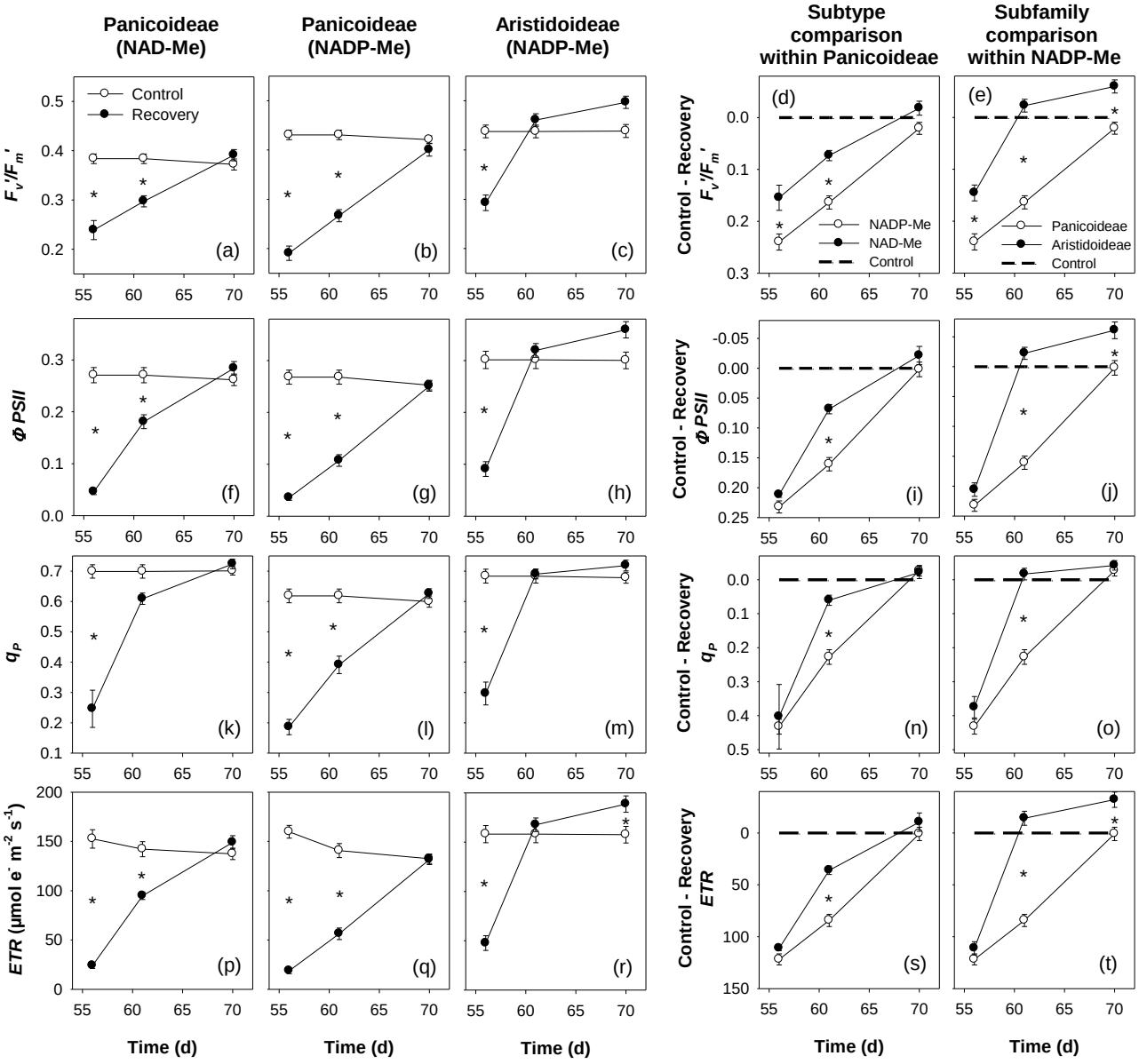

Figure 2.7: Recovery (a-c) *PSII* maximum efficiency (F_v'/F_m'), (f-h) *PSII* operating efficiency (*ΦPSII*), (k-m) photochemical quenching (q_P) and (p-r) electron transport rate (*ETR*) for Panicoideae NAD-ME, Panicoideae NADP-ME and Aristidoideae NADP-ME species. Control minus drought F_v'/F_m', Φ*PSII*, q_P and *ETR* (d,i,n,s) for "subtype comparison within Panicoideae" and (e,j,o,t) for "subfamily within comparison within NADP-Me". (*) symbol indicates significant differences between treatments and controls at the corresponding days (a-c, f-h, k-m, p-r) and between treatments at the corresponding days (d-e, i-j, n-o, s-t). n= 12–18 for each data point (mean ± SE).

Table 2.5: General Linear Model (GLM) results of a comparison of photosynthetic rate (*A*), stomatal conductance (g_{ST}), intrinsic water-use efficiency (A/g_{ST}) and *Ci/Ca* between photosynthetic subtypes (represented as species nested in photosynthetic subtype) in response to decreasing *SWC* (dry-down) and re-watering after drought (recovery). To account for the time effects of the controls in the GLM results, treatments were deducted from the mean of the controls at corresponding days. n.s. (not significant), *= $p < 0.05$, **= $p < 0.01$ and ***= $p < 0.001$.

	Phase	Species	Species x Day	Species (Subtype)	Subtype	Day	Subtype x Day
A	Dry-down	** $F_{5,179}= 3.7$	* $F_{20,179}= 1.7$	** $F_{4,179}= 4.4$	*n.s.* $F_{1,179}= 0.03$	*** $F_{4,179}= 246$	*n.s.* $F_{4,179}= 2$
	Recovery	*** $F_{4,89}= 31$	*** $F_{8,89}= 4.2$	*** $F_{3,89}= 17.7$	*** $F_{1,89}= 59.3$	*** $F_{2,89}= 401$	*** $F_{2,89}= 8.1$
g_{ST}	Dry-down	*n.s.* $F_{5,174}= 1.2$	* $F_{20,174}= 1.8$	*n.s.* $F_{4,174}= 1.4$	*n.s.* $F_{1,174}= 0.48$	*** $F_{4.174}= 76$	*n.s.* $F_{4,174}= 0.45$
	Recovery	* $F_{4,86}= 3.2$	*n.s.* $F_{8,86}= 1.8$	*n.s.* $F_{3,86}= 2.6$	* $F_{1,86}= 5.7$	*** $F_{2,86}= 90$	*n.s.* $F_{2,86}= 0.58$
A/g_{ST}	Dry-down	*n.s.* $F_{5,175}= 1.8$	** $F_{20,175}= 2.1$	*n.s.* $F_{4,175}= 1.7$	*n.s.* $F_{1,175}= 2.3$	*** $F_{4,175}= 161$	*n.s.* $F_{4,175}=0.9$
	Recovery	*n.s.* $F_{4,86}= 2$	* $F_{8,86}= 2.6$	*n.s.* $F_{3,86}= 2.3$	*n.s.* $F_{1,86}= 0.6$	*** $F_{2.86}= 114$	* $F_{2,86}= 3.3$
C_i/C_a	Dry-down	*n.s.* $F_{5,173}= 1.7$	** $F_{20,173}= 2.2$	*n.s.* $F_{4,173}= 1.6$	*n.s.* $F_{1,173}= 1.3$	*** $F_{4,173}= 160$	*n.s.* $F_{4,173}= 14$
	Recovery	*n.s.* $F_{4,84}= 1.8$	** $F_{8,84}= 3.2$	*n.s.* $F_{3,84}= 2$	*n.s.* $F_{1,84}= 0.4$	*** $F_{2,84}= 120$	* $F_{2,84}= 4.8$

Table 2.6: General Linear Model (GLM) results of a comparison of photosynthetic rate (*A*), stomatal conductance (g_{ST}), intrinsic water-use efficiency (A/g_{ST}) and *Ci/Ca* between subfamilies (represented as species nested in subfamily) in response to decreasing *SWC* (dry-down) and re-watering after drought (recovery). To account for the time effects of the controls in the GLM results, treatments were deducted from the mean of the controls at corresponding days. n.s. (not significant), *= $p < 0.05$, **= $p < 0.01$ and ***= $p < 0.001$.

	Phase	Species	Species x Day	Species (Subfamily)	Subfamily	Day	Subfamily x Day
A	Dry-down	*** $F_{5,140}$= 7.4	** $F_{15,140}$= 2.5	* $F_{4,140}$= 2.5	*** $F_{1,140}$=29.2	*** $F_{3,140}$= 176	*** $F_{3,140}$= 6.4
	Recovery	*** $F_{5,104}$= 21	*** $F_{10,104}$= 5.3	** $F_{4,104}$= 4.5	*** $F_{1,104}$= 90.5	*** $F_{2,104}$= 271	*** $F_{2,104}$= 23.3
g_{ST}	Dry-down	*** $F_{5,139}$= 7.8	*n.s.* $F_{15,139}$= 1.7	* $F_{4,139}$= 3	*** $F_{1,139}$= 27.7	*** $F_{3,139}$= 73	* $F_{3,139}$= 3.3
	Recovery	*** $F_{5,104}$= 11	*n.s.* $F_{10,105}$= 1.3	* $F_{4,104}$= 2.5	*** $F_{1,104}$= 43.3	*** $F_{2,104}$= 93.4	*n.s.* $F_{2,104}$= 0.6
A/g_{ST}	Dry-down	* $F_{5,136}$= 2.7	* $F_{15,136}$= 2	* $F_{4,136}$= 2.6	*n.s.* $F_{1,136}$= 3	*** $F_{3,136}$= 107	*n.s.* $F_{3,136}$= 2
	Recovery	* $F_{5,99}$= 2.8	** $F_{10,99}$= 3.1	*n.s.* $F_{4,99}$= 1	** $F_{1,99}$= 7.3	*** $F_{2,99}$= 74.5	*n.s.* $F_{2,99}$= 2.9
C_i/C_a	Dry-down	* $F_{5,133}$= 2.8	* $F_{15,133}$= 2	* $F_{4,133}$= 2.5	*n.s.* $F_{1,133}$= 2	*** $F_{3,133}$= 106	*n.s.* $F_{3,133}$= 1.2
	Recovery	* $F_{5,96}$= 3.1	*** $F_{10,\ 133}$= 3.4	*n.s.* $F_{4,96}$= 1.2	* $F_{1,96}$= 6	*** $F_{2,96}$= 72.5	* $F_{2,96}$= 3.2

Table 2.7: General Linear Model (GLM) results of a comparison of *PSII* maximum efficiency (F_v'/F_m'), *PSII* operating efficiency (*ΦPSII*), photochemical quenching (q_P) and electron transport rate (*ETR*) between

photosynthetic subtypes (represented as species nested in photosynthetic subtype) in response to decreasing *SWC* (dry-down) and re-watering after drought (recovery). To account for the time effects of the controls in the GLM results, treatments were deducted from the mean of the controls at corresponding days. n.s. (not significant), *= $p < 0.05$, **= $p < 0.01$ and ***= $p < 0.001$.

	Phase	Species	Species x Day	Species (Subtype)	Subtype	Day	Subtype x Day
F_v'/F_m'	Dry-down	*** $F_{5,142}$= 4.9	*** $F_{15,142}$= 3.5	*n.s.* $F_{4,142}$= 2.4	*** $F_{1,142}$= 13.3	*** $F_{3,142}$= 142	*** $F_{3,142}$= 9.8
	Recovery	*** $F_{4,88}$= 16.6	*n.s.* $F_{8,88}$= 1.5	*** $F_{3,88}$= 7.4	*** $F_{1,88}$= 43	*** $F_{2,88}$= 104	*n.s.* $F_{2,88}$= 2.4
ΦPSII	Dry-down	*** $F_{5,142}$= 4.7	* $F_{15,142}$= 2	** $F_{4,142}$= 4.5	*n.s.* $F_{1,142}$= 3	*** $F_{3,142}$= 199	*n.s.* $F_{3,142}$= 1.3
	Recovery	*** $F_{4,88}$= 27	*** $F_{8,88}$=4.3	*** $F_{3,88}$= 20.8	*** $F_{1,88}$= 41	*** $F_{2,88}$= 342	*** $F_{2,88}$= 10.5
q_P	Dry-down	*n.s.* $F_{5,142}$= 1.7	*n.s.* $F_{15,142}$= 1.7	*n.s.* $F_{4,142}$= 0.38	* $F_{1,142}$= 6	*** $F_{3,142}$= 101	*n.s.* $F_{3,142}$= 0.7
	Recovery	*n.s.* $F_{4,88}$= 1.4	*n.s.* $F_{8,88}$= 1.5	*n.s.* $F_{3,88}$= 0.4	* $F_{1,88}$= 4.9	*** $F_{2,88}$= 78.7	* $F_{2,88}$= 3.4
ETR	Dry-down	** $F_{5,142}$= 4.67	*n.s.* $F_{15,142}$= 1.9	** $F_{4,142}$= 4.4	*n.s.* $F_{1,142}$= 3.1	*** $F_{3,142}$= 199	*n.s.* $F_{3,142}$= 1.28
	Recovery	*** $F_{4,88}$= 27	*** $F_{8,88}$= 4.3	*** $F_{3,88}$= 20.6	*** $F_{1,88}$= 39.8	*** $F_{2,88}$= 330	*** $F_{2,88}$= 10.1

Table 2.8: General Linear Model (GLM) results of a comparison of *PSII* maximum efficiency (F_v'/F_m'), *PSII* operating efficiency (*ΦPSII*), photochemical quenching (q_P) and electron transport rate (*ETR*) between subfamilies (represented as species nested in subfamily) in response to decreasing *SWC* (dry-down) and re-

watering after drought (recovery). To account for the time effects of the controls in the GLM results, treatments were deducted from the mean of the controls at corresponding days. n.s. (not significant), *= $p < 0.05$, **= $p < 0.01$ and ***= $p < 0.001$.

	Phase	Species	Species x Day	Species (Subfamily)	Subfamily	Day	Subfamily x Day
F_v'/F_m'	Dry-down	*** $F_{5,138}$= 13.7	*** $F_{15,138}$= 3	*** $F_{4,138}$= 5.6	*** $F_{1,138}$= 41.2	*** $F_{3,138}$= 125	** $F_{3,138}$= 5.4
	Recovery	*** $F_{5,104}$= 33.8	** $F_{10,104}$= 3.2	*** $F_{4,104}$= 5.6	*** $F_{1,104}$= 141.4	*** $F_{2,104}$= 149.5	*** $F_{2,104}$= 11
ΦPSII	Dry-down	*** $F_{5,138}$= 7.1	* $F_{15,138}$= 2.2	** $F_{4,138}$= 3.7	*** $F_{1,138}$= 19	*** $F_{3,138}$= 167	* $F_{3,138}$= 3.7
	Recovery	*** $F_{5,104}$= 27.1	*** $F_{10,104}$= 6.4	*** $F_{4,104}$= 6.6	*** $F_{1,104}$= 112	*** $F_{2,104}$= 282	*** $F_{2,104}$= 30
q_P	Dry-down	* $F_{5,138}$= 2.6	*n.s.* $F_{15,138}$= 1.1	*n.s.* $F_{4,138}$= 1.2	** $F_{1,138}$= 8.3	*** $F_{3,138}$= 216	* $F_{3,138}$= 2.8
	Recovery	*** $F_{5,104}$= 9.2	*** $F_{10,104}$= 4.1	*n.s.* $F_{4,104}$= 1.7	*** $F_{1,104}$= 40.9	*** $F_{2,104}$= 235	*** $F_{2,104}$= 17.8
ETR	Dry-down	*** $F_{5,138}$= 3.1	*n.s.* $F_{15,138}$= 1.5	*n.s.* $F_{4,138}$= 2.1	* $F_{1,138}$= 6.4	*** $F_{3,138}$= 114	* $F_{3,138}$= 2.8
	Recovery	*** $F_{5,104}$= 23.8	*** $F_{10,104}$= 6.3	*** $F_{4,104}$= 5.8	*** $F_{1,104}$= 98	*** $F_{2,104}$= 262	*** $F_{2,104}$= 30.3

2.3.8 Individual species responses

Leaf water relations, gas exchange and cholorophyll fluorescence GLM comparisons between subtypes and subfamilies (species nested in subtype/subfamily) were effective as individual species

within photosynthetic subtypes responded to progressive drought and drought recovery with little variablity (Fig. 2.8, 2.9, 2.10). The major exception was *P. virgatum* (Fig. 2.8, 2.9, 2.10) which showed signs of leaf senescence at full drought and subsequently did not recover to pre-drought status for another six months. *A. semialata* maintained high Ψ_{leaf} at day 42 compared to the low Ψ_{leaf} of *H. contortus and T. leucothrix* from the same group (Fig. 2.8 d,e,f).

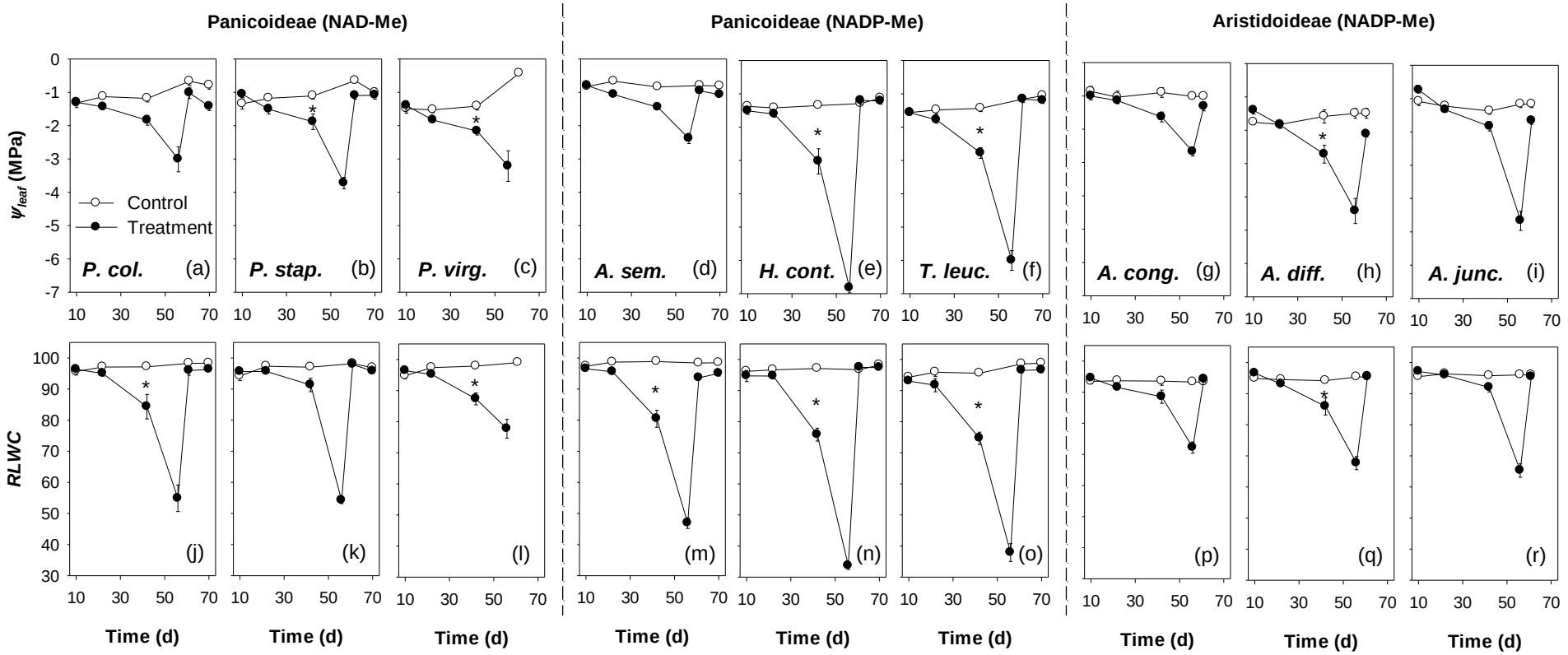

Figure 2.8: (a-i) Leaf water potential (Ψ_{leaf}) and (j-r) relative leaf water content (*RLWC*) for the dry-down and recovery phase of the experiment for all the species. n= 4–6 for each data point (mean ± SE) and asterisks symbol (*) indicates significant differences between treatments and controls at the corresponding days. All treatments at day 56 were compared to the controls at day 61 and are significantly different. Plants were re-watered at day 58.

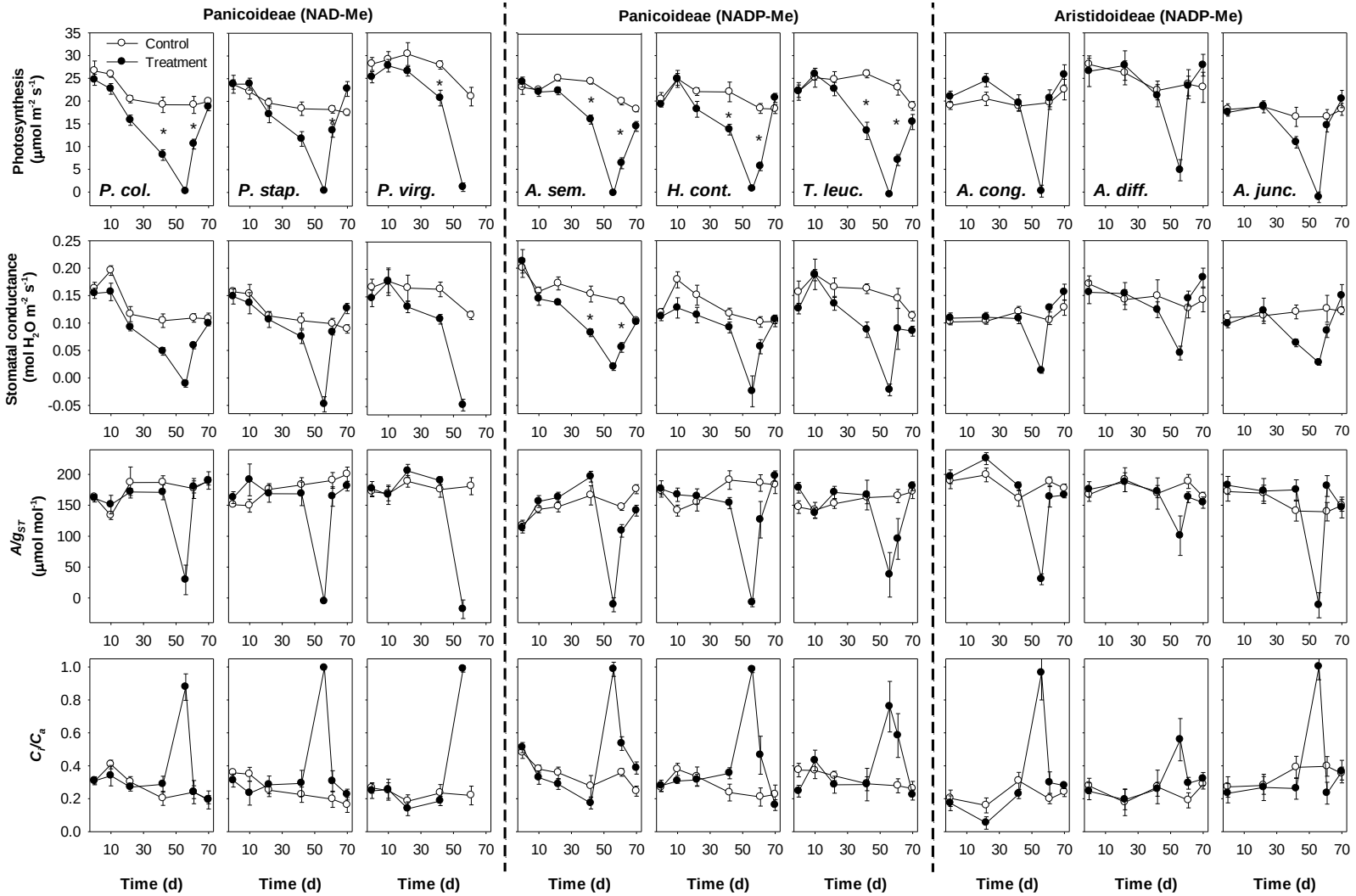

Figure 2.9: Gas exchange dry-down and recovery parameters A, g_{ST}, A/g_{ST} and C_i/C_a for species grouped by subtype/subfamily. n= 4–6 for each data point (mean ± SE) and asterisks symbol (*) indicates significant differences between treatments and controls at the corresponding days. All treatments at day 56 were compared to the controls at day 61 and are significantly different. Plants were re-watered at day 58.

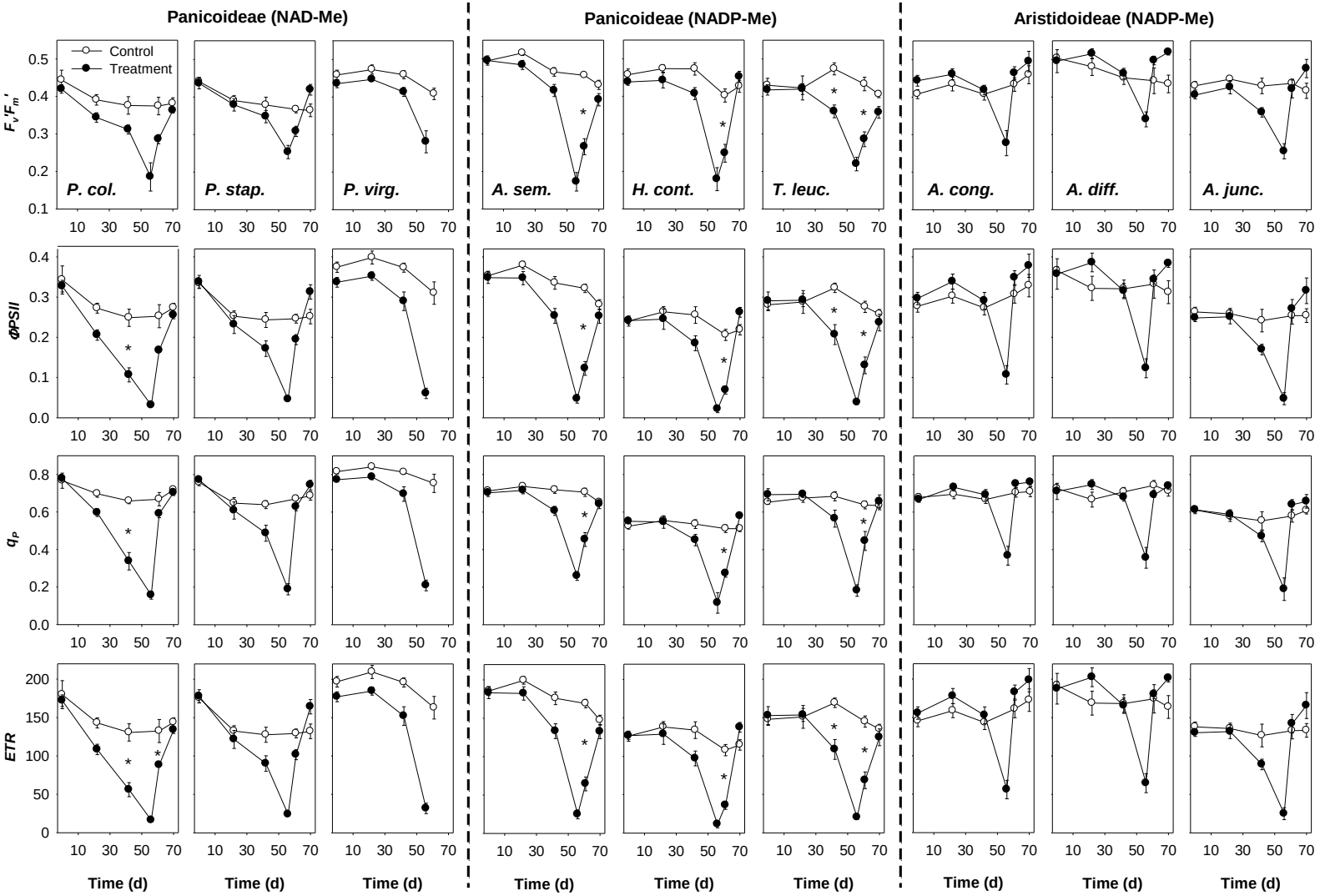

Figure 2.10: Chlorophyll fluorescence dry-down and recovery parameters F_v'/F_m', *ΦPSII*, q_P *and ETR* for species grouped by subtype/subfamily. n= 4–6 for each data point (mean ± SE) and asterisks symbol (*) indicates significant differences between treatments and controls at the corresponding days. All treatments at day 56 were compared to the controls at day 61 and are significantly different. Plants were re-watered at day 58.

2.3.9 *RLWC* correlations

The rate of photosynthetic (*A*) recovery was correlated to the extent to which leaves were dehydrated during the progressive drought and to light reaction performance (Fig. 2.11). Species that maintained higher *RLWC* and F_v'/F_m' values showed the fastest *A* recovery and *visa- versa*. Plants that maintained higher *RLWC* during the drought also showed higher F_v'/F_m' values at severe drought (Fig. 2.12). This was an indication that less dehydrated leaves likely maintained light reaction integrity, and photosynthesis subsequently recovered faster upon re-watering. These correlations showed a strong subtype/subfamily response, where the three groups showed distinct clustering at different positions on the regression. *Panicum virgatum* was an outlier (Fig 2.11), as it maintained high *RLWC* and F_v'/F_m' values during drought but did not recover.

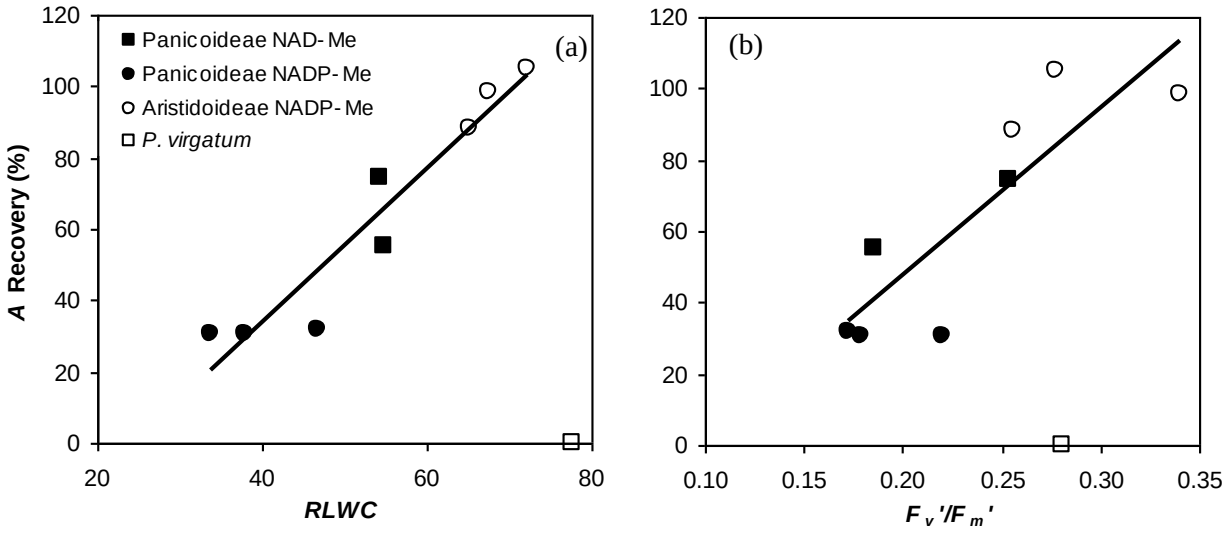

Figure 2.11: Recovery of photosynthesis (*A*) after three days of re-watering related to (a) the relative leaf water content (*RLWC*) and (b) *PSII* maximum efficiency (F_v'/F_m') after 56 days of drought (~3.5% *SWC*). Regression stats (a); (R^2= 0.126, p< 0.350), excluding *Panicum virgatum* (R^2= 0.906, p< 0.0004) and (b); (R^2= 0.26, p< 0.17), excluding *P. virgatum* (R^2= 0.73, p< 0.007) Species are grouped by subfamily and subtype and *P. virgatum* is indicated by (□) symbol.

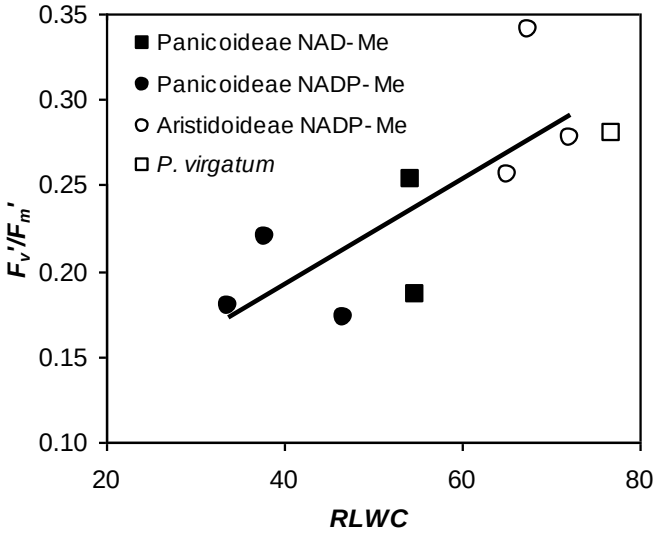

Figure 2.12: *PSII* maximum efficiency (F_v'/F_m') after 56 days of drought (~3.5% *SWC*) related to the *RLWC* on the same day. Regression stats; (R^2= 0.57, p< 0.019), excluding *P. virgatum* (R^2= 0.558, p< 0.034). Species are grouped by subfamily and subtype and *P. virgatum* is indicated by (□) symbol. Abbreviation: relative leaf water content (*RLWC*).

2.4 Discussion

The response of the Aristoid species supported the hypothesis that this subfamily was the most tolerant of progressive drought. However contrary to the photosynthetic subtype hypothesis, the response to progressive drought was not different between Panicoideae NAD-Me and NADP-Me subtypes. Conversely, drought recovery results showed a photosynthetic and subfamily interaction. Panicoideae NAD-Me and Aristidoideae NADP-Me subtypes recovered from the progressive drought significantly faster than the Panicoideae NADP-Me subtypes.

The decline in *A* and associated parameters for all groups responded in a similar manner as the C_4 grass species from Ripley *et al.* (2010), but there was variability in these responses. The *A* decline in response to drought for the Panicoid and Aristoid species could initially be attributed to the steady decline in g_{ST}. This supported what Lawlor (2002) reviewed, that as *RLWC* drops g_{ST} declines so does associated *A* but after a certain *RLWC* the decline in *A* could be attributed to non-stomatal effects. Treatment A/g_{ST} ratios remained the same as the controls which indicated the rate of *A* decline was equal to the rate of decline in $g_{ST.}$ However at 6.5% *SWC* (day 42), a threshold was encountered where the decline in A/g_{ST} ratio increased significantly, indicating that *A* and g_{ST} had fallen to near zero. At this threshold, C_i increased to a concentration similar to that of ambient air. This indicated that the rapid decline in *A* beyond this threshold was a non-stomatal (metabolic) effect and that intercellular

CO_2 was no longer being assimilated via photosynthesis. The Aristoid NADP-Me response to drought was less rapid than that of the Panicoid NADP-Me subtype, but at full drought (~3.5% *SWC*) the photosyntheic rate was not dissimilar between subfamilies. Although Aristoid NADP-Me species also experienced the same threshold from day 42, this was less severe than the Panicoid NADP-Me species, inidcating that in the Aristoid species photosynthetic metabolism was less affected by drought.

Chlorophyll flourescence parameters measured showed trends similar to the photosynthetic gas exchange reponses during the advanced stages of drought, with the exception of *PSII* maximum efficiency (F_v'/F_m'). The reduction in *PSII* operating efficiency ($\Phi PSII$) and photochemical quenching (q_P) with drought was a result of decreased photochemistry, due to photosynthetic down-regulation. The down-regulation of photosynthesis likely decreased the reduction potential of the quinine acceptor (Q_A) and light energy was dissipated as heat (Baker, 2008). The plants' F_v'/F_m' response to drought was attributed to reductions of F_m' and F_o'. All groups showed similar reductions in F_m', which was associated with a reduction in photochemistry and heat dissipation. F_o' decreased for all the groups which was also an indication of increased heat dissipation, possibly associated with the xanthophyll cycle, whereas an increase in F_o' is generally interpreted as a dissociation of the light harvesting complex of *PSII* reaction centres and subsequent degradation (Armond *et al.,* 1980; Efeoğlu *et al.*, 2009). The lower F_o' values of the Panicoid NAD-Me and Aristoid species could have indicated increased heat dissipation via the xanthophyll cycle, resulting in less impaired *PSII*. The higher F_v'/F_m' values for the Panicoid NAD-Me and Aristoid NADP-Me species indicated less compromised *PSII*, and their ability to maintain photochemistry performance under severe drought and this was likely linked to maintenance of higher *RLWC*.

Panicoideae NAD-Me and Aristoid NADP-Me species photosynthetic rate recovered from the progressive drought significantly faster than the Panicoideae NADP-Me species. This photosynthetic recovery from drought was correlated to the maintenance of leaf water status and higher F_v'/F_m' values during the drought (Fig. 2.11). During the progressive drought, Panicoideae NAD-Me and Aristidoideae NADP-Me species maintained higher *RLWC* compared to Panicoideae NADP-Me species. High *RLWC* was not maintained by differences in stomatal conductance (g_{ST}) but by different Ψ_{leaf} (R^2= 0.34; removal of the outlier *A. semialata*, R^2= 0.65, data not shown), as the Panicoid species showed no stomatal response differences during drought. Plants that maintained higher *RLWC* also had higher Ψ_{leaf}, indicating an additional mechanism such as osmotic adjustment (*OA*). Between the NADP-Me species, Aristoid species maintained significantly higher g_{ST} and *RLWC* during drought.

The correlation of *RLWC* to F_v'/F_m' at severe drought (~3.5% *SWC*) showed that higher F_v'/F_m' values were associated with higher *RLWC* (Fig. 2.12). By maintaining *PSII* integrity during drought,

Panicoid NAD-Me and Aristoid NADP-Me species could recover faster upon re-watering (Fig. 2.11 b). *Panicum virgatum* however, maintained high *RLWC* and F_v'/F_m' during drought but senescenced its leaves under extreme drought conditions. This supported the findings of Barney *et al.,* (2009) that showed when exposed to *SWC* of ~3% *P. virgatum* did not recover and showed marked leaf senescence.

Results further confirmed that the slower rate of recovery for Panicoideae NADP-Me species in contrast to Panicoideae NAD-Me and Aristoid NADP-Me species was of a metabolic origin. This was evident from the C_i/C_a ratio after three days of re-watering, which showed that Panicoid NAD-Me and Aristoid NADP-Me species treatments C_i/C_a values were the same as the control values. Conversely, Panicoid NADP-Me C_i/C_a ratios remained high, but there was no stomatal limitation as g_{ST} values were no different to those of the NAD-Me species. This is an indication that Panicoid NADP-Me species were unable to utilise the available intercellular CO_2, indicating that the light reactions were compromised by leaf dehydration, supporting the findings of Saccardy *et al.,* (1998) who showed for *Z. mays* that *PSII* efficiency was negatively affected at a *RLWC* below 60%.

The loss of photosynthetic metabolism at a distinct threshold suggests that once soil water potential declines sufficiently the plants are no longer able to source water, and dramatic metabolic perturbations ensue. Maintaining higher *RLWC* and a favourable soil to leaf water potential gradient via osmotic adjustment would counteract this, allowing for the maintenance of leaf turgor. This may be important for maintaining the continuum between mesophyll and bundle sheath cells and the transfer of metabolites via plasmodesmata, whose function is known to require positive turgor pressure (Clifford *et al.,* 1998, Jones and Corlett 1992). To further investigate the role of metabolic limitations and the relationship to turgor loss, *Z. mays* (Panicoid NADP-Me) was used as a model species in Chapter 3 to conduct rapid drought experiments.

These results offer a mechanistic explanation of why biogeographic distribution patterns of grass subfamilies are evident in southern Africa, and are related to drought. The mechanism whereby Aristoid species, which tolerate more severe drought and recover faster on re-watering, could explain why the Aristoid subfamily in general are distributed in the more xeric regions of southern Africa (Visser *et al.,* 2012; 2014). Research indicates that NAD-Me photosynthetic subtypes also have a preference for more xeric environments (Ellis *et al*., 1980; Vogel *et al.,* 1986; Taub, 2000; Cabido *et al.,* 2008), but it is suggested that this response is complicated by phylogeny, due to the oversampling of Chloridoideae NAD-Me species. These progressive drought results support the idea that the association to rainfall gradients are stronger amongst subfamilies compared to C_4 photosynthetic subtype (Taub, 2000). The photosynthetic recovery from drought supports the idea that differences in

physiological traits of photosynthetic subtype offer competitive advantages under different ecological conditions (Sage and Monson, 1999).

Chapter 3

Turgor loss as a mechanism for metabolic limitation: Developing a model system using *Zea mays*

3.1 Introduction

Partitioning of the photosynthetic enzymes between the mesophyll (MC) and bundle sheath cells (BSC) requires the intercellular transport of metabolites (Wang *et al.,* 2014). Some of these metabolites include the C_4 acids (malate and aspartate) and the C_3 acids (pyruvate and alanine). If photosynthesis is to operate efficiently, a large volume of these metabolites are required to move rapidly between these cells (Bilska and Sowiński, 2010). This intercellular transport of metabolites is generally performed via apoplastic and/or symplastic processes. Apoplastic transport is the movement between plasma membranes (cell walls) whereas symplastic transport is the movement between the cytoplasm of the neighbouring cells via plasmodesmata. Transport of the metabolites along the plasmodesmata are achieved mainly through diffusive processes (symplastic) which are maintained by concentration gradients between MC and BSC, and the diffusive permeability is further governed by the Stokes radius of molecules (Ohnishi *et al.,* 1990; Leegood, 2000; Roberts and Oparka, 2003). It was suggested by Sowiński (2008) that the transfer of metabolites between the MC and BSC in C_4 photosynthesis can not be adequately explained by simple-diffusion processes, however the hypothesised alternatives have not been experimentally shown.

It has been proposed that metabolic processes are more sensitive to changes in turgor and cell volume than absolute water potential, as cells need to maintain structural integrity since intermolecular distances are critical for metabolic activity (Clifford *et al.,* 1998, Jones and Corlett 1992). It has been suggested that changes in turgor pressure can cause plasmodesmata to act as pressure sensitive valves (Oparka and Prior, 1992). A decrease in plasmodesmata number and conductivity can disrupt the metabolite pathway and have noticeable effects on C_4 photosynthetic metabolism (Sowiński *et al.,* 2008) as the number of plasmodesmata show a positive correlation to net photosynthetic rate found in various C_4 grasses (Sowiński *et al.,* 2007). Plasmodesmata are also important for the export of photosynthetic products and sucrose in *Z. mays,* and export is slowed if plasmodesmata at the BSC/VP (vascular parenchyma) interface are blocked by callose polysaccharides (Botha *et al.,* 2000). Turgor loss and the subsequent plasmolysis can lengthen/stretch plasmodesmata and thereby decrease the diameter which can restrict metabolite movement (Robinson-Beers and Evert, 1990; Sowiński *et al.,* 2007). Plasmolysis can also be destructive, such that as it worsens, cellular membranes crack at the plasmodesmata level (Gonzalez and Rogers, 2003). These effects on the plasmodesmata are

expected to develop at the threshold where cell turgor is lost, thereby affecting photosynthetic processes. Bilska and Sowiński (2010) showed that low temperatures inhibited photosynthesis in two *Z. mays* lines. Low temperatures affected transport between the BS and MS cells due to swelling at the either ends of the plasmodesmata, which restricting metabolite diffusion. Findings like these support our hypothesis that water stress may affect C_4 photosynthetic metabolism due to reduced metabolite diffusion from damage or structural changes to the plasmodesmata as result of turgor loss.

Photosynthesis (*A*) and stomatal responses (g_{ST}) in C_4 species have been shown to be sensitive to leaf water contents below ~90% with *A* and g_{ST} progressively declining to zero at the same rate, when leaf water contents decreased to ~60%. (Saccardy *et al.,* 1996; Ghannoum, 2003). Saccardy *et al.,* (1996) concluded that this decline in *A* for *Z. mays* was mainly attributed to drought induced decreases in stomatal conductance, and not metabolic limitations, as elevated CO_2 restored *A* of water stressed leaves. These findings are however in contrast to the findings of Ghannoum, (2003), who concluded that the decline in *A* of four C_4 species of grasses was of metabolic origin. Various drought studies on C_4 species have since shown that the response of *A* to water stress is mainly attributed to metabolic and not stomatal limitations (Carmo-Silva *et al.,* 2010; Ripley *et al.,* 2007, 2010). The mechanisms whereby water stress affects photosynthetic metabolism in C_4 grasses are yet to be fully elucidated as metabolic impairment theories differ (Ghannoum, 2009; Lawlor and Tezara, 2009). As C_4 photosynthesis requires the symplastic transport of metabolites between the MC and BSC, damage or modification to the plasmodesmata could result in negative effects on the C_4 photosynthetic metabolism. Based on the research of the effects of water stress on plasmodesmata discussed here, turgor pressure loss in C_4 plants may impair plasmodesmata function, and this turgor loss threshold could initiate the onset of metabolic limitations.

The aims of this chapter were to determine for *Z. mays*; (1) if metabolic and not stomatal limitations are responsible for the majority decrease in photosynthesis during severe drought and (2) if metabolic limitations (photosynthesis) are initiated once the leaves lose positive turgor pressure?

3.2 Materials and methods

3.2.1 Method rationale

To test whether C_4 photosynthetic metabolism was affected at the turgor loss threshold, *Z. mays* was used as a model species, as it is well represented in the literature and it can be rapidly cultivated from seed. The rationale was to induce drought of a range of severities and to assess stomatal and non-

stomatal limitations of photosynthesis, before destructively sampling leaves to determine relative leaf water contents (*RLWC*)**.** Rather than construct complete CO_2 response curves, stomatal and non-stomatal limitations were determined by making leaf gas exchange measurements, one at ambient CO_2 (400 μmol mol^{-1}) and then repeated at saturating CO_2. Additional leaves were used to construct pressure-volume curves which allowed components of leaf water potential (osmotic and turgor) potential to be determined across a range of *RLWC*. These were then used to derive water (Ψ_{leaf}), osmotic (Ψ_{π}) and turgor (Ψ_{P}) potentials for control and drought treated leaves based on their relative leaf water contents.

3.2.2 Plant material, gravimetric soil water content and soil water potential

A single *Zea mays* L. (Kalahari cultivar) seed was sown per pot containing 2.5 Kg of a homogenous soil mixture. Plant were grown in the same polythene tunnel used in Chapter 2 and soil water content (*SWC*) for the potted plants were calculated according to the methods used in Chapter 2.

The relationship between soil water potential (Ψ_{soil}) and *SWC* was determined for the topsoil used for potting plants. Oven dried soil (70°C for 48 hours) was mixed with water to prepare soils of known *SWC*. Subsamples of this soil were placed in triplicate glass vials each with a calibrated soil psychrometer. Vials were sealed and left in a temperature controlled environment for a minimum of 48 hours. Subsequent water potential measurements were made using a Wescor HR-33T microvolt meter and *SWC* was correlated to Ψ_{soil} using a hyperbolic function (y = a+b/x) using CurveExpert© (Version 1.4, Daniel Hyams).

3.2.3 Pressure-volume curves

Pressure volume (PV) curves were constructed by determining the relationship between relative leaf water content (*RLWC*) and leaf water potential (Ψ_{leaf}). This was done by sequentially dehydrating leaves and determining Ψ_{leaf} and *RLWC* at regular intervals. Initially well-watered potted rooted plants were bagged overnight to ensure the leaves reached full turgor potential. For 11 replicate plants, the fully expanded second or third leaf produced after the cotyledon was excised, weighed, and the corresponding Ψ_{leaf} was obtained by using the Schőlander pressure chamber. Subsequent leaves were allowed to slowly dehydrate in a humidified bell jar and Ψ_{leaf} and *RLWC* were measured at repeated intervals. *RLWC* was calculated according to the following formula:

$$RLWC = \frac{leaf\ wet\ mass - leaf\ dry\ mass}{leaf\ turgor\ mass - leaf\ dry\ mass} \times 100$$

To determine individual components of leaf water potential ($\Psi_{leaf} = \Psi_P + \Psi_\pi$) at any *RLWC*, the reciprocal of the Ψ_{leaf} was plotted against *RLWC*, and a model was fitted to the data using the equations of Schulte and Hinckley (1985) (Figure 3.1). Turgor potential (Ψ_P) was calculated according to Figure 3.1 and the turgor loss point (*TLP*) values, expressed as *RLWC* and Ψ_{leaf} were determined where Ψ_P= 0 MPa.

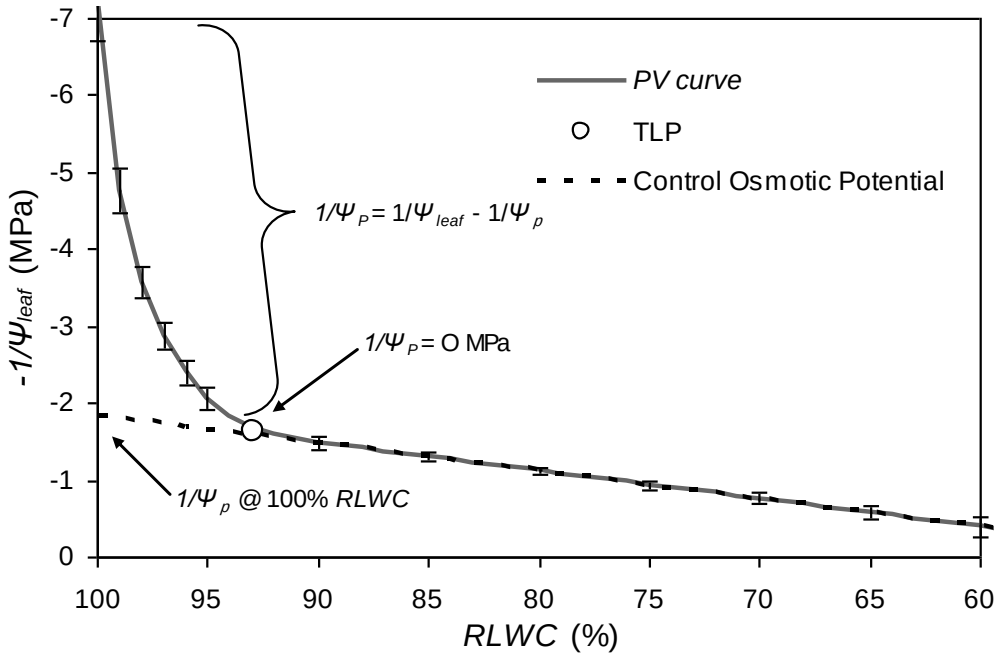

Figure 3.1: Control *Z. mays* pressure-volume curve (——) with SE bars plotted using the equations of Schulte and Hinckley (1985). The curvilinear portion indicates the effect of osmotic (Ψ_π) and turgor (Ψ_P) potential and the straight line (– – and ——) represents the osmotic potential (Ψ_π). The turgor loss point (*TLP*) is denoted by the open circle (O) and this is where Ψ_P = 0 MPa. Turgor potential (Ψ_P) is calculated by subtracting Ψ_π from Ψ_{leaf}. Abbreviation: relative leaf water content (*RLWC*).

3.2.4 Rapid drought protocol

A rapid drought protocol was developed to investigate the relationship between turgor loss and metabolic limitation. The relationship between *SWC* to *RLWC* showed that decreases in *RLWC* were only evident once the *SWC* had decreased below 8% (Results, Fig. 3.4 a). Hence water was withheld from replicate plants such that a range of decreasing *RLWC* was attained. This dehydration protocol was initiated with batches of 23 replicate plants from which water was withheld, starting on successive days to ensure a regular supply of plants of differing *RLWC* for assessing metabolic limitation.

3.2.5 Metabolic and stomatal limitation measurements

Leaf CO_2 and H_2O gas exchange parameters were measured on the second or third fully expanded leaf developed after the cotyledon, using a Li-Cor 6400 photosynthesis system with a blue–red LED light source (LI-6400; Li-Cor, Inc., Lincoln, NE, USA). Conditions in the cuvette were maintained as follows: leaf temperature was set at 29ºC, *VPD* at < 2.3 KPa and *PPFD* of 1200 µmol m^{-2} s^{-1} (97.4% of saturation, S.E. ± 0.31, n=3). Spot gas exchange measurements were performed instead of entire CO_2 response curves, as the literature indicated that A_{max} saturated at a C_i of approximately 400 µmol mol^{-1} under normal and water stress conditions (Naidu and Long, 2004; Markelz *et al*., 2011). Pre-drought photosynthetic measurements were made at ambient and elevated CO_2 concentrations on the same section of leaf area. Where possible, CO_2 concentrations were elevated such that the leaf intercellular CO_2 concentration (C_i) was maintained at approximately 400 µmol mol^{-1}. Measurements were repeated after three to four days of drought when *SWC* had declined to ≤ 13%, and leaves were also excised at this point (the leaf area that was inserted in the cuvette) to determine *RLWC*. The wet mass of the excised leaf portion was obtained and placed in a vial containing water that just covered the excised end of the leaf for four hours to allow the leaf to rehydrate and attain full turgidity. Using the *RLWC* calculated from the experimental plants, the corresponding leaf water potential components (Ψ_{leaf}, Ψ_{π} and Ψ_P) were derived from the PV curve (Fig. 3.4). The same procedure was followed for controls plants except under well-watered conditions (~16% *SWC*).

Photosynthetic parameters were calculated according to von Caemmerer and Farquhar (1981). Stomatal limitation of photosynthesis (S_L) was calculated according to Farquhar and Sharkey (1982), showing the effect of stomata on photosynthesis for drought stressed plants. Relative metabolic limitations (R_{ML}) were calculated according to Figure 3.2 which explained effects of the drought relative to the initial measurements on the well-watered plants.

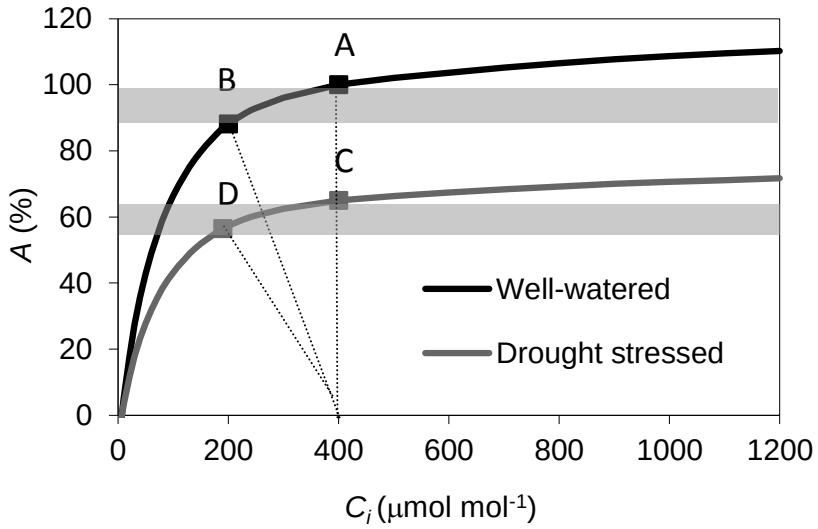

Figure 3.2: Calculation of stomatal limitation (S_L) and relative metabolic limitation (R_{ML}). The two lines represent hypothetical CO_2 response curves (A:C_i) for well-watered and drought stressed leaves. For the well-watered leaf S_L = [((A - B) / A) x 100] where A is the photosynthetic rate corresponding to a C_i of 400 μmol m^{-2} s^{-1} CO_2 (infinite g_{st}) and B is the photosynthetic rate corresponding to a C_i at finite g_{st} (ambient CO_2). For the drought treatment S_L = [((C - D) / C) x 100]. The R_{ML} for the well-watered leaf is by definition = 0. For the drought stressed leaf R_{ML} = [(A – C) / A) x 100]. The shaded areas indicate stomatal limitations for each curve (Ripley *et al.*, 2007). Abbreviations: intercellular CO_2 concentration (C_i), photosynthetic rate (A).

3.2.6 Statistics and model fitting

Coefficient of determination (R^2) and p-values were determined for the linear and non-linear regressions of R_{ML} and S_L to declining *RLWC*, Ψ_{leaf} and Ψ_P. Controls were treated independently as these plants did not experience a water deficit. Values of R_{ML} and S_L were compared using a one-way ANOVA, while differences in C_i values were compared using Student *t*-tests. All statistics were performed using Statistica© (Version 10, StatSoft, Inc) except best fit models were fitted using CurveExpert© (Version 1.4, Daniel Hyams).

3.3 Results

3.3.1 Pressure-volume curve

The leaf water potential parameters for fully hydrated *Z. mays* leaf tissue (100% *RLWC*) were as follows: Ψ_{leaf} = -0.136 MPa (SE ± 0.065), Ψ_{π} = -0.567 MPa (SE ± 0.034) and Ψ_P = 0.424 MPa (SE ± 0.029). Ψ_P = 0 MPa (*TLP*) at a *RLWC* of 92.9% (SE ± 0.46) and a corresponding Ψ_{leaf} of -0.652 MPa (SE ± 0.084) (Fig. 3.3).

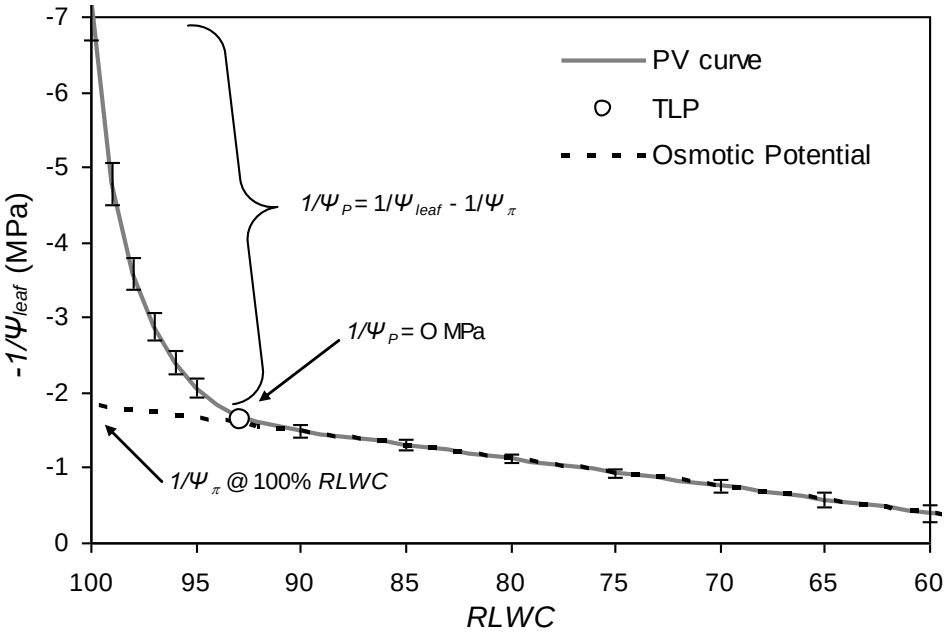

Figure 3.3: Pressure-volume curve (——) constructed for *Z. mays* (n= 11) with SE bars using the equations of Schulte and Hinckley (1985). The curvilinear portion indicates the effect of osmotic (Ψ_{π}) and turgor (Ψ_P) potential and the straight line (– – and ——) represents the osmotic potential (Ψ_{π}). Turgor loss point (*TLP*) is denoted by the open circle (O) and this is where Ψ_P = 0 MPa. Turgor potential (Ψ_P) is calculated by subtracting Ψ_{π} from Ψ_{leaf}. Abbreviation: relative leaf water content (*RLWC*).

3.3.2 Soil and leaf water parameters

Mean soil water content (*SWC*) and Ψ_{soil} for the control, pre and post-*TLP* groups were significantly different (Table 3.1). The means for *RLWC*, Ψ_{leaf} and Ψ_P for control and pre-*TLP* groups were not different, whereas mean values for *RLWC*, Ψ_{leaf} and Ψ_P at the post-*TLP* groups were different to control and pre-*TLP* groups. This was an indication that there were significant changes in soil water

characteristics between pre and post-*TLP*, and also that control plants did not experience soil water deficits, although the leaf water properties did not indicate a difference between controls and pre-*TLP* values**.**

Table 3.1: Average values (± SE) for soil water content (*SWC*), soil water potential (Ψ_{soil}), relative leaf water content (*RLWC*), leaf water potential (Ψ_{leaf}), leaf osmotic potential (Ψ_{π}) and leaf turgor potential (Ψ_{P}) of plants group according to their leaf turgor status. Pre-*TLP* refers to parameters measured before leaf turgor is lost, while post-*TLP* refers to parameters measured after leaf turgor is lost. Abbreviation: turgor loss point (*TLP*).

	Leaf turgor status		
Parameter	Control (n= 7)	Pre-*TLP* (n= 15)	Post-*TLP* (n= 8)
SWC (%)	15.6 ± 0.5 [a]	8.68 ± 0.4 [b]	6.83 ± 0.32 [c]
Ψ_{soil} (MPa)	-0.46 ± 0.02 [a]	-1.11 ± 0.05 [b]	-1.49 ± 0.08 [c]
RLWC	95.7 ± 0.41 [a]	95.3 ± 0.34 [a]	87.1 ± 1.9 [b]
Ψ_{leaf} (MPa)	-0.44 ± 0.03 [a]	-0.47 ± 0.025 [a]	-0.76 ± 0.05 [b]
Ψ_{π} (MPa)	-0.59 ± 0.005 [a]	-0.46 ± 0.09 [a]	-0.74 ± 0.05 [a]
Ψ_{P} (MPa)	0.15 ± 0.025 [a]	0.13 ± 0.02 [a]	-0.016 ± 0.0028 [b]

Different lower-case letters indicate significant differences between means for the values confined to a row $P < 0.05$ (Tukey HSD test).

3.3.3 Effect of soil water on leaf water relations

RLWC remained fairly constant at 95% with decreasing *SWC* until ~8% *SWC*, where a threshold was reached and a rapid decline in *RLWC* occurred (Fig. 3.4 a). At a *SWC* between 5 and 8%, the *RLWC* had declined from 95% to around 75%, indicating the sensitivity of *RLWC* to *SWC* below this threshold. Leaf water potential (Ψ_{leaf}) showed a steadier decline from about 15% *SWC*, with a less apparent threshold at a *SWC* of approximately 8% (Fig 3.4 b). The *TLP* occurred at a *SWC* of approximately 7.4%, which may explain the exponential decline of *RLWC* and Ψ_{leaf} below 8% *SWC*. The non-linear response of Ψ_{leaf} was either the result of simple passive accumulation of solutes due to leaf dehydration, or the net solute accumulation from osmotic adjustment (*OA*) (Girma and Krieg, 1992) combined with the loss of turgor at ~8% *SWC*.

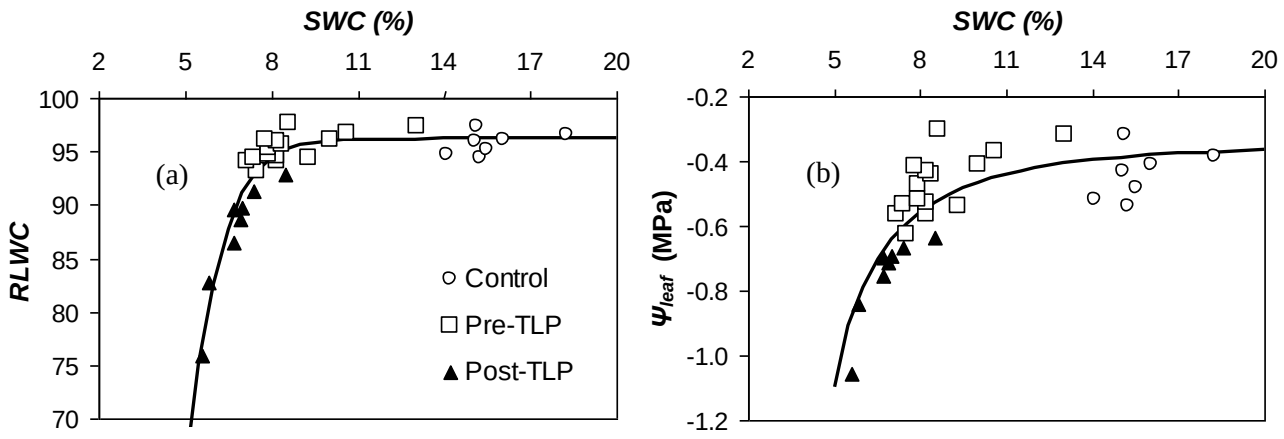

Figure 3.4: Response of *Z. mays* (a) *RLWC* and (b) Ψ_{leaf} to decreasing *SWC*. Lines fitted to all the data including the controls using the following best fit model y=a/(1+b*exp(-cx)). *RLWC* R^2= 0.91; Ψ_{leaf} R^2= 0.94. Each point represents an individual leaf from a separate plant. Abbreviations: relative leaf water content (*RLWC*), leaf water potential (Ψ_{leaf}), soil water content (*SWC*), turgor loss point (*TLP*).

3.3.4 Leaf gas exchange drought response

Both photosynthesis (*A*) and stomatal conductance (g_{ST}) for drought stressed plants decreased in response to drought, but the responses varied according to the way in which leaf water status was assessed (Fig. 3.5). For all the parameters, *SWC*, *RLWC* and Ψ_{leaf} there was no difference in *A* and g_{ST} between the control and drought stressed leaves pre-*TLP* (left of the dashed line) (Fig. 3.5 a-f). *A* and g_{ST} decreased exponentially at the *TLP* threshold when compared against *SWC*, and to a lesser degree for Ψ_{leaf} (Fig. 3.5 a,c,d,f). *A* and g_{ST} decreased progressively with *RLWC*, with no discernable threshold at the *TLP* (Fig 3.5 b,e).

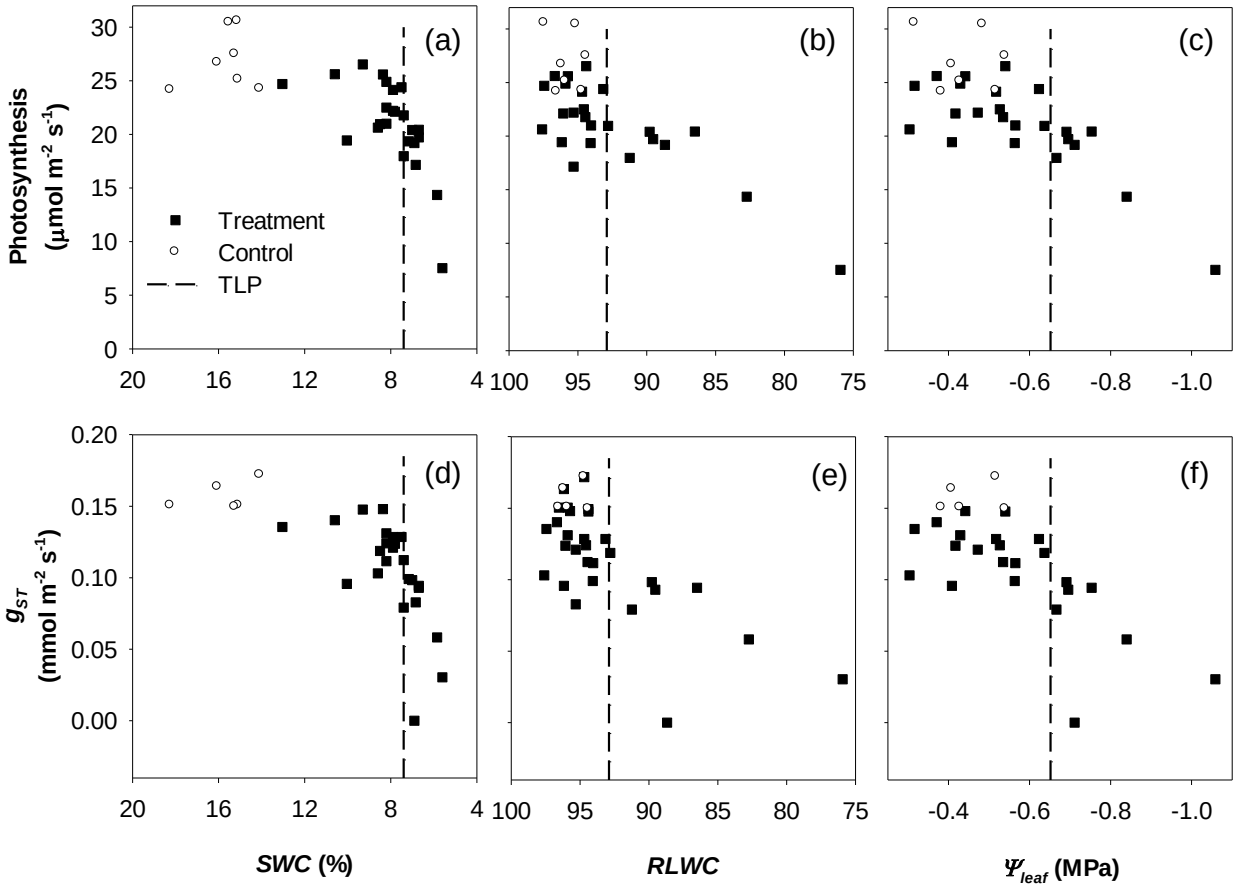

Figure 3.5: (a-c) *Z. mays* photosynthetic rate (*A*) and (d-f) stomatal conductance (g_{ST}) with decreasing *SWC*, *RLWC* and Ψ_{leaf} measured at ambient CO_2 concentrations (400 μmol mol^{-1}). The vertical dashed line (- - -) represents the *TLP* of *Z. mays* leaves for each independent variable. Drought treatment (■) and control leaves (○) while each point represents an individual leaf from a separate plant. Abbreviations: soil water content (*SWC*), relative leaf water content (*RLWC*), leaf water potential (Ψ_{leaf}), turgor loss point (*TLP*).

3.3.5 Intercellular CO_2

Under water stressed conditions CO_2 diffusion into the intercellular leaf spaces can become restricted due to the reduction in stomatal apertures, this being particularly evident when measuring photosynthetic responses at different CO_2 concentrations. This was apparent from the different Post-*TLP* "well-watered" and "drought" C_i values when measured under saturating CO_2 (Table 3.2). However based on CO_2 response data from various studies on water stressed *Z. mays* (Naidu and Long, 2004; Markelz *et al.*, 2011), all C_i values used in this experiment were within the concentrations required to saturate photosynthesis and to achieve A_{max} (maximum photosynthetic rates) (Table 3.2).

Table 3.2: Average C_i (μmol mol^{-1}) (± SE) for plants according to their leaf turgor status at saturating CO_2 for the well-watered and drought plants photosynthetic measurements.

	Saturating CO_2	
Leaf turgor status	Well-watered C_i	Drought C_i
Control	1065 ± 121 *	
Pre-*TLP*	958 ± 59 [a]	894 ± 49 [a]
Post-*TLP*	1212 ± 85 [a]	427 ± 88 [b]

* Mean C_I for the controls were also measured on two occasions but with no drought treatment. Different lower-case letters indicate significant differences between means for the values confined to a row $p < 0.05$ (Student *T*- test). Abbreviations: intercellular CO_2 concentration (C_i), turgor loss point (*TLP*).

3.3.6 Metabolic limitations

Metabolic limitations (R_{ML}) were calculated for the drought stressed plants relative to when these plants were well-watered (Fig. 3.2). Metabolic limitations (R_{ML}) for water stressed *Z. mays* leaves showed an increase in response to decreasing *RLWC* and Ψ_{leaf} (Fig. 3.6 a-b; Table 3.1). The coefficient of determination (R^2) values for linear and non-linear regressions for R_{ML} against *RLWC* were not different (Fig. 3.6 a; Table 3.1). The non-linear regressions for R_{ML} against Ψ_{leaf} (R^2= 0.86 vs. R^2= 0.75) had higher R^2 values than the linear regressions, which indicated no apparent threshold where R_{ML} increased (Fig. 3.6 b; Table 3.1). An ANOVA test indicated that the control and pre-*TLP* R_{ML} means were not different, but these were different to the post-*TLP* R_{ML} mean ($F_{2,27}$= 25.2, p< 0.0001).

If a separate linear and non-linear regression was fitted to the data pre-*TLP* for *RLWC*, the R^2 value for the non-linear fit (R^2= 0.13) was considerably higher than that of the linear fit (R^2= 0.05), indicating that R_{ML} increases non-linearly as the *TLP* approaches (Table 3.1). This trend was also evident when separate linear (R^2= 0.86) and non-linear (R^2= 0.94) regressions were fitted to the data post-*TLP*, indicating R_{ML} increased somewhat exponentially as the leaf dehydrated. For Ψ_{leaf}, the non-linear fit (R^2= 0.14) for the pre-*TLP* data had a higher R^2 than the linear regression (R^2= 0.05), but the R^2 values for the post-*TLP* data did not differ.

3.3.7 Stomatal limitations

Stomatal limitations (S_L) were calculated for the drought stressed plants (Fig. 3.2). S_L for the water stressed leaves showed no trends to decreasing *RLWC* and Ψ_{leaf}, and the treatments did not differ to the controls (Fig. 3.6 c-d; Table 3.1). When a separate linear and non-linear regression was fitted to the data pre and post-*TLP* for *RLWC* and Ψ_{leaf}, R^2 values did not differ. This indicated that the decrease in *RLWC*, Ψ_{leaf} and the *TLP* threshold had no significant effect on the stomatal limitations. An ANOVA test indicated that the control, pre and post-*TLP* S_L means were not different ($F_{2,28}$= 28.1, p= 0.73).

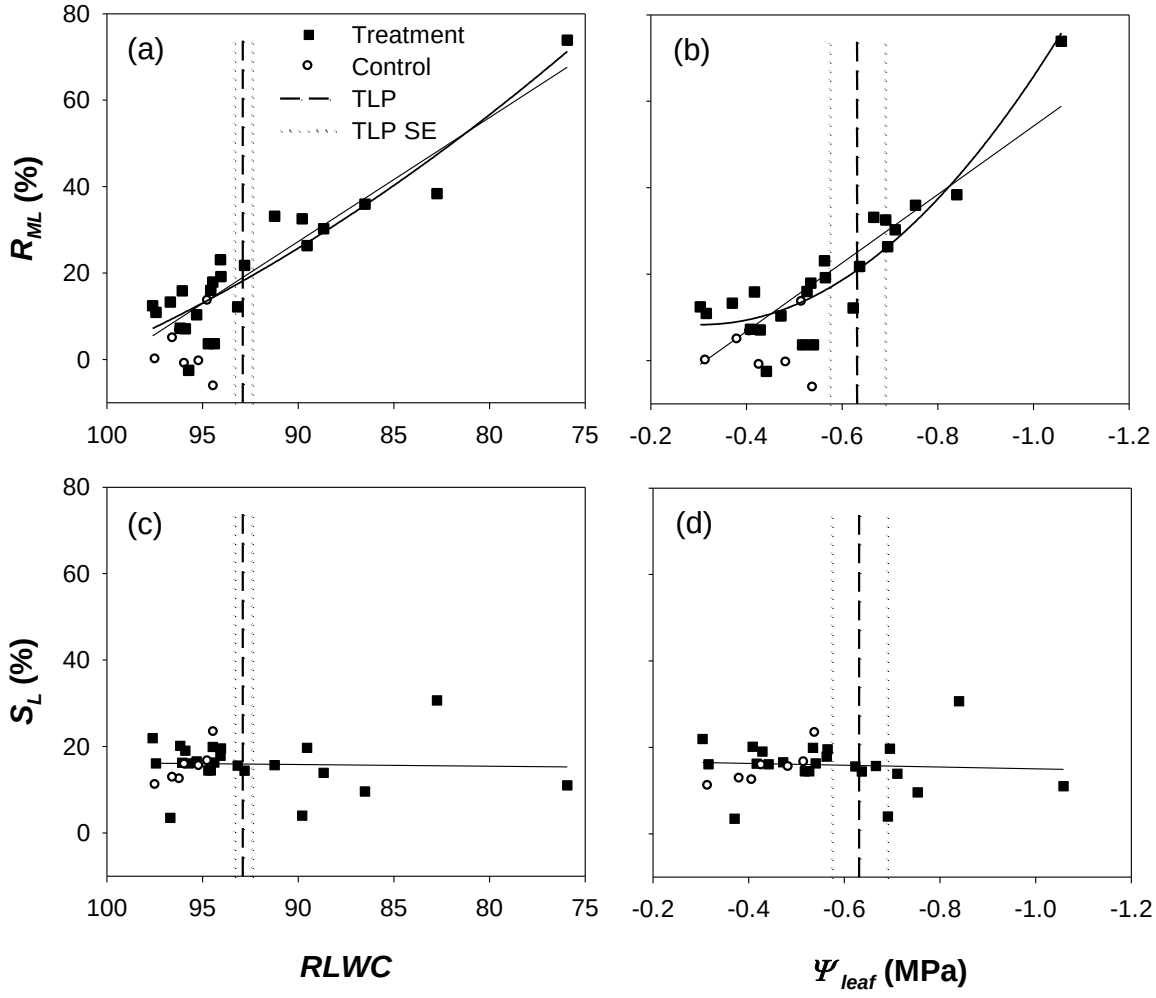

Figure 3.6: *Z. mays* relative metabolic (a-c) and stomatal limitations (d-e) with decreasing *RLWC* and Ψ_{leaf}. The vertical dashed line (- - -) represents the *TLP* and the dotted line (⋯) represents the *TLP* SE of *Z. mays* leaves for each independent variable. Drought treatment (■) and control leaves (○) and each point represents an individual plant. Linear lines fitted to (a-d) and non-linear (2nd order polynomial) lines fitted to (a-b). Non-linear lines are not displayed on (c-d) as they did not differ to the linear fits. Lines fitted to treatment data only. All R^2 values are presented on Table 3.1.

Table 3.3: Linear and non-linear coefficient of determination (R^2) values and level of significance for relative metabolic (R_{ML}) and stomatal (S_L) limitations in response to decreasing *RLWC* and Ψ_{leaf} (MPa) for control and drought plants pre- and post-turgor loss.

		RLWC		Ψ_{leaf} (MPa)	
		Linear	Non-linear	Linear	Non-linear
		R^2			
R_{ML}	Control	0.0006 n.s.	0.07 n.s.	0.0006 n.s.	0.07 n.s.
	Pre-*TLP*	0.051 n.s.	0.13 n.s.	0.051 n.s.	0.144 n.s.
	Post-*TLP*	0.864 ***	0.94 ***	0.923 ***	0.951 ***
	All (excl. control)	0.837 ***	0.843 ***	0.753 ***	0.861 ***
S_L	Control	0.741 *	0.813 *	0.741*	0.813 *
	Pre-*TLP*	0.005 n.s.	0.012 n.s.	0.006 n.s.	0.015 n.s.
	Post-*TLP*	0.018 n.s.	0.12 n.s.	0.007 n.s.	0.021 n.s.
	All (excl. control)	0.001 n.s.	0.0054 n.s.	0.004 n.s.	0.004 n.s.

Control (n= 7), Pre-*TLP* (n= 15), Post-*TLP* (n= 8) and All (excl. control) (n= 23). Levels of significance for the regressions are indicated as: n.s. (not significant) P > 0.05; *****P < 0.05; ******P < 0.01; *******P < 0.001.

3.3.8 Effect of *SWC* on metabolic limitations

Soil moisture content had a strong influence on *RLWC* and hence also on R_{ML}, and at approximately 8% *SWC* a threshold developed where R_{ML} increased exponentially (Fig. 3.7). This indicated the direct effect of soil moisture availability on photosynthetic metabolism, and that after a specific *SWC* threshold *Z. mays* plants could not avoid the effects of soil dehydration on photosynthesis.

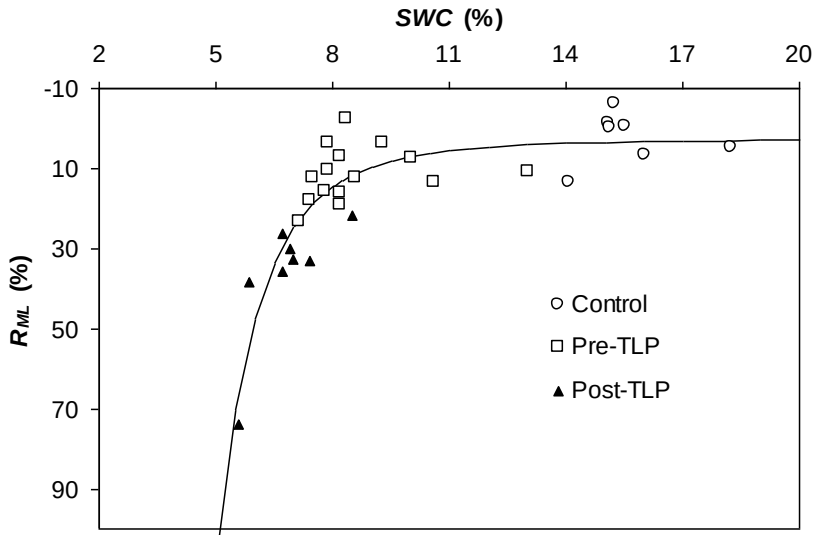

Figure 3.7: Relative metabolic limitation (R_{ML}) for individual *Z. mays* leaves against *SWC*. Line fitted to all the data including the controls using the following best fit model y=a/(1+b*exp(-cx)) (R^2=0.91). Abbreviations: soil water content (*SWC*), turgor loss point (*TLP*).

3.4 Discussion

These results supported the hypothesis that as the leaf water deficit increased, metabolic and not stomatal limitations, significantly affected the photosynthetic output. Metabolic limitations increased with decreasing relative leaf water content (*RLWC*) and leaf water potential (Ψ_{leaf}), while stomatal limitations showed no change. This response supports the findings of research conducted on various C_4 grasses that increasing water deficits (drought) affects the C_4 photosynthetic metabolism to a greater extend than the limitations to photosynthesis imposed by stomata (Lawlor, 2002; Ghannoum, 2003; Ripley *et al.*, 2007, 2010).

Metabolic limitations (R_{ML}) showed a linear increase with decreasing *RLWC* and Ψ_{leaf}, with no apparent threshold at the *TLP* (Fig 3.6 a-b). Irrespective of whether considered in response to *RLWC* or Ψ_{leaf}, R_{ML} subsequent to the *TLP* was significantly higher than values prior to the *TLP*. The linear increase in R_{ML} with decreasing *RLWC* supported the "Type 2" response originally presented by Lawlor (2002). Lawlor, (2002) suggested two different photosynthetic responses to decreasing leaf water deficits: "Type 1" response where *A* and g_{ST} both decrease linearly and roughly in parallel with decreasing leaf water content during which elevated CO_2 can restore *A* to A_{max}, indicating the photosynthetic metabolism is not intrinsically affected. As leaf water content falls further (well beyond the *TLP*), elevated CO_2 no longer effectively restores *A* to A_{max}, indicating the onset of metabolic limitations. For a "Type 2" response, *A* and g_{ST} decrease much the same as the "Type 1",

however elevated CO_2 only partially restores *A* to A_{max}. A_{max} consequently shows a progressive decrease with decreasing leaf water, and the effect of stomata are shown to be less important in restoring A_{max}. This indicates A_{max} is metabolically inhibited starting at high leaf water contents.

For *Z. mays* only a small reduction in *RLWC* (~4.7%) resulted in the loss of photosynthetic metabolism, which decreased progressively as *RLWC* fell further. Owing to this "Type 2" response, a clear threshold at the *TLP* would not be expected. Lawlor (2002) suggested that this "Type 2" response may be the result of leaf regulatory mechanisms failure to maintain ionic and osmotic homeostasis (osmotic adjustment - *OA*), resulting in metabolic impairment. Studies by Lawlor and Khanna-Chopra (1984), Meyer *et al.*, (1992) and Tezara *et al.*, (1999) noted a progressive decrease in ATP with falling *RLWC*, which was an indication of inhibited ATP synthase. This implies that metabolic impairment from reduced ATP synthase may be linked to osmotic adjustment (Zhang *et al.*, 1999).

When measured under ambient conditions, the decrease in *A* and g_{ST} with decreasing *SWC* and leaf water properties, showed the classical trend demonstrated by Lawlor (2002). The decline in *A* with increasing water stress could be attributed to the interactive effect of stomata and photosynthetic metabolism, and these trends were also not dissimilar to *Z. mays* and C_4 grasses from various drought studies (Saccardy *et al.*, 1996; Ward *et al.*, 1999; Carmo-Silva *et al.*, 2010; Ripley *et al.*, 2010; Ogbaga *et al.*, 2014), indicating the plants responded as expected to drought.

From the results and the experimental methods, it was not possible to ascertain if plasmodesmata were directly affected by the water stress, but it is known that turgor maintenance is important in both apoplastic and symplastic (plasmodesmata transport) pathways. Turgor potential retains cell membrane integrity and solute exchange (Thorpe and Minchin, 1996; Blackman and Overall, 2001; Roberts and Oparka, 2003). The observed metabolic response (Type 2) indicated a possible lack of osmotic homeostasis and by definition, osmotic adjustment (Lawlor, 2002). It therefore seems the loss of turgor was not as damaging as leaf dehydration, and the linear response of metabolic loss to leaf dehydration, with no apparent threshold at the point where turgor was lost supports this idea. Progressive leaf dehydration and not sudden turgor loss, may have resulted in impaired plasmodesmata transport function and/or reduced ATP synthase (Lawlor, 2002) which possibly affected metabolic processes. Disruption to plasmodesmata transport could also have resulted in the BSC metabolism being deprived of substrates, and in the case of *Z. mays* (NADP-Me), reductant in the form of reduced malate.

If C_4 photosynthetic metabolism is to remain uninhibited during water stress, it would stand to reason that C_4 plants need to maintain favourable leaf water statuses. Maintaining high leaf water is not

exclusively achieved by morphological adaptations (vessel diameters, leaf hairs etc.), but also through mechanisms such as osmotic adjustment (Zhang *et al.,* 1999; Nayyar, 2003; Kusaka *et al.,* 2005; Molinari *et al.,* 2007). Chapter 4 will examine the metabolic responses of the C_4 species used in the long-term 58 day drought experiment, to see if this link of metabolic loss to the maintenance of leaf water status is applicable under long-term drought conditions.

Chapter 4
Metabolic limitation mechanisms

4.1 Introduction

When C_4 species are exposed to severe drought, their photosynthetic output is affected to a larger extend by metabolism than limitations to CO_2 diffusion imposed on by stomata (Lawlor, 2002; Ghannoum *et al.*, 2003; Flexas *et al.*, 2006; Ibrahim *et al.*, 2008; Ripley *et al.*, 2007, 2010; Taylor *et al.*, 2011). Within C_4 grasses, photosynthetic subtypes have also shown different responses under water stress conditions whereby NAD-Me species maintain higher water use efficiencies over the NADP-Me species, (Ghannoum *et al.*, 2002) and Carmo-silva *et al.*, (2007) demonstrated smaller photosynthetic susceptibility of a NAD-Me species compared to a NADP-Me species. This empirical data also supports the biogeography of C_4 grasses where the number of NADP-Me species increases with increased precipitation while the number of NAD-Me species shows the reciprocal response (Ellis *et al*., 1980; Vogel *et al.*, 1986; Taub, 2000; Cabido *et al.*, 2008). This association with rainfall gradients is not restricted to C_4 photosynthetic subtypes but also lineages (Taub, 2000; Cabido *et al.*, 2008), which suggests an interaction between subtype and phylogeny. The distribution of C_4 grasses in South Africa indicates that Panicoideae species (mainly NADP-Me but also NAD-Me species) show a preference for mesic habitats, while Aristidoideae species show the converse response (Visser *et al.*, 2012). To elucidate this differential drought response amongst subtypes and lineages, photosynthetic metabolic performance and osmotic adjustment were investigated to determine the mechanisms responsible for these metabolic responses.

The response of CO_2 assimilation to intercellular CO_2 ($A:C_i$ curve) can be used to determine the effects of drought on the limitation of photosynthesis (A) imposed by CO_2 diffusion across the stomata and by biochemical (metabolic) limitations. Results for *Z. mays* (Chapter 3) clearly showed that reductions in photosynthesis under severe water stress were almost wholly attributed to metabolic limitations. To determine which metabolic processes are affected, the y-intercept, initial slope and the saturated portion of the $A:C_i$ curve were analysed using the models of von Caemmerer and Farquhar (1981) and von Caemmerer (2000).

Mitochondrial respiration in the light (R_d), PEPcase efficiency (k) and maximum Rubisco activity (V_{max}) are biochemical parameters derived from $A:C_i$ curves, which can give insight into the effects of photosynthetic metabolism when exposed to water deficits. A review by Atkin and Macherel (2009) showed that drought elicits a variety of responses in leaf R_d, but the majority of species showed a decrease in R_d. In comparison to the reduction in photosynthesis, changes in R_d are minor, but they

propose that maintenance of mitochondrial ATP synthesis during drought aids faster photosynthetic recovery from drought. The rate of phosphoenol pyruvate (PEP) carboxylation or PEPcase efficiency is calculated from the initial slope (*k*), where CO_2 is limiting and the C_4 cycle (rate of C_4 acid decarboxylation) is assumed to be equivalent to the PEPcase efficiency (von Caemmmerer, 2000). Maximum Rubisco activity (V_{max}) is calculated from the saturated portion of the curve where CO_2 is not limiting (von Caemmerer 2000). Studies on C_4 grasses from the three photosynthetic subtypes have shown that drought reduces *k* and V_{max} (Carmo-Silva *et al.*, 2008; Ripley *et al.*, 2010; Alfonso and Bruggemann, 2012). Reductions in *k* may be attributed to a decrease in the C_4 cycle rate by the reduction in PEPcase efficiency (von Caemmerer, 2000), and reductions in V_{max} are most likely due to ribulose bisphosphate (RuBP) regeneration limitations, PEP regeneration limitations and RuBP carboxylase/oxygenase (Rubisco) enzymes limitations (von Caemmerer, 2000; Lawlor, 2002; Sage, 2002). Lawlor (2002) however suggested that Rubisco enzyme limitations are not likely to affect V_{max} drought responses, but that these result from PEP and RuBP regeneration limitations caused by ATP synthase impairment. More drought tolerant species should be able to better maintain *k* and V_{max}, and this may be associated with osmotic adjustment (*OA*), which should play a role by maintaining leaf water status, resulting in less inhibition of metabolic processes.

The main purpose of *OA* is to maintain favourable leaf water status in response to water stress, and this can be achieved by sustaining leaf turgor potential so cells can continue important metabolic processes such as photosynthesis (Jones and Turner, 1978; Zhang *et al.*, 1999). By lowering the osmotic potential, higher *RLWC* can be maintained, and the turgor loss point (*TLP*) can also be shifted such that the *TLP* occurs at a slightly lower *RLWC* (Jones and Turner, 1978; Michelena and Boyer, 1982; Girma and Krieg, 1992). *OA* has been shown for various C_4 grass species that were subject to soil water deficits, such as *Sorghum bicolour* (Jones and Turner 1978; Girma and Krieg 1992), *Zea mays* (Michelena and Boyer, 1982), *Pennisetum setaceum*, *Heteropogon contortus* (Williams and Black, 1994), *Hyparrhenia rufa* and *Tracypogon plumosus* (Baruch and Fernández, 1993). *OA* in C_4 plants is not always shown to increase drought tolerance, but for the following species it has been shown that an association with drought tolerance exists: *Z. mays*, *Saccharum officinarum* (sugarcane) and *Pennisetum americanum* (pearl millet) (Nayyar, 2003; Kusaka *et al.*, 2005; Molinari *et al.*, 2007). Changes in the *TLP* after *OA* was shown for *H. rufa* and *T. plumosus* (Baruch and Fernández, 1993) and *S. bicolour* (Jones and Turner, 1978), but these changes were slight (2-3% *RLWC*) and although not statistically significant, a slight shift in the *TLP* could confer additional water stress tolerance. However results from Chapter 3 show that the point where turgor is lost does not show a relationship to metabolic decline, but in fact this decline is progressive with leaf dehydration.

Current research demonstrates that C_4 grasses suffer mainly from metabolic and not stomatal limitations under severe drought, but this has primarily been restricted to species from the Panicoideae

lineage, with little or no research conducted on Aristidoideae species. In addition to this, studies have not always correctly accounted for phylogeny when comparing photosynthetic subtypes, specifically NADP-Me and NAD-Me species.

The aims of this chapter were to determine if; (1) metabolic limitations were more important in determining the decline of photosynthesis than stomatal limitations; (2) Aristidoideae NADP-Me and Panicoideae NAD-Me species showed less metabolic limitations to progressive drought than Panicoideae NADP-Me species; (3) drought tolerance mechanism (osmotic adjustment) was correlated to lessening metabolic limitations and (4) that metabolic limitations intensify with decreasing leaf water status and do not show a threshold response related to the loss of leaf turgor.

4.2 Methods

These hypotheses were tested by deriving parameters from the photosynthetic response (*A*) to intercellular concentrations of CO_2 (C_i) (*A:C*$_i$ curves) and pressure-volume curves (PV curves) of the nine species. Potted plants were subjected to a controlled dehydration over a 58 day period and gas exchange and leaf water relation measures made on several occasions (see Fig. 2.2 Chapter 2). Additionally, drought responses of the gas exchange parameter, stomatal conductance (g_{ST}) and chlorophyll fluorescence emission parameter, *PSII* maximum efficiency (F_v'/F_m') reported in Chapter 2, was also compared to *A:C*$_i$ and PV curve parameters.

4.2.1 *A:C*$_i$ curves

The photosynthetic response (*A*) to intercellular concentrations of CO_2 (C_i) were measured using a Li-6400 photosynthesis system (Li-Cor Inc., Lincoln, NE, USA). During the dry-down phase treated plants were measured on day 10 (control: ~15% *SWC*), day 30 (~10% *SWC*) and day 45 (~6.5% *SWC*) (Fig. 2.2). Plants were acclimated under a sodium vapour light at a photosynthetic photon flux density (*PPFD*) similar to that used in the cuvette. Measurements were made on the youngest fully-expanded leaf (first down from the apical bud) between 10:30 am and 3:30 pm under laboratory conditions. Cuvette conditions were maintained as follows: a PPFD of 1200 μmol m^{-2} s^{-1} was supplied by a blue-red led light source, leaf temperature was set at 29°C, vapour pressure deficits (VPD) ranged between 1 – 2.5 kPa. External CO_2 concentrations (C_a) were supplied in the following sequence: 400, 250, 150, 100, 50, 400, 500, 1000, 1300, 1600 μmol mol^{-1}. Leaf areas were measured manually and CO_2 response curves were modelled according to von Caemmerer & Furbank (1999), with the following parameters being obtained: R_d, mitochondrial respiration rate in the light (μmol m^{-2} s^{-1}) was calculated

from the y-intercept of the initial slope of the $A:C_i$ curve. R_d is determined by the mitochondrial respiration occurring in the mesophyll and bundle sheath cells and is not associated with photorespiration (von Caemmerer, 2000). The initial slope (k) (PEPcase efficiency) of the $A:C_i$ curve (mol m^{-2} s^{-1}) was calculated from linear regression between the C_i and A for the first three points. V_{max}, the maximum Rubisco activity (μmol m^{-2} s^{-1}), was determined from the CO_2 saturated portion of the $A:C_i$ curve. Stomatal limitation of photosynthesis (S_L) for each curve was calculated according to Farquhar and Sharkey (1982) (Fig. 4.1). Relative stomatal limitations (R_{SL}) and relative metabolic limitations (R_{ML}) of the water stressed plants were calculated according to Fig. 4.1. R_{SL} shows the effect of stomata on photosynthesis for a treatment relative to the control while S_L is the actual limitation to photosynthesis imposed on by the stomata.

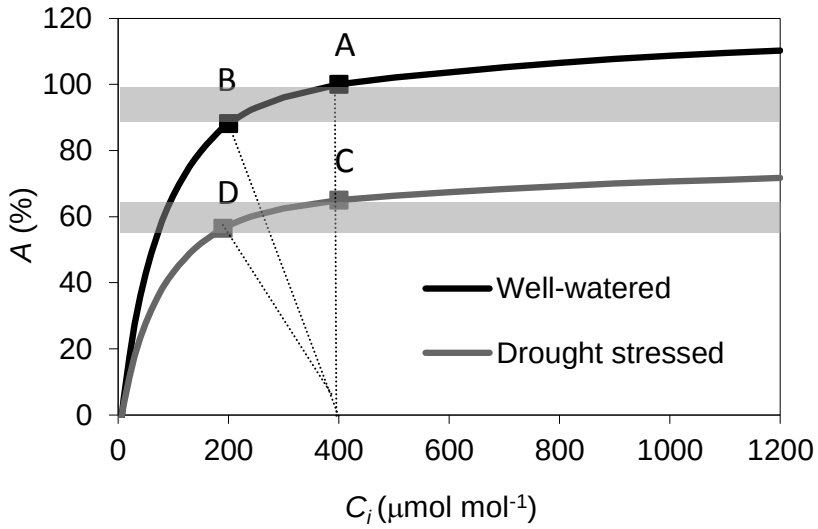

Figure 4.1: The two lines represent hypothetical CO_2 response curves (A:C_i) for well-watered and drought stressed leaves. For the well-watered leaf the stomatal limitation (S_L) = [((A - B) / A) x 100] where A is the rate equal to 400 μmol mol^{-1} (infinite g_{st}) and B is the rate corresponding to C_i at finite g_{st} (ambient CO_2). For the drought treatment the S_L = [((C - D) / C) x 100]. Relative stomatal limitation (RL_S) for the well-watered leaf is the same as S_L but for the water stressed leaf R_{SL} = [(C - D) / B) x 100]. Relative metabolic limitation (R_{ML}) for the well-watered leaf is by definition = 0 and for the drought stressed leaf R_{ML} = [(A – C) / A) x 100]. The shaded areas indicate the S_L for each curve (Ripley *et al.*, 2007). Abbreviation: photosynthetic rate (A), intercellular CO_2 concentration (C_i).

As leaves age or depending on non-treatment environmental factors, their photosynthetic rates change, even in well-watered plants. This must be accounted for by comparing rates for drought treated plants to rates for control plants of the same age. However, for practical reasons relating to the number of species used in these experiments, it was not feasible to replicate $A:C_i$ curves on well-watered controls at each sampling date. Hence, we accounted for the age effects by correcting

photosynthetic rates by changes in rates that had been observed when making gas exchange measurements on the control plants of the same species (Chapter 2). This control *A* data from the gas exchange spot measurements (Chapter 2) was used to correct the $A{:}C_i$ treatment data.

The percentage change in photosynthetic rates of control plants from day 10 to 30, and from day 10 to 45, was calculated and the drought treated photosynthetic rates measured in response to C_i on days 30 and 45 were increased or decreased accordingly.

$$\text{Corrected A : Ci} = \frac{\text{Control A day 10}}{\text{Control A day 30}} \times \text{A : Ci A day 10}$$

4.2.2 Pressure-volume curves

Pressure-volume curves (PV curves) constructed from control leaves were used to determine individual components of leaf water potential ($\Psi_{leaf} = \Psi_P + \Psi_\pi$). The reciprocal of the Ψ_{leaf} was plotted against *RLWC* and a model was fitted to the data using the equations of Schulte and Hinckley (1985). The *TLP* ($\Psi_P = 0$ MPa) was defined as the *RLWC* at which Ψ_{leaf} equalled Ψ_π (osmotic potential). Ψ_π at 100% *RLWC* was calculated as the y-intercept of the straight line (Fig. 4.2). See Chapter 3 for full methods and Fig. 3.1.

To determine the osmotic adjustment (*OA*) of treated plants, their Ψ_{leaf} and *RLWC* were measured at various intervals during the dry down experiment, once *RLWC* had declined sufficiently to ensure that $\Psi_P = 0$ and that changes in $1/\Psi_{leaf}$ were solely dependent on $1/\Psi_\pi$. This response of $1/\Psi_{leaf}$ to *RLWC* was fitted with a straight line and $1/\Psi_\pi$ at 100% *RLWC* (y-intercept) was calculated. Osmotic adjustment was defined as the difference between Ψ_π of control and drought treated plants at 100% *RLWC*. As different species showed inherently different Ψ_π, *OA* was expressed as a percentage of the control value (relative *OA*) to allow the comparison of *OA* between species. Only the data from one species (*Aristida junciformis*) was used to illustrate the Ψ_π calculations shown in Figure 4.2.

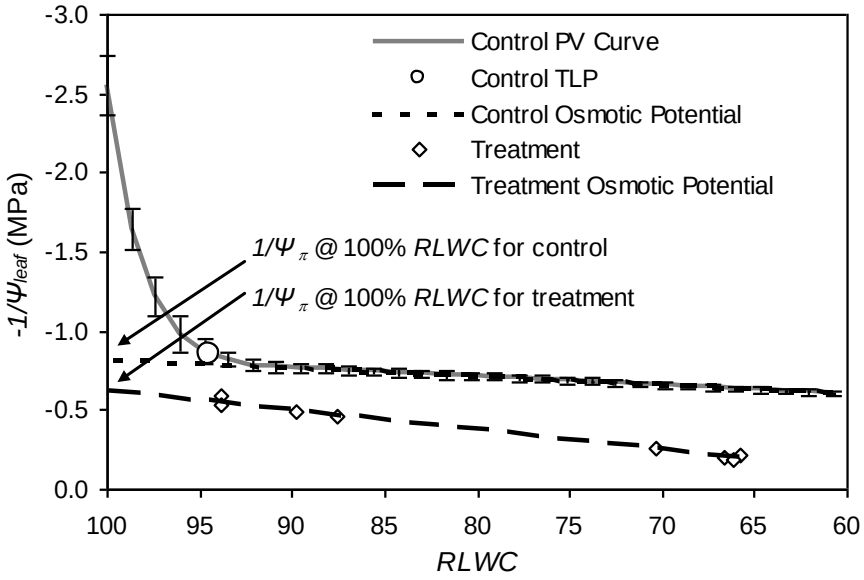

Figure 4.2: Pressure-volume curve (——) constructed for *Aristida junciformis* well-watered leaves (n= 3) with SE bars using the equations of Schulte and Hinckley (1985). The short dashed line (– –) represents the osmotic potential (Ψ_π) of well-watered leaves while the long dashed line (— —) represents the Ψ_π of the *A. junciformis* water stressed leaves. Diamonds (◊) represent mean data at two sampling intervals for *A. junciformis* (n= 4 plants). The difference between the y-intercept of the two lines was calculated as osmotic adjustment (*OA*). Turgor loss point (*TLP*) is denoted by the open circle (O) and this is where Ψ_P = 0 MPa. Abbreviation: leaf water potential (Ψ_{leaf}), relative leaf water content (*RLWC*).

4.2.3 Statistics

As in Chapter 2, the same statistical design (Nested General Linear Models) was used to detect the effects of drought on species, date, photosynthetic subtype/subfamily and their interactions with R_d, k, V_{max}, S_L, R_{SL} and R_{ML}. In addition to the GLM analysis, Student *t*-tests were used to detect differences in 1) R_{ML} and R_{SL} for Panicoid subtypes and for NADP-Me subfamilies and 2) differences in absolute osmotic adjustment between individual species. Lastly, regression analysis was performed on all linear relationships to determine the coefficient of determination (R^2) and p-values (significance).

4.3 Results

4.3.1 Average *A:C*$_i$ curves

Figure 4.3 shows the average CO_2 response curves (*A:C*$_i$) constructed for Panicoid and Aristoid species. Comparisons between Panicoid NADP-Me and NAD-Me species (subtypes) show similar results for the well-watered and treatments curves, but the comparison between NADP-Me Panicoid and Aristoid species (subfamily) show different curve shapes and treatment responses. Panicoid species control curves saturated at a C_i of approximately 400 µmol mol^{-1} with an operating point (C_i value at an ambient CO_2 of 400 µmol mol^{-1}) of 190 and 205 µmol mol^{-1} for NADP-Me and NAD-Me species respectively. Aristoid species control curves did not show complete saturation at a C_i of 400 µmol mol^{-1}, and the operating point was at 130 µmol mol^{-1}. Operating points at ~6.5% *SWC* decreased to 155 µmol mol^{-1} for Panicoid NADP-Me species, 146 µmol mol^{-1} for NAD-Me species and 120 µmol mol^{-1} for Aristoid species (~6.5% *SWC*). This equated to drought induced decreases in C_i operating points of 22.5 and 29% for Panicoid NADP-Me and NAD-Me species respectively, and 8% for Aristoid species. To further analyse the *A:C*$_i$ curves in detail, the following parameters: R_d, k, V_{max}, S_L, R_{SL} and R_{ML} were derived from individual curves and compared between subtypes and subfamilies.

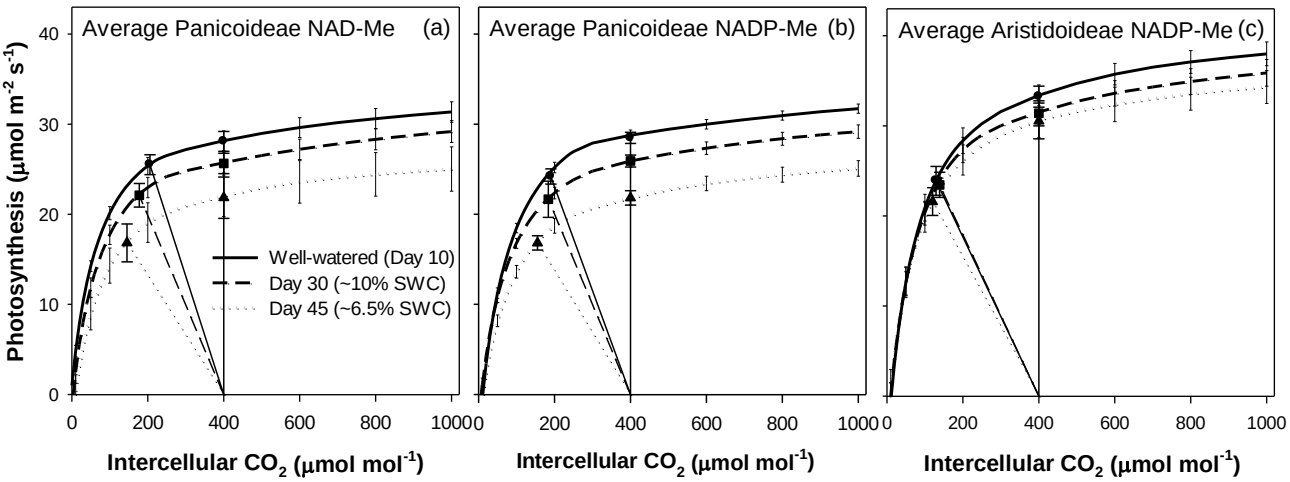

Figure 4.3: Average *A:C*$_i$ responses of (a) Panicoideae NAD-Me, (b) Panicoideae NADP-Me and (c) Aristidoideae NADP-Me species in response to drought. The solid line (**—**) indicates the well-watered (control) curve at day 10 (15% *SWC*), the dashed line (**— —**) indicates day 30 (~10% *SWC*) and the dotted line indicates (**⋯**) day 45 (~6.5% *SWC*). The curves at day 30 and 45 were adjusted according to the control values of the gas exchange measurements at the corresponding days. The vertical solid line (**—**) represents *A* at ambient CO_2 concentration (400 µmol mol^{-1}) assuming no stomatal limitations for all curves. The three diagonal lines (**—**, – –, **·····**) which correspond to the respective CO_2 response curves at the well watered and drought treatments represent the limitation on *A* imposed by CO_2 diffusion through the stomata. The plotted curves represent mean ± SE, n= 9-12.

4.3.2 *A:C$_i$* responses compared between Panicoid subtypes

Panicoid species showed *A:C$_i$* curves characteristic of Panicoid C_4 grasses (Ripley *et al.*, 2010) and photosynthetic saturation occurred at a C_i of approximately 400 μmol mol^{-1} for all the species (Fig. 4.4 a-f). Species curves showed relative uniformity, with the exception of *Panicum coloratum*, which showed a significant reduction at day 45 (~6.5% *SWC*), contrasting with the response of *P. virgatum* which did not show a reduction at the same *SWC* (Fig. 4.4 a,c). Mitochondrial respiration (R_d) remained unchanged for NADP-Me species whereas R_d for the NAD-Me species increased significantly with drought resulting in a subtype x day interaction (Fig. 4.5; Table 4.1). *P. virgatum* was the exception within the NAD-Me species, as it showed no change in R_d with drought (Fig. 4.5 a,b,d). The initial slope (*k*) for the NAD-Me species showed no change in response to drought whereas the NADP-Me species *k* was significantly lower than the control value by day 45 (Fig. 4.5 f,g,i). However this did not result in different trends between subtypes, and subtype x day interactions were not significant (Table 4.1). Maximum Rubisco activities (V_{max}) between subtypes did not differ, and both subtypes showed near identical decreases in response to drought, with the exception of *P. coloratum* which showed a significant decrease in V_{max} after day 30 (~10% *SWC*) when compared to the other Panicoid species (Fig. 4.5 k,l,n; Table 4.1).

4.3.3 *A:C$_i$* responses compared between subfamilies

A:C$_i$ curves for Aristoid species did not show the responses typical of Panicoid *A:C$_i$* curves where photosynthesis (*A*) saturated at a C_i of approximately 400 μmol m^{-2} s^{-1}. Aristoid curves did not appear to fully plateau but instead there was progressive increase of *A* with increasing C_i (Fig. 4.4 g-i). This was most notable for the *A. congesta* curves and the *A. junciformis* control curve (Fig. 4.4 g,i). Despite the differences in shapes of *A:C$_i$* curves for subfamilies, parameters derived from the curves showed similarities when compared statistically. Mitochondrial respiration (R_d) rates for both subfamilies showed no change in response to drought (Fig. 4.5 b,c,e; Table 4.2), but there was variability among the Aristoid species, with *Aristida junciformis* having significantly higher values than *A. diffusa* (Fig. 4.5 c). Values for the initial slope (*k*) were different between subfamilies, but both decreased with drought (Fig. 4.5 g,h,j; Table 4.2). Like *k*, maximum Rubisco activities (V_{max}) were different between subfamilies but both decreased with drought (Fig. 4.5 l,m,o; Table 4.2).

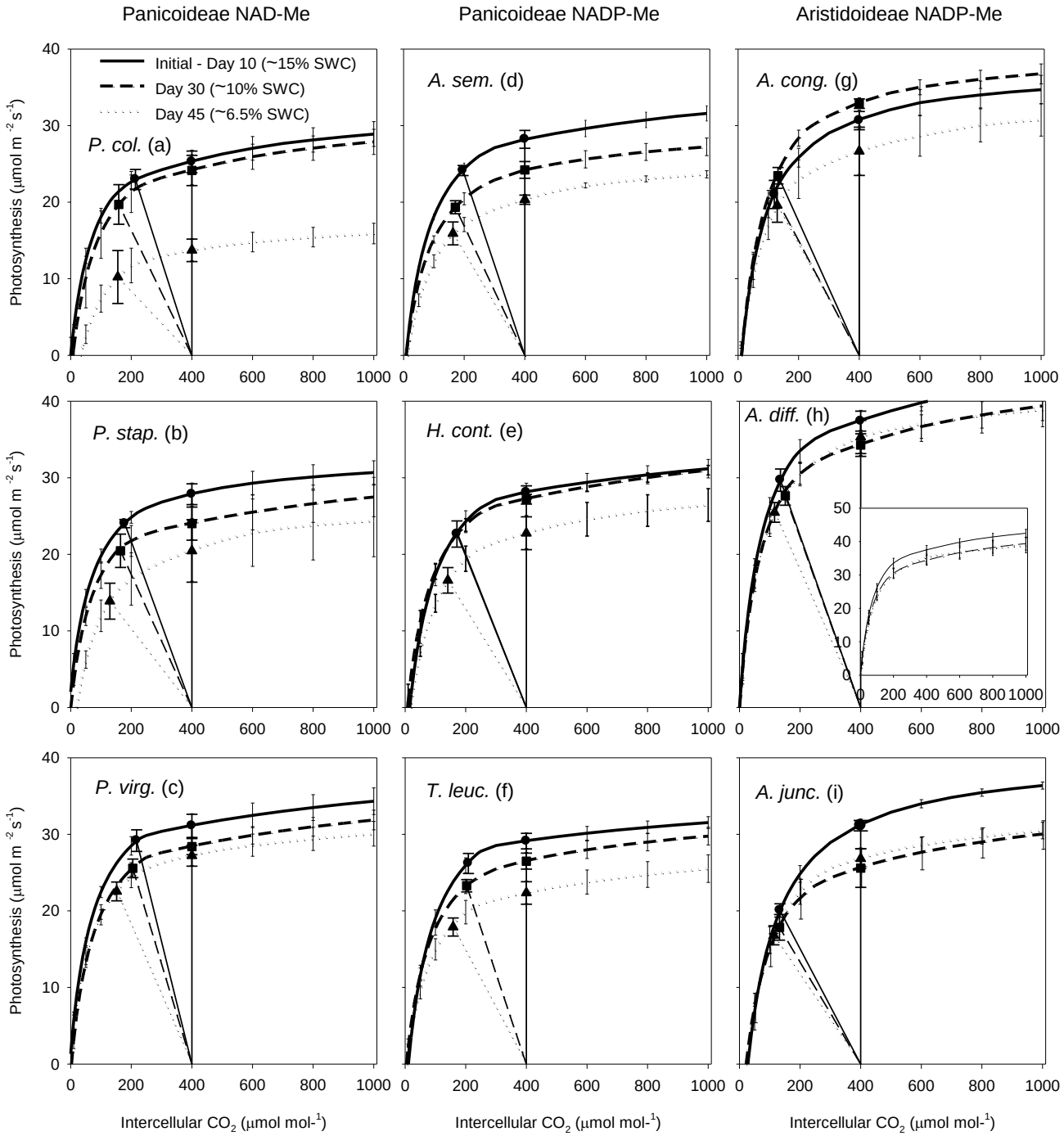

Figure 4.4: *A:C*$_i$ responses of (a-c) Panicoideae NAD-Me, (d-f) Panicoideae NADP-Me and (g-i) Aristidoideae NADP-Me species. The solid line (**—**) indicates the well-watered (control) curve at day 10 (~15% *SWC*), the dashed line (**— —**) indicates day 30 (~10% *SWC*) and the dotted line indicates (**⋯**) day 45 (~6.5% *SWC*). The curves at day 30 and 45 were adjusted according to the control values of the gas exchange measurements at the corresponding days. The inset on *A. diffusa* graph (h) indicates the full *A:C*$_i$ curves as the *A* rates were too high to be included in the scale of the other species. The vertical solid line (—) represents *A* at ambient CO_2 concentration (400 μmol mol^{-1}) assuming no stomatal limitations for all curves. The three diagonal lines (**—, – –, ·····**) which correspond to the respective CO_2 response curves at the well watered and drought treatments represent the limitation on *A* imposed by CO_2 diffusion through the stomata. The plotted curves represent mean ± SE and n= 2-5 per curve.

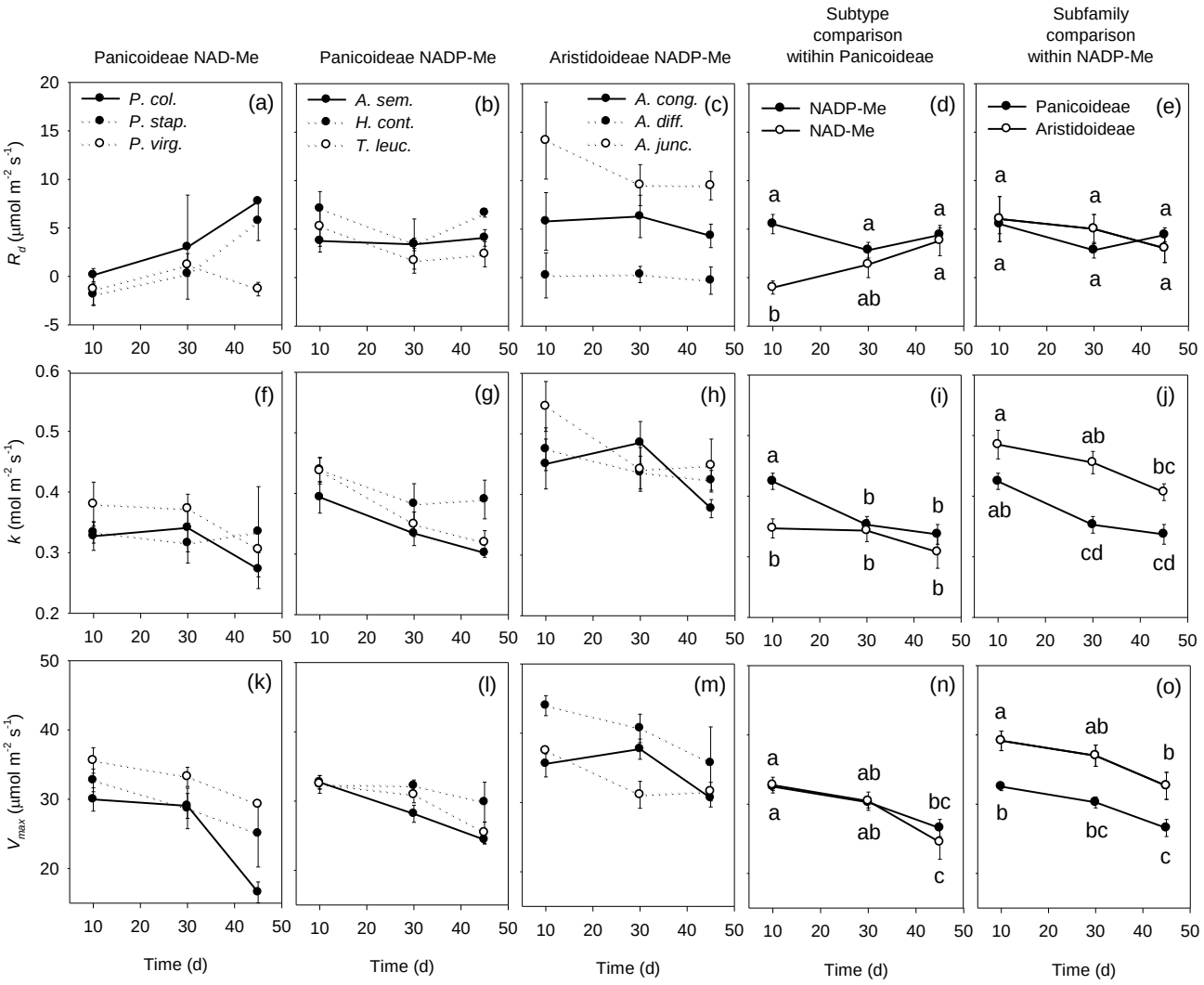

Figure 4.5: (a-e) Mitochondrial respiration rates (R_d), (f-j) initial slope (k) and (k-o) maximum Rubisco activity (V_{max}) for Panicoideae NAD-Me species, Panicoideae NADP-Me species, Aristidoideae NADP-Me species and average Panicoideae (NAD-Me vs. NADP-Me) and average NADP-Me (Panicoideae vs. Aristidoideae). Day 10 indicates the control. The plotted data points represent mean ± SE, n= 2-5 per species and n= 9-12 for subtype/subfamily. Small case letters signify homogenous groups.

Table 4.1: General Linear Model (GLM) results for mitochondrial respiration (R_d), the initial slope (k) and maximum Rubisco activity (V_{max}) between Panicoideae photosynthetic subtypes exposed to drought treatments. n.s. (not significant), *= p < 0.05, **= p < 0.01 and ***= p < 0.001.

Model parameter	Species	Species x Day	Species (Subtype)	Subtype	Day	Subtype x Day
R_d	*** $F_{5,66}$= 5	* $F_{10,66}$= 2.2	* $F_{4,66}$= 2.5	** $F_{1,66}$= 11.6	n.s. $F_{1.66}$= 2.66	** $F_{1,66}$= 5.6
k	** $F_{5,66}$= 3.6	n.s. $F_{10,66}$= 0.9	* $F_{4,66}$= 2.7	** $F_{1,66}$= 9.2	*** $F_{2,66}$= 7.8	n.s. $F_{2,66}$= 2
V_{max}	*** $F_{5,66}$= 5.2	n.s. $F_{10,66}$= 1.1	*** $F_{4,66}$= 5.5	n.s. $F_{1,66}$= 0.8	***. $F_{1.66}$= 22	n.s. $F_{1,66}$= 0.8

Table 4.2: General Linear Model (GLM) results for mitochondrial respiration (R_d), the initial slope (k) and maximum Rubisco activity (V_{max}) between Panicoideae and Aristoideae NADP-Me photosynthetic subtypes exposed to drought treatments. n.s. (not significant), *= p < 0.05, **= p < 0.01 and ***= p < 0.001.

Model parameter	Species	Species x Day	Species (Subfamily)	Subfamily	Day	Subfamily x Day
R_d	*** $F_{5,67}$= 10.1	n.s. $F_{10,67}$= 0.52	*** $F_{4,67}$= 13.7	n.s. $F_{1,67}$= 2.5	n.s. $F_{2,67}$= 1.6	n.s. $F_{2,67}$= 0.6
k	*** $F_{5,68}$= 9.5	n.s. $F_{10,68}$= 1.1	* $F_{4,68}$= 2.6	*** $F_{1,68}$= 37	*** $F_{2,68}$= 13	n.s. $F_{2,68}$= 0.7
V_{max}	*** $F_{5,68}$= 14	n.s. $F_{10,67}$= 14.5	*** $F_{4,67}$= 5.7	*** $F_{1,67}$= 42	*** $F_{2,67}$= 15.6	n.s. $F_{2,67}$= 0.07

4.3.4 Stomatal and metabolic limitations compared between Panicoid subtypes

Comparisons between metabolic (R_{ML}) and stomatal limitations (R_{SL}) revealed that R_{ML} was the major factor determining the decline in photosynthesis amongst Panicoid NADP-Me and NAD-Me species (Fig. 4.6 a-b).

R_{ML} accounted for approximately 25% of the decrease in photosynthetic rates in comparison to R_{SL} which accounted for less than 10% of the decrease (Fig. 4.7 k,l,n; Table 4.3). There was species variation amongst NAD-Me species, with *Panicum coloratum* showing the highest R_{ML} of 45% and *P. virgatum* the lowest R_{ML} of 13%.

R_{SL} between subtypes did not alter with drought and both NADP-Me and NAD-Me subtypes responded similarly (Fig. 4.7 f,g,i; Table 4.1). *Heteropogon conturtus* showed some variability amongst NADP-Me species with a negative R_{SL} at day 45 (~6% *SWC*).

Drought induced a constant increase in stomatal limitations (S_L) for the NADP-Me and NAD-Me Panicoid species and by day 45, S_L were significantly higher than day 10, with an increase of <15% for both subtype groups (Fig. 4.7; a,b,d; Table 4.3). Species responded with little variability and there were no significant outliers.

4.3.5 Stomatal and metabolic limitations compared between subfamilies

Relative metabolic limitations (R_{ML}), as opposed to R_{SL}, was the major factor determining the decline in photosynthesis for Panicoid species, however for the Aristoid species, both R_{ML} and R_{SL} showed near identical contributions to the decline of photosynthesis of about 10% (Fig. 4.6 b-c).

R_{ML} did not show an increase in response to drought for Aristoid species, which was ~10% compared to Panicoid species which was ~25% (Fig. 4.7 l,m,o; Table 4.4 – subfamily x day interaction). *Aristida congesta* showed a significant increase in R_{ML} between day 30 and 45, but this was due to treatment photosynthetic rates that were higher than the controls at day 30 (~10% *SWC*) (Fig. 4.4 g).

R_{SL} values of the Aristoid species were significantly higher than the Panicoid species but drought values were not different to the controls for each subfamily, with the overall the trends not different and this being evident from the insignificant subfamily x day interaction (Fig. 4.7 g,h,j; Table 4.4). Aristoid species showed variability as R_{SL} values for *A. junciformis* were significantly higher than for *A. diffusa*.

Aristoid species had higher S_L values, but these did not change with drought, unlike the Panicoid species (Fig. 4.7 b,c,e). Overall the S_L trends in response to drought were not different between subfamilies, this being evident from the insignificant subfamily x day interaction (Table 4.4). This indicated that Aristoid species operated with intrinsically higher S_L but unlike Panicoid species, drought did not alter the effect of stomata on *A*. There was slight variability amongst Aristoid species, where *A. junciformis* had higher S_L values than *A. diffusa*, but the trends were alike.

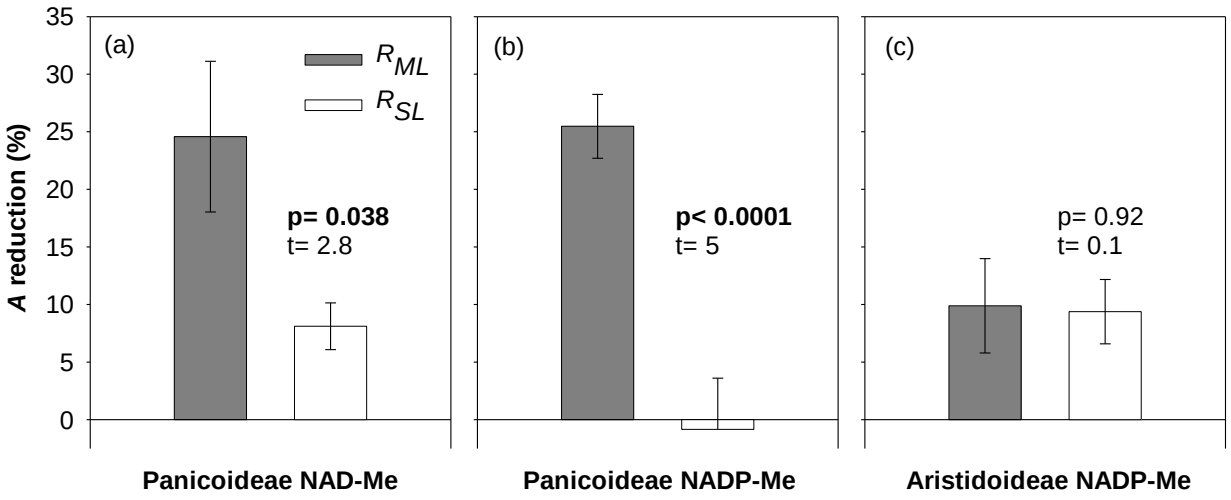

Figure 4.6: Relative metabolic limitations (R_{ML}) and relative stomatal limitations (R_{SL}) and their contribution to the reduction in the photosynthetic rate (*A*) measured at an ambient CO_2 concentration of 400 μmol mol^{-1} for drought stressed (a) Panicoideae NAD-Me, (b) Panicoideae NADP-Me and (c) Aristidoideae NADP-Me species. Values for R_{ML} and R_{SL} were calculated by deducting the control value (Day 10 = well watered) from the final value (Day 45: ~6.5% *SWC*). R_{ML} control values were zero. The bars represent mean ± SE, n= 9-12. Abbreviation: photosynthetic rate (*A*).

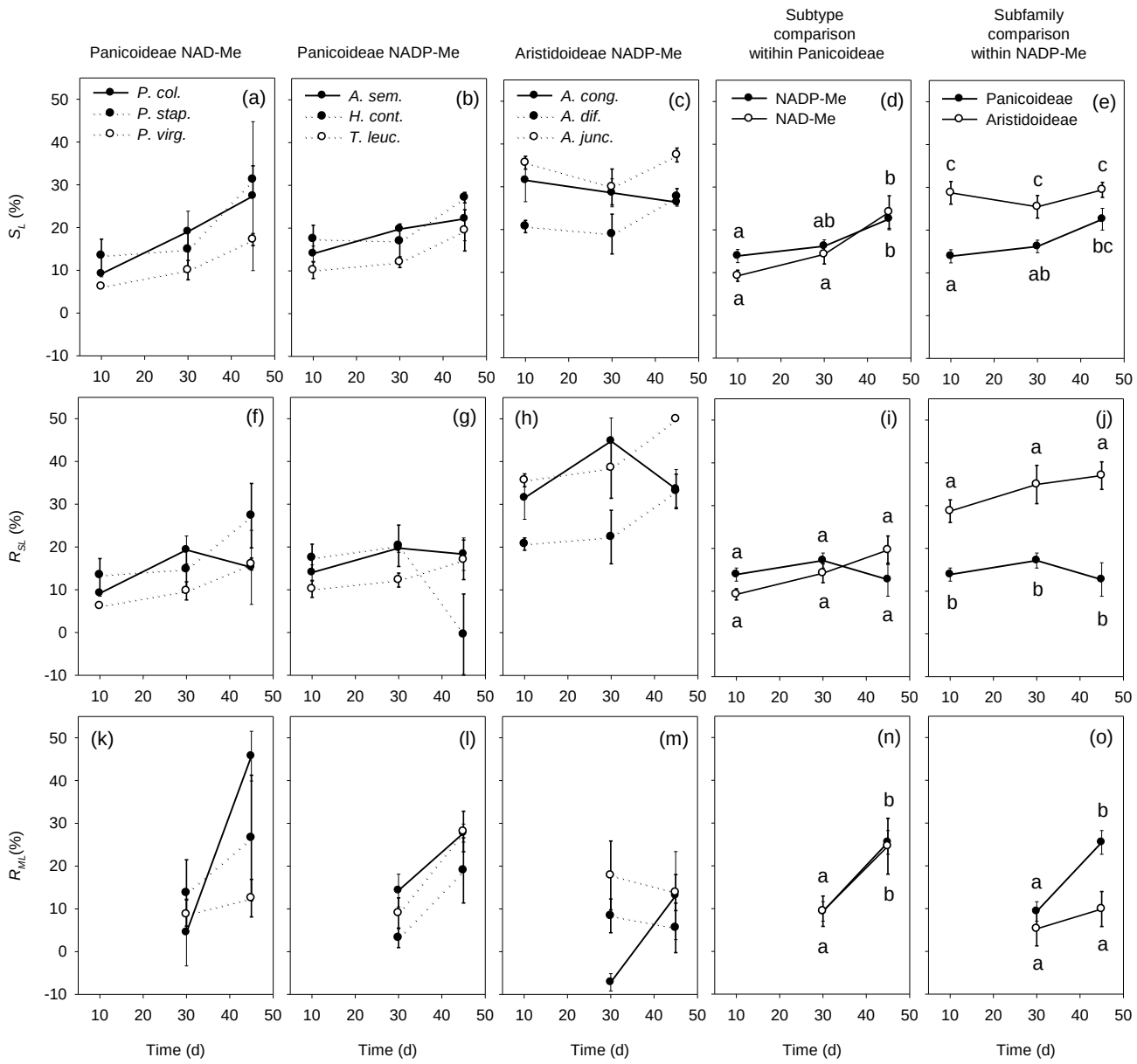

Figure 4.7: (a-e) Stomatal limitations (S_L), (f-j), relative stomatal limitations (R_{SL}) and (k-o) relative metabolic limitations (R_{ML}) for Panicoideae NAD-Me species, Panicoideae NADP-Me species, Aristidoideae NADP-Me species and average Panicoideae (NAD-Me vs. NADP-Me) and average NADP-Me (Panicoideae vs. Aristidoideae). Day 10 for S_L and R_{SL} (same value for both) indicates the controls whereas the R_{ML} could only be calculated from day 30 onwards. The plotted data points represent mean ± SE, n= 2-4 per species and n= 9-12 for subtype/subfamily averages. Small case letters signify homogenous groups.

Table 4.3: General Linear Model (GLM) results for stomatal limitations, relative stomatal limitations and relative metabolic limitations between Panicoideae photosynthetic subtypes exposed to drought treatments. * = $p < 0.05$, ** = $p < 0.01$ and *** = $p < 0.001$.

Parameter	Species	Species x Day	Species (Subtype)	Subtype	Day	Subtype x Day
Stomatal Limitations (S_L)	** $F_{5,64}$= 3.4	n.s. $F_{10,64}$= 0.7	** $F_{4,64}$= 4.2	n.s. $F_{1,64}$= 0.75	*** $F2_{,64}$= 19	n.s. $F_{2,64}$= 1.3
Relative Stomatal Limitations (R_{SL})	n.s. $F_{5,64}$= 2.0	** $F_{10,64}$= 2.9	n.s. $F_{4,41}$= 1.9	n.s. $F_{1,64}$= 0.0	n.s. $F_{1.64}$= 2.2	* $F_{1,64}$= 3.5
Relative Metabolic Limitations (R_{ML})	n.s. $F_{5,41}$= 1.65	n.s. $F_{5,41}$= 1.73	n.s. $F_{4,41}$= 1.6	n.s. $F_{1,41}$= 0.06	*** $F_{1.41}$= 18.5	n.s. $F_{1.41}$= 0.00

Table 4.4: General Linear Model (GLM) results for stomatal limitations, relative stomatal limitations and relative metabolic limitations between Panicoideae and Aristidoideae NADP-Me photosynthetic subtypes exposed to drought treatments. * = $p < 0.05$, ** = $p < 0.01$ and *** = $p < 0.001$.

Parameter	Species	Species x Day	Species (Subfamily)	Subfamily	Day	Subfamily x Day
Stomatal Limitations (S_L)	*** $F_{5,64}$= 13.5	n.s. $F_{10,64}$= 1.1	*** $F_{4,64}$= 6.4	*** $F_{1,64}$= 50.4	** $F_{2,64}$= 5.3	n.s. $F_{2,64}$= 2.2
Relative Stomatal Limitations (R_{SL})	*** $F_{5,41}$= 21	* $F_{5.41}$= 2.6	** $F_{4,41}$= 4.6	*** $F_{1,41}$= 76	n.s. $F_{1,41}$= 1.7	n.s. $F_{1,41}$= 1.9
Relative Metabolic Limitations (R_{ML})	** $F_{5,41}$= 4	n.s. $F_{5,41}$= 2.1	n.s. $F_{4,41}$= 2.5	* $F_{1,41}$= 7.1	** $F_{1,41}$= 11.6	n.s. $F_{1,41}$= 3.3

4.3.6 Osmotic adjustment

Osmotic adjustment (*OA*) was calculated from the change in Ψ_π (osmotic potential) with drought stress. This was expressed in absolute terms or relative to the values for well-watered controls. All species showed some degree of *OA*, although this was not always significant. *H. contortus* showed the highest relative *OA* of 45.3% (Table 4.5). Statistically, the mean *OA* of subtype/subfamily groups were not different, as species within the groups showed a high degree of *OA* variability in response to

drought. Species from the Aristoid subfamily however all showed significant *OA* with the least variability.

Table 4.5: Average osmotic adjustment (*OA*) in MPa and the relative *OA* (%) for species (grouped by subfamily/subtype) used the drought experiment. n.s. (not significant), *= $p < 0.05$, **= $p < 0.01$ and ***= $p < 0.001$. n= 2-4 per species.

Subfamily (Subtype)	Species	*OA* (MPa)	Relative *OA* (%)
Panicoideae (NAD-Me)	*P. coloratum*	0.11 n.s.	7.8
	P. stapfianum	0.25 n.s.	17.4
	P. virgatum	0.59 ***	37.4
	Mean	**0.31**	**20.9**
Panicoideae (NADP-Me)	*A. semialata*	0.22 **	19.5
	H. contortus	1.05 *	45.3
	T. leucothrix	0.43 ***	23.1
	Mean	**0.57**	**29.3**
Aristidoideae (NADP-Me)	*A. congesta*	0.32 *	22.4
	A. diffusa	0.67 *	34.0
	A. junciformis	0.37 ***	23.4
	Mean	**0.45**	**26.6**

4.3.7 Relationship between metabolic limitations and osmotic adjustment

Relative metabolic limitations (R_{ML}) were significantly correlated to the degree that leaves osmotically adjusted (*OA*) during the drought phase of the experiment (Fig. 4.8 a). Species that had higher *OA* relative to the controls, showed less photosynthetic metabolic limitations. *Heteropogan contortus* was an outlier, which when removed from the regression analysis, dramatically changed the R^2 value from 0.5 to 0.75.

To determine which components of the photosynthetic metabolism were affected by *OA*, different relationships with relative *OA* were investigated. Mitochondrial respiration rates in the light (R_d), which is the y-intercept of the $A:C_i$ curves, showed a significant relationship of increasing R_d with decreasing *OA* (R^2= 0.6) when the outlier *H. contortus* was removed (Fig. 4.8 b). This was an indication that species which showed higher levels of *OA* maintained lower respiration rates, which may have reduced net carbohydrate consumption, i.e. glucose metabolism. Maximum Rubisco activity (V_{max}), which was derived from the saturated portion of the $A:C_i$ curve, showed a significant relationship of decreasing V_{max} with *OA* (R^2= 0.5) (Fig. 4.8 c). This implied that pyruvate (PEP)

regeneration rates were likely affected by the ability of a species to osmotically adjust (*OA*). In addition to parameters derived from A:C_i curves, *PSII* maximum efficiency (F_v'/F_m') (results from Chapter 2) was also shown to have a significant relationship to *OA* (R^2= 0.67) (Fig 4.8 d). Species that had higher *OA* therefore maintained higher F_v'/F_m' values, indicating that *OA* played a role in the maintenance of *PSII* photochemistry. In contrast, when *OA* was correlated to R_{SL} and S_L, no relationship (data not shown) was apparent, indicating that *OA* had no influence on stomatal limitations of photosynthesis. Absolute g_{ST} values calculated from gas exchange (results from Chapter 2) showed a significant relationship to *OA*, indicating changes to osmotic potential (Ψ_π) influenced stomatal responses (Fig 4.8 e). However, these correlative analyses must be treated with some caution as they might vary independently of one another as a common response to increasing drought.

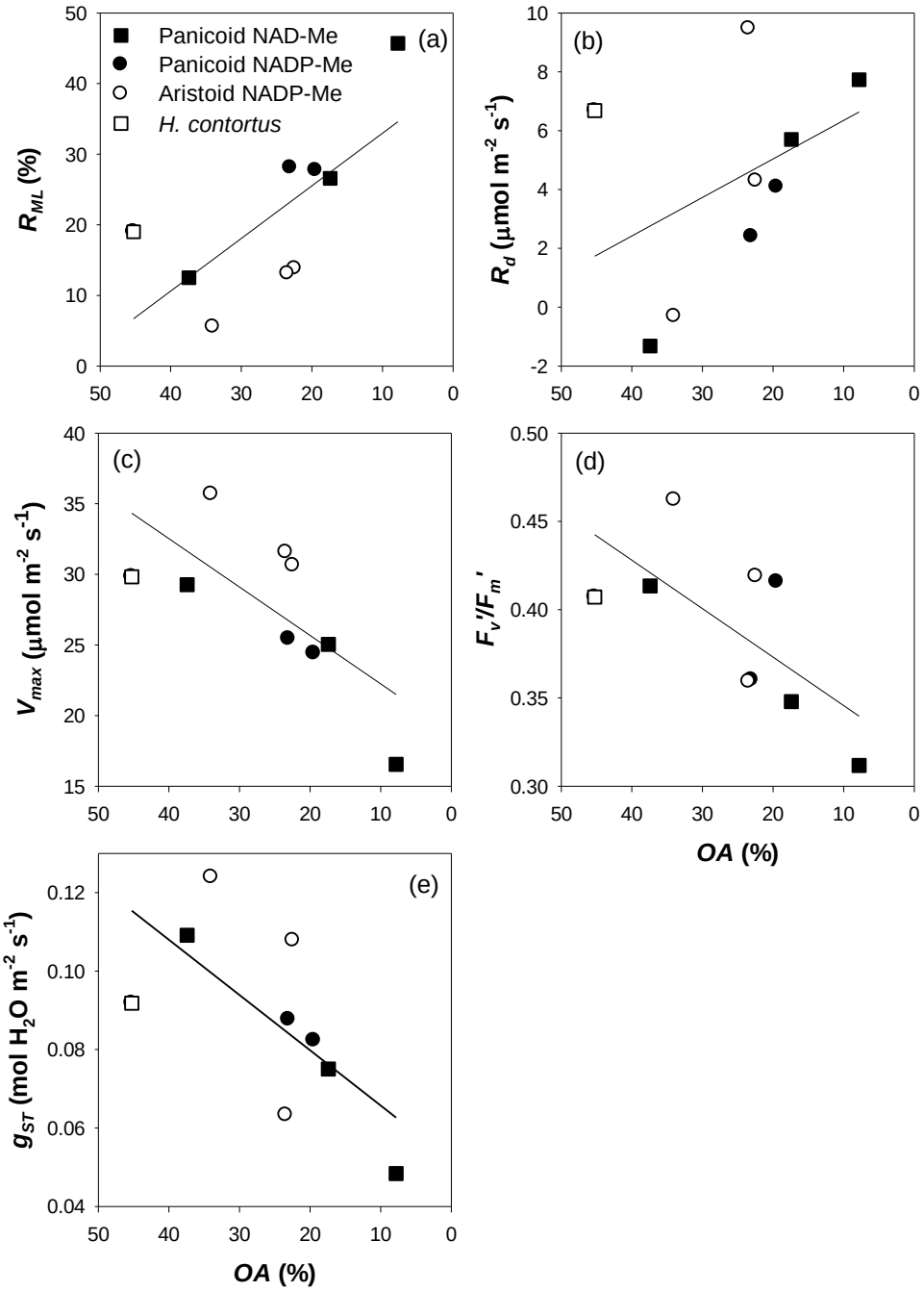

Figure 4.8: (a) Relative metabolic limitations (R_{ML}), (b) mitochondrial respiration (R_d), (c) maximum Rubisco activity (V_{max}), (d) *PSII* maximum efficiency (F_v'/F_m') and stomatal conductance (g_{ST}) at day 42 (~6.5% *SWC*) related to the relative osmotic adjustment (*OA*) of leaves during the drought experiment. Regression stats (a); (R^2= 0.5, p= 0.035), excluding *H. contortus* (R^2= 0.75, p= 0.0057), (b); (R^2= 0.17; p= 0.26), excluding *H. contortus* (R^2= 0.61, p= 0.022), (c) (R^2= 0.51, p= 0.03), excluding *H. contortus* (R^2= 0.66, p= 0.014;), (d); (R^2= 0.67, p= 0.047), excluding *H. contortus* (R^2= 0.76, p= 0.027) and (e); (R^2= 0.46; p= 0.046). Data points represent individual species means (n= 2-4). Species are grouped by subfamily and subtype and *H. contortus*, indicated by (□) symbol.

Chapter 2 indicated that species post-drought photosynthetic recovery was related to *PSII* photochemistry (F_v'/F_m') status during drought. It was therefore of interest to determine if F_v'/F_m' of water stressed leaves showed a relationship to metabolic limitations. Relative metabolic limitations (R_{ML}) were significantly correlated to the F_v'/F_m' (R^2= 0.6) (Fig. 4.8 a). Plants that maintained higher F_v'/F_m' values during drought showed less R_{ML} indicating that reduced *PSII* photochemistry performance contributed to the inhibition of photosynthetic metabolism. V_{max} values showed a significant decrease with decreasing F_v'/F_m' values (R^2= 0.6) which may indicate that the light reactions and ATP supply limited PEP regeneration or Rubisco activity.

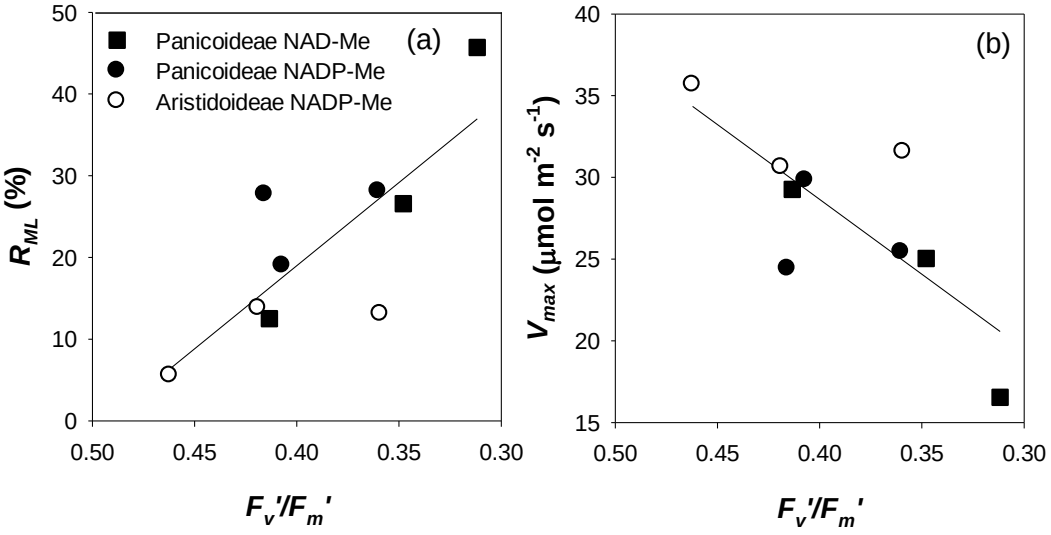

Figure 4.9: (a) Relative metabolic imitations (R_{ML}) and (b) maximum Rubisco activity (V_{max}) at day 42 (~6.5% *SWC*) related to the *PSII* maximum efficiency (F_v'/F_m') on the same day. Regression stats (a); (R^2= 0.61, p= 0.013) and (b); (R^2= 0.6, p=0.01). Data points represent individual species means (n= 2-4). Species are grouped by subfamily and subtype.

4.3.8 Turgor potential loss

The difference between the *RLWC* measured for control plants and the *RLWC* at which water stressed plants lost turgor (*TLP*), indicated the percentage of leaf water content that could be lost before the *TLP* resulted. The loss of leaf water content to reach *TLP* for Panicoid NAD-Me and NADP-Me species was 3.2 and 6.3%, respectively, and this difference was significant at p< 0.0001 (Table 4.6). The loss of leaf water content required to reach *TLP* for the Aristoid species was 2% (Table 4.6). This was an indication that under normal well-watered conditions, Aristoid species *RLWC* operated nearer the *TLP*, indicating that in these species, the change in leaf water content between near full turgor and

TLP is smaller. However osmotic adjustment (*OA*) may help maintain leaf water and also avoid turgor loss in Aristoids, whereas *OA* may not be as effective in Panicoids as they were unable to effectively maintain favourable leaf water status under drought.

Table 4.6: Species (grouped by subfamily/subtype) average turgor loss point (*TLP*) calculated from PV Curves represented as *RLWC* and the average *RLWC* of the control plants throughout the drought and recovery experiment. *TLP* and control *RLWC* were compared within each subfamily/subtype group using a *t*-Test.

Subfamily (Subtype)	Species	*RLWC*		*t*-Test result (*TLP* vs. Control)
		TLP	Control	
Panicoideae (NAD-Me)	*P. coloratum*	93.7 (0.053)	97.3 (0.49)	*t*-value= -7.1; df= 21; p< 0.000001
	P. stapfianum	92.5 (0.85)	96.7 (0.68)	
	P. virgatum	93.7 (0.13)	97.2 (0.9)	
	Mean	**93.3 (0.33)**	**97.1 (0.37)**	
Panicoideae (NADP-Me)	*A. semialata*	94.0 (1.47)	98.3 (0.26)	*t*-value= -7; df= 22; p< 0.000001
	H. contortus	90.1 (1.59)	97.0 (0.34)	
	T. leucothrix	88.9 (0.59)	96.6 (0.88)	
	Mean	**91.0 (1.0)**	**97.3 (0.36)**	
Aristidoideae (NADP-Me)	*A. congesta*	89.6 (0.18)	93.5 (0.07)	*t*-value= -2.7; df= 22; p= 0.013
	A. diffusa	94.0 (0.56)	94.7 (0.24)	
	A. junciformis	94.5 (1.03)	95.9 (0.15)	
	Mean	**92.7 (0.85)**	**94.7 (0.29)**	

Species *TLP* n= 3, Control n= 4-5 and Mean n= 9-15, ± SE in parenthesis.

The percentage loss of leaf water required to decrease turgor potential to zero (*TLP*) showed a significant relationship to R_{ML} when the outlier *P. coloratum* was removed (Fig. 4.9 a). This meant that species which were required to lose the largest relative volume of leaf water before turgor was lost, were more affected by metabolic limitations with progressive drought. R_{ML} showed a significant relationship to stomatal conductance (g_{ST}). Plants that operated with higher g_{ST} during drought exhibited the lowest R_{ML}. If the outlier *A. junciformis* was removed, the R^2 value increased from 0.6 to 0.96, indicating g_{ST} close association with metabolic limitations.

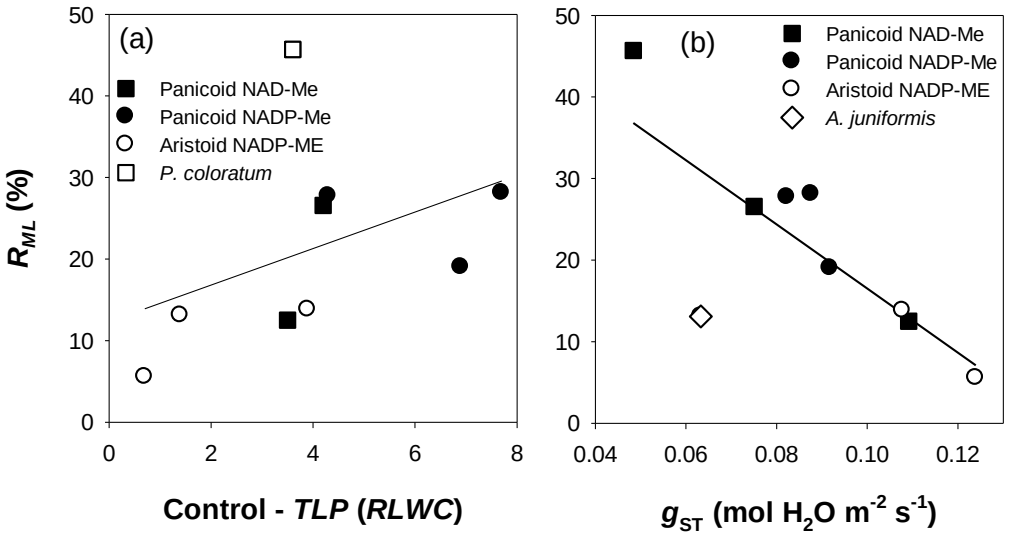

Figure 4.10: Relative metabolic limitations (R_{ML}) at day 42 (~6.5% *SWC*) related to (a) the percentage leaf water loss required to decrease turgor to zero and (b) stomatal conductance (g_{ST}) on the same day . Regression stats (a); (R^2= 0.17; p= 0.27) and excluding *P. coloratum* outlier (R^2= 0.52, p= 0.044) and (b); (R^2= 0.6; p= 0.014) and excluding *A. junicformis* outlier (R^2= 0.96; p= 0.00002). Data points represent an individual species (n= 2-4). Species are grouped by subfamily and subtype and (a) *P. coloratum* and (b) *A. junciformis* indicated by (□) and (◊) symbols respectively.

4.4 Discussion

As has been shown in much of the literature (Lawlor, 2002; Ghannoum *et al.*, 2003; Flexas *et al.*, 2006; Ibrahim *et al.*, 2008; Ripley *et al.*, 2007, 2010; Taylor *et al.*, 2011) the photosynthetic response to drought was a combination of reduced stomatal conductance (or increased stomatal limitation – S_L) and increased metabolic limitation (R_{ML}). For the Panicoideae species S_L increased two fold from day 10 to day 45, while the increase in R_{ML} between days 30 and 45 was more variable increasing between 2 to 8 fold depending on species (Fig. 4.7 d,i,n). In contrast, the Aristidoideae species showed little increase in S_L with drought, although these values were intrinsically higher than those for the Panicoid species at all levels of drought. The Aristidoideae species also showed the smallest increase in R_{ML}, which confirmed the findings in Chapter 2, showing their superior drought tolerance compared to the Panicoid NADP-Me species.

What was more notable was the degree to which species osmotic adjustment (*OA*) correlated to metabolic limitations, parameters derived from $A{:}C_i$ curves, chlorophyll fluorescence emission (F_v'/F_m') and stomatal conductance (g_{ST}). Previous studies have shown an association of *OA* to

drought tolerant species (Jones and Turner 1978; Girma and Krieg 1992; Nayyar, 2003; Kusaka *et al.*, 2005; Molinari *et al.*, 2007), however this result shows the direct effect of *OA* on photosynthetic metabolism. All the species used in this experiment showed a degree of *OA* which was comparable to results obtained for various C_4 species (Jones and Turner, 1978; Knapp, 1984; Williams and Black, 1994). Plants that osmotically adjusted, maintained higher stomatal conductance and demonstrated lower metabolic limitations. Increased osmotic adjustment meant that light reactions remained more functional (F_v'/F_m'), Rubisco activity (V_{max}) was higher, and plants had lower rates of mitochondrial respiration (R_d) (Fig. 4.8). Species that showed less *OA* suffered larger metabolic limitations, decreased light reaction performance, and Rubisco activity and rates of mitochondrial respiration (R_d) increased significantly with drought (Fig. 4.8).

At a species level, *OA* was correlated to photosynthetic parameters, however these parameters also showed subtype and lineage responses. Panicoid species (NADP-Me and NAD-Me) in this study supported the current literature (Lawlor 2002; Ghannoum *et al.*, 2003; Marques da Silva and Arrabaca, 2004; Ripley *et al.*, 2007, 2010) which showed that metabolic limitation was a significant contributor to the decline in photosynthesis in droughted C_4 grasses. Panicoid NAD-Me and NADP-Me species showed the same declines in metabolism (Fig. 4.7 n; Table 4.3), but subfamily differences were apparent when Panicoideae and Aristidoideae grasses were compared (Fig. 4.7 o; Table 4.3). Aristidoideae grasses suffered smaller metabolic limitations during drought, and lost leaf water at a slower rate compared to Panicoid species early in the drought because of lower g_{ST}. As drought progressed g_{ST} did not decrease as much as the Panicoid species, and leaf water was likely maintained by *OA* (Fig. 4.8 e). Despite these differences all species showed progressive changes with increasing drought from initial stomatal limitations to subsequent metabolic limitations.

Stomata limited photosynthesis during initial drought, but as drought advanced this became less important. This confirmed what Lawlor (2002) suggested, that as drought progresses past a threshold, metabolic limitations become more prevalent than stomatal limitations in C_4 plants. Between NADP-Me species, the Aristidoideae species photosynthetic decline was equally attributed to metabolic and stomatal limitations. This metabolic decline for Aristidoideae species was significantly lower than that of the Panicoid NADP-Me species. The Aristoid species response to drought was similar to that of C_3 grasses where the decline in photosynthesis was a combination of both stomatal and metabolic limitations (Ripley *et al.*, 2010), which contrasted the Panicoid species response which was dominated by non-stomatal limitations.

Photosynthetic biochemical parameters: V_{max}, k and R_d showed changes in response to drought, but these changes were not always significant and consistent within subtypes/subfamilies. All subtype/subfamily groups showed a significant decrease in maximum Rubisco activity (V_{max}),

although Aristoid species maintained higher values than the Panicoid NADP-Me species. V_{max} showed similar trends as R_{ML}, but this was to be expected as both parameters were derived from the saturated portion of the $A:C_i$ curves. Lawlor (2002) suggested that reductions in V_{max} are most likely due to RuBP limitations resulting from impaired ATP synthesis from progressive inactivation or loss of the Coupling Factor, due to increasing concentrations of ionic Mg^{2+}. Being C_4 species, V_{max} would also likely have been affected by limitations to PEP regeneration which relies on ATP for the reaction (von Caemmerer 2000).

Panicoid and Aristoid NADP-Me species showed a significant decline in the initial slope (*k*) which could be interpreted as a decrease in the C_4 cycle rate (PEPcase efficiency) (von Caemmerer, 2000). Within the Panicoid subtype comparison, *k* did not decline for NAD-Me species. This implied that under conditions of severe drought and limiting CO_2, NADP-Me Panicoideae and Aristitoideae species showed an analogous response of reduced C_4 cycle rates. The *k* response for Panicoid NADP-Me species in this study showed the same response as drought stressed Panicoideae NADP-Me species reported by Ripley *et al.*, (2010), indicating a uniform response amongst these species.

As has been demonstrated in previous studies (Flexas *et al.*, 2005; Atkin and Macherel, 2009), mitochondrial respiration (R_d) did not show a uniform drought response. Panicoid NAD-Me species showed an increase, while NADP-Me species showed no increase in response to severe drought. This increase in R_d for Panicoid NAD-Me species could reflect a change in energetic demands resulting from limitations to photosynthesis. Despite different metabolic limitations at severe drought, no change in R_d for NADP-Me Panicoideae and Aristoideae species indicated a strong subtype response which was likely related to their underlying photosynthetic biochemistry. These results confirmed what Flexas *et al.*, (2005) suggested, that drought may alter R_d but it would not be totally impaired.

As the chlorophyll fluorescence emission, F_v'/F_m' showed a correlation to photosynthetic recovery (Chapter 2), it was therefore of interest to determine if the light reactions showed an association to photosynthetic metabolism. Results here showed a relationship of photosynthetic metabolic parameters R_{ML} and V_{max} to F_v'/F_m'. Panicoid and Aristoid NADP-Me species showed distinct responses which were grouped along the regression, whereas Panicoid NAD-Me species showed stronger species responses. Species that maintained higher F_v'/F_m' performance showed less metabolic limitations (R_{ML}) and higher V_{max} values. These correlations of metabolism to F_v'/F_m' demonstrated that as light adapted *PSII* activity decreased, the photosynthetic metabolism decreased. It could however be argued that the decreases in these metabolic processes caused the down-regulation of *PSII* photochemistry. Lu and Zhang, (1999) suggested that in water stressed wheat (C_3) leaves, reduced F_v'/F_m' was attributed to down-regulation of the photosynthetic electron chain to

match a decrease in CO_2 assimilation. Results from Chapter 2 suggested the link of decreased F_v'/F_m' to active/inactive xanthophyll cycling.

Results showed that species which operated at higher leaf water contents tended to osmotically adjust the most, maintain leaf water potential (Ψ_{leaf}), and maintain more positive stomatal conductance during moderate to severe drought. It is also these species that were required to lose the least amount of leaf water before turgor was lost. Aristoid species were required to lose the least amount of water (2%) before turgor was lost and it was these species that were consistently capable of higher *OA* and showed the least R_{ML}. Panicoid species showed larger decreases in leaf water (3.8 – 6.3%) before turgor was lost and they were less capable of *OA* and showed more R_{ML} under drought stress conditions. There was however some species variability in this response. Leaf water results from Chapter 2 showed that at ~6.5% *SWC*, Aristoid species maintained *RLWC* significantly higher than the Panicoid NADP-Me species, which may be an indication that the Aristoid species maintained *RLWC* above or just within the turgor loss range under drought conditions. This indicated possible leaf water sensitivity under drought conditions in the Aristoid species, and was likely mitigated by *OA*. Panicoid species tended to show less sensitivity in leaf water to decreasing *SWC*, and low *RLWC* during drought indicated that *OA* was possibly less effective in mitigating leaf dehydration. These linear correlations between leaf water status and photosynthetic performance suggest a continuum in response from species that are isohydric to those that are anisohydric (McDowell *et al.,* 2008).

The Aristoid species tended to show properties associated with anisohydric plants, which keep their stomata open, irrespective of Ψ_{leaf}, and maintain higher photosynthetic rates during mild to moderate drought conditions. Anisohydric plants are generally accepted as drought tolerant (McDowell *et al.,* 2008). Panicoid species tended to resemble the behaviour of isohydric plants, which operate at lower stomatal conductances during drought to maintain constant leaf water potentials, resulting in lower photosynthetic rates under drought situations (McDowell *et al.,* 2008; Sade *et al*., 2012). Isohydric regulation is seen as a mechanism to avoid hydraulic failure (cavitation), whereas anisohydric plants are vulnerable to hydraulic failure due to small hydraulic safety margins during drought episodes (McDowell *et al.,* 2008). Aristioid species shown here however maintained high leaf water contents during drought, thereby mitigating the effects of cavitation. Ogle *et al.,* (2012) suggested an anisohydric response for *Heteropogon contortus* (Panicoid NADP-Me) as it exhibited minimal stomatal response to decreasing Ψ_{soil} and vapour pressure deficits (VPD). Stomatal conductance values for H. contortus from this study support this idea, however it showed some of the lowest *RLWC* and Ψ_{leaf}, which is not indicative of anisohydric regulation. Furthermore it has been shown that under severe drought conditions, isohydric and anisohydric grasses showed little difference in their photosynthetic responses (Alvarez *et al.,* 2007), and results here showed that the Panicoid and Aristoid species all responded similarly at severe drought (~3.5% *SWC*).

Aristoid species showed greater drought tolerance when compared to the Panicoid species, this being evident by their less impaired photosynthetic metabolism. Results indicated that this was achieved by osmotic adjustment, which likely maintained higher leaf water status, subsequently sustaining physiological processes (Jones and Turner, 1978; *Zhang et al.*, 1999). Results also showed no evidence of a threshold at the *TLP* where metabolism declined. Furthermore, phylogenetic groups or photosynthetic subtype responses were not always uniform, with the exception of the Aristidoideae species, which showed the least variability in stomatal and metabolic responses. By increasing the sampling of Aristidoideae species, their drought responses should show consistent differences to the Panicoideae species.

Chapter 5
General Discussion

5.1 Introduction

The main aim of this study was to determine the photosynthetic drought tolerance and recovery responses amongst C_4 grasses from different photosynthetic subtypes and phylogenetic clades, and the mechanism/s that govern these responses. This was done by comparing plants with different photosynthetic subtypes from the same lineage (Panicoideae) and plants sharing the same biochemistry (NADP-Me), but from different lineages (Panicoideae and Aristoideae). Treatment plants were subject to a progressive dry-down over a period of 58 days upon which they were re-watered and maintained in a well-watered state. At select intervals during the progressive drought and recovery phases, parameters such as gas exchange, chlorophyll fluorescence emissions, CO_2 response curves and leaf water status were measured. In addition to the progressive drought experiment, a second drought experiment was conducted on *Zea mays* to determine if photosynthetic metabolic loss was related to the loss of turgor. Owing to the natural distributions of C_4 grasses within South Africa and their association to rainfall gradients, it was hypothesised that Panicoid NAD-Me and Aristoid NADP-Me species would exhibit greater drought tolerance over Panicoid NADP-Me species. The differences in lineage recovery from drought would be related to the magnitude of metabolic limitations, and that metabolic limitations would be inversely related to the ability to maintain favourable leaf water status during severe drought.

The main finding from the progressive drought experiment was that Aristoid species exhibited the greatest photosynthetic (*A*) drought tolerance and fastest photosynthetic recovery upon re-watering in comparison to Panicoid NADP-Me species. This drought tolerance was linked to a low level of metabolic inhibition, and this study for the first time showed that osmotic adjustment (*OA*) was inversely related to photosynthetic metabolic limitations. By increasing *OA* and avoiding metabolic limitations, Aristoid species were able to achieve this drought tolerance while operating at higher stomatal conductances under severe drought (Fig. 4.8 a). Aristoid species also maintained high leaf water potentials (Ψ_{leaf}) and relative leaf water contents (*RLWC*) throughout the drought (Fig. 2.3). This drought response also supported the Aristoid species biogeography in South Africa, whereby xeric areas tend to have a higher number of species of *Aristida* as opposed to mesic areas (Visser *et al.*, 2012).

Further findings from the progressive drought and recovery experiment indicated a photosynthetic subtype by subfamily interaction. Although Panicoid NADP-Me and NAD-Me species showed

similar responses during the drought phase of the experiment, NAD-Me species showed significantly faster recovery rates (Fig. 2.4 & 2.5). Ghannoum *et al.*, (2002) showed that during drought, NAD-Me species increased their *WUE* relative to the NADP-Me species, however this result was complicated by phylogeny as most NAD-Me species used were from the Chloridoideae subfamily. Results from the subfamily comparison using NADP-Me species supported the hypothesis that species from Aristidoideae were more drought tolerant and recovered faster than species belonging to Panicoideae. Panicoideae NAD-Me and Aristidoideae species which maintained high *RLWC* during drought showed significantly faster recovery rates, as opposed to Panicoid NADP-Me species which had slow photosynthetic recovery rates which were correlated to severely dehydrated leaves at full drought. The mechanisms for differences in response to, and recovery from drought, were related to differences in stomatal and metabolic limitations to photosynthesis.

5.2 Metabolic or stomatal limitations

Research has demonstrated that in the majority of drought experiments conducted on C_4 grasses, stomatal limitations initially affected the photosynthetic decline until a *RLWC* threshold was encountered, after which metabolic limitations were the major contributor to photosynthetic decline (Ghannoum, 2003; Ripley *et al.*, 2007, 2010). In this experiment, Panicoid species (NAD-Me and NADP-Me) demonstrated greater metabolic limitations (R_{ML}) than Aristoid species, and consequently it was the Panicoid species which showed greater susceptibility to drought compared to the Aristoid species. Metabolic limitations for the Panicoid species were approximately 25% at a *SWC* of ~6.5%, whereas the stomatal (R_{SL}) influence was less than 10% for NAD-Me and negligible for NADP-Me species, with these R_{SL} values being no different to initial well-watered R_{SL} values (Fig. 4.6). This was an indication that metabolism was almost wholly responsible for the drought induced photosynthetic decline. At the same *SWC* of ~6.5%, Aristoid species had still not shown a significant decline in photosynthesis, and similarly R_{ML} was less than 10% as was R_{SL}. Neither R_{ML} nor R_{SL} values were different to their initial well-watered values, indicating the exceptional drought tolerance of Aristoid species. All species however ceased photosynthetic activity by the end of the drought treatment (Day 56; ~3.5% *SWC*), and this would have been due to the observed metabolic limitations, full stomatal closure and photosynthetic down-regulation processes (Lawlor, 2002). Results from the rapid drought experiment using *Z. mays* (Panicoid NADP-Me) showed the same response as the Panicoid species whereby R_{ML} was almost entirely responsible for the decline in photosynthesis (Fig. 3.6). At the same *SWC* of ~6.5%, both the Panicoid species and the *Z. mays* plants had comparable R_{ML} values, which were not different at 25% (SE ± 4.7) and 30% (SE ± 2.3), respectively. This was a good indication of how two very different experiments yielded the same results for different species from the same lineage, which highlights the notion of phylogenetic conservatism (Webb, 2000; Donoghue, 2008).

Photosynthetic recovery showed a subtype by subfamily response, whereby NAD-Me and Aristoid species recovered significantly faster than Panicoid NADP-Me species. Although NAD-Me species did not show a full recovery after three days (day 61) of being re-watered, their photosynthetic rates were significantly higher than that of the Panicoid NADP-Me species (Fig. 2.6). Metabolic limitations were likely responsible for the slow recovery of Panicoid NADP-Me species as intercellular CO_2 concentrations (C_i) at day 61 measured 208 μmol mol^{-1}, while stomotal conductance (g_{ST}) values were no different to the NAD-Me species (Fig 2.6). This was an indication that photosynthetic processess were unable to utilise the available intercellular CO_2, and hence draw the C_i down to values of 108 μmol mol^{-1} CO_2 seen for NAD-Me and Aristoid species alike.

5.3 Mechanisms

5.3.1 Osmotic adjustment and the C_4 cycle

Various leaf physiological criteria were investigated to determine possible mechanisms responsible for photosynthetic metabolic impairment in response to drought. A major finding was the link of osmotic adjustment (*OA*) to photosynthetic metabolic limitations (R_{ML}). At a subtype/subfamily level there was some variability within the groups, but at a species level there was a significant relationship whereby increasing *OA* was associated with lower R_{ML} (Fig. 4.8 a). It is well documented that plants utilise *OA* as a mechanism to maintain leaf turgor potential by lowering the leaf water potential in response to drought. This allows cells to maintain important metabolic processes such as photosynthesis (Jones and Turner, 1978; Michelena and Boyer, 1982; Girma and Krieg, 1992; Baruch and Fernández, 1993; Williams and Black, 1994). Findings from the *Zea mays* experiment (Fig. 3.6) however showed no real link between turgor loss and metabolic loss, instead indicating the role of *OA* in maintaining favourable leaf water statuses, as opposed to sustaining leaf turgor potential. These findings have highlighted the link of *OA* to drought tolerance like previous studies (Jones and Turner, 1978; Baruch and Fernandez, 1993), however results here demonstrated that *OA* plays a role in the maintenance of photosynthetic metabolism in C_4 grasses.

Results for PEPcase efficiency (k) and mitochondrial respiration (R_d) showed subtype trends despite different levels of metabolic impairment amongst these subtypes. Panicoideae species showed similar metabolic limitations in response to drought, but k and R_d trends were different between the NADP-Me and NAD-Me species (Fig. 4.5). Conversely, NADP-Me species from the Panicoideae and Aristidoideae subfamilies showed different metabolic responses, but the same trends for k and R_d. This was possibly due to the different energetic demands between NADP-me and NAD-Me species (Furbank, 2011), which became important under conditions of limiting CO_2 and water stress. All

groups showed a reduction in Rubisco velocity (V_{max}) as drought progressed. At a species level, V_{max} showed a significant relationship with decreasing *OA* (Fig. 4.8 c). This was an indication of the grasses ability to maintain maximum Rubisco activity and PEP regeneration (von Caemmerer 2000; Lawlor, 2002) under water stress by *OA*. Mitochondrial respiration (R_d) also showed a relationship to *OA* whereby increased *OA* was associated with decreased R_d, but biological interpretation of this result would require further investigation.

5.3.2 Chlorophyll fluorescence

Chlorophyll fluorescence emission parameter F_v'/F_m' (*PSII* maximum efficiency) showed associations to photosynthetic metabolic responses and leaf water relations during the drought and recovery phases of the experiment. Maintenance of light reactions (F_v'/F_m') showed relationships to leaf water content and osmotic adjustment (*OA*). By keeping the leaves hydrated during severe drought, it appears the *PSII* performance was less impaired. Species which maintained higher F_v'/F_m' values during drought showed lower metabolic limitations and less inhibited maximum Rubisco activity (Fig. 4.9). These species also showed the fastest photosynthetic recovery upon re-watering, and this relationship showed a subtype and subfamily effect where Panicoid NAD-Me and Aristoid species recovered faster than the Panicoid NADP-Me species.

Analysis of F_v'/F_m' parameters indicated a possible link to increased xanthophyll cycling for NAD-Me and Aristidoideae species. All species showed a similar decline in relative F_m', which is generally interpreted as decreased photochemistry (Baker, 2008), however the afore mentioned groups showed a larger relative decrease in F_o'. A decrease in F_o' could be associated with heat dissipation, the net result of the xanthophyll cycle (Armond *et al.*, 1980). Panicoid NADP-Me species which demonstrated a smaller relative decrease in F_o' compared to NAD-Me and Aristoid species, could possibly be interpreted as a dissociation of the light harvesting complex of *PSII* reaction centres and subsequent degradation (Armond *et al.*, 1980; Efeoğlu *et al.*, 2009). However as no direct measurements of the xanthophyll cycle were performed, the above interpretation using chlorophyll fluorescence parameters is merely proposed.

5.4 Ecological implications

From an ecological perspective, changes in southern African climate patterns may very well affect the distribution of these C_4 grasses and additionally the species composition of these grasslands. Grasslands ecosystems are particularly sensitive, as changes to species compositions from altered selective pressures are exacerbated by these species short life histories (Smith and Donoghue, 2008).

Climate models have predicted desertification expanding west to east in South Africa (Shongwe *et al.*, 2009; IPCC 5, 2013). Results here have shown Aristidoideae species are more drought tolerant than other lineages and we predict that the shift in drought may allow this lineage to expand eastwards, thereby outcompeting Panicoideae species. Furthermore, mesic grasslands that contain a higher percentage of Panicoids species may become vulnerable to changes in functional type compositions where increased duration and severity of drought events (Christinson *et al.*, 2007) could favour the more drought tolerant Aristoid species.

5.5 Conclusion

Photosynthetic results indicated a stronger phylogenetic response to drought compared to photosynthetic subtype. Aristoid species exhibited greater drought tolerance over Panicoid NADP-Me species. Amongst Panicoid species, both NADP-Me and NAD-Me species showed the same drought responses. Post-drought photosynthetic recovery showed a subtype by subfamily interaction where Panicoid NAD-Me and Aristioid species showed faster recovery rates compared to Panicoideae NADP-Me species. Photosynthetic recovery was linked to the maintenance of leaf water contents and light reaction performance (*PSII*) during severe drought and this showed distinct subtype by subfamily responses. This indicated that species within these groups which were able to limit leaf dehydration maintained greater light reaction performance. Furthermore, plants that osmotically adjusted maintained leaf water potential, higher stomatal conductances and consequently experienced less metabolic limitations. This response was most prevalent in the Aristidoideae species. By osmotically adjusting, key metabolic process such as Rubisco activity (and/or PEP regeneration) and light reaction performance were maintained, and allowed photosynthesis to continue under conditions of decreasing soil water. The relationship of metabolic limitations to osmotic adjustment showed species responses, although the Aristidoideae species showed a more uniform response than the Paincoideae species. Patterns entirely confined to phylogenetic groups or photosynthetic subtypes were not always distinct, but Aristidoideae species showed the least variability in both stomatal and metabolic responses, and more sampling of Aristidoideae should show that their drought response are consistently different to that of the Panicoideae. Moreover, results presented here offer a mechanistic explanation to the biogeographic distributions of the Aristidoideae, which are mostly NADP-Me or C_3 species, and their ability to cope in arid environments.

5.6 References

Alfonso S.U., Brüggemann W. 2012. Photosynthetic responses of a C_3 and three C_4 species of the genus *Panicum* (s.l.) with different metabolic subtypes to drought stress. *Photosynthetic Research* 112: 175-191.

Alvarez E., Scheiber S.M., Beeson R.C., Sandrock D.R. 2007. Drought tolerance responses of purple Lovegrass and 'Adagio' maiden grass. *HortScience* 42: 1695-1699.

Armond P.A., Björkman O., Staehelin L.A. 1980. Dissociation of supramolecular complexes in chloroplast membranes: A manifestation of heat damage to the photosynthetic apparatus. *Biochimica et Biophysica Acta* 601: 433–462.

Asada K. 2006. Production and scavenging of reactive oxygen species in chloroplasts and their functions. *Plant Physiology* 141: 391-396.

Atkin O.K., Macherel D. 2009. The crucial role of plant mitochondria in orchestrating drought tolerance. *Annals of Botany* 103: 581-597.

Badger M.R., von Caemmerer S., Ruuska S., Nakano H. 2000. Electron flow to oxygen in higher plants and algae: rates and control of direct photoreduction (Mehler reaction) and rubisco oxygenase. *Philosophical Transactions of the Royal Society B* 355: 1433-1446.

Baker N.R., 2008. Chlorophyll Fluorescence: A Probe of Photosynthesis In Vivo. *Annual Revue of Plant Biology* 59: 89–113.

Barney J.N., Mann J.J., Kyser G.B., Blumwald E., Van Deynze A., DiTomasa J.M. 2009. Tolerance of switchgrass to extreme soil moisture stress: Ecological implications. *Plant Science* 177: 724-732.

Baruch Z., Fernández D.S. 1993. Water relations of native and introduced C_4 grasses in a neotropical savanna. *Oecologia* 96: 179-185.

Batanouny K.H., Stichler W., Ziegler H. 1988. Photosynthetic pathways, distribution, and ecological characteristics of grass species in Egypt. *Oecologia* 75: 539-548.

Becker T.W., Fock H.P. 1986. Effects of water stress on the gas exchange, the activities of some enzymes of carbon and nitrogen metabolism, and on the pool sizes of some organic acids in maize leaves. *Photosynthesis Research* 8: 175–181.

Bernacchi C.J., Pimentel C., Long S.P. 2003. *In vivo* temperature response functions of parameters required to model RuBP-limited photosynthesis. *Plant, Cell and Environment* 26: 1419-1430.

Berner R.A., Kothavala Z. 2001. GEOCARB III: A revised model of atmospheric CO_2 over Phanerozoic time. *American Journal of Science* 304: 397–437.

Bilska A., Sowiński P. 2010. Closure of plasmodesmata in maize (*Zea mays*) at low temperature: a new mechanism for inhibition of photosynthesis. *Annals of Botany* 106: 675-686.

Blackman L.M., Overall R.L. 2001. Structure and function of plasmodesmata. *Australian Journal of Plant Physiology* 28: 709-727.

Bond W.J. 2008. What limits trees in C_4 grasslands and savannas? *Annual Review of Ecology, Evolution, and Systematics* 39: 641-659..

Botha C.E.J., Cross R.H.M., van Bel A.J.E., Peter C.I., 2000. Phloem loading in the sucrose-export-defective (*SXD-1*) mutant maize is limited by callose deposition at plasmodesmata in bundle sheath vascular parenchyma interface. *Protoplasma* 214: 65-72.

Boutton T.W., Hamson A.T., Smith B.N. 1980. Distribution of biomass of species differing in photosynthetic pathway along an altitudinal transect in southeastern Wyoming grassland. *Oecologia* 45: 287-298.

Bowman J.L., Smyth D.R., Meyerowitz E.M. 1989. Genes directing flower development in Arabidopsis. *Plant Cell* 1: 37-52.

Brown P.S., Knievel D.P., Pell E.J. 1995. Effects of moderate drought on ascorbate peroxidase and glutathione reductase activities in mesophyll and bundle sheath cells of maize. *Physiologia Plantarum* 95: 274–280.

Brown R.H. 1999. Agronomic implications of C_4 photosynthesis. In: Sage R.F., Monson, R.K., eds. *C_4 Plant Biology*. Academic Press, San Diego, CA, USA. p. 473-503.

Brugnoli E., De Tullio M.C., Monteverdi M.C., Lauteri M., Scartazza A. 1995. Xanthophyll cycle components and energy dissipation in sun and shade leaves of C_3 and C_4 plants. In: Mathis P., ed. *Photosynthesis: From Light to Biosphere Vol. IV*. Kluwer Academic Publishers, Dordrecht, The Netherlands. P. 79–82.

Cabido M., Pons E., Cantero J.J., Lewis J.B., Anton A. 2008. Photosynthetic pathway variation among C_4 grasses along a precipitation gradient in Argentina. *Journal of Biogeography* 35: 131-140.

Carmo-Silva A.E., Soares A.S., Marques da Silva J., Bernardes da Silva A., Keys A.J., Arrabaça M.C. 2007. Photosynthetic response of three C_4 grasses of different metabolic subtypes to water deficit. *Functional Plant Biology* 34: 204-213.

Carmo-Silva A.E., Keys A.J., Andralojc P.J., Powers S.J., Arrabaça., Parry M.A.J. 2010. Rubisco activities, properties, and regulation in three different C_4 grasses under drought. *Journal of Experimental Botany* 61: 2355–2366.

Carmo-Silva A.E., da Silva A.B., Keys A.J., Parry M.A.J., Arrabaça M.A. 2008. The activities of PEP carboxylase and the C_4 acid decarboxylases are little changed by drought stress in three C_4 grasses of different subtypes. *Photosynthesis Research* 97: 223-233.

Cerros-Tlatilpa R., Columbus J.T., Barker N.P. 2011. Phylogenetic relationship of *Arsitida* and relatives (Poaceae, Aristidoideae) based on noncoding chloroplast (*TRNL-F, RPL16*) and nuclear (ITS) DNA sequences. *American Journal of Botany* 98: 1868-1886.

Christin P.A., Besnard G., Samaritani E., Duvall M.R., Hodkinson T.R., Savolainen V., Salamin N. 2008. Oligocene CO_2 decline promoted C_4 photosynthesis in grasses. *Current Biology* 18: 37-43.

Christin P.A., Salamin N., Kellog E.A., Vicentini A,. Besnard G. 2009. Integrating phylogeny into studies of C_4 variation in the grasses. *Plant Physiology* 149: 82-87.

Christensen J.H., Hewitson B., Busuioc A., Chen A., Gao X., Held I., Jones R., Kolli R.K., Kwon W.-T., Laprise R., Magaña Rueda V., Mearns L., Menéndez C.G., Räisänen J., Rinke A., Sarr A., Whetton P. 2007. Regional Climate Projections. In: *Climate Change 2007: The Physical Science Basis. Contribution of Working Group I to the Fourth Assessment Report of the Intergovernmental Panel on Climate Change* [Solomon, S., Qin D., Manning M., Chen Z., Marquis M., Averyt K.B., Tignor M., Miller H.L. (eds.)]. Cambridge University Press, Cambridge, United Kingdom and New York, NY, USA.

Clifford S.C., Arndt S.K., Corlett J.E., Joshi S., Sankhla N., Popp M., Jones H.G. 1998. The role of solute accumulation, osmotic adjustment and changes in cell wall elasticity in drought tolerance in *Ziziphus mauritiana* (Lamk.). *Journal of Experimental Botany* 49: 967–977.

Cornic G. 2000. Drought stress inhibits photosynthesis by decreasing stomatal aperture not by affecting ATP synthesis. *Trends in Plant Sciences* 5: 187-188.

Cornic G., Fresneau C. 2002. Photosynthetic carbon reduction and carbon oxidation cycles are the main electron sinks for Photosystem II activity during a mild drought. *Annnals of Botany* 89: 887-894.

DeCosta M., Huang B. 2006. Integrating phylogeny into studies of C_4 variation in the grasses. *Journal of the American Society for Horticultural Science* 131: 338-344.

Dengler N.G., Dengler R.E., Donnelly P.M., Hattersley P.W. 1994. Quantitative leaf anatomy of C_3 and C_4 grasses (Poaceae): Bundle sheath and mesophyll surface area relationships. *Annals of Botany* 73: 242-255.

Donoghue M.J. 2008. Colloquium paper: a phylogenetic perspective on the distribution of plant diversity. *Proceedings of the National Academy of Sciences of the USA* 105: 11549-11555.

Du Y.C., Kawamitsu Y., Nose A., Hiyane S., Murayama S., Wasno K., Uchida Y. 1996. Effects of water stress on carbon exchange rate and activities of photosynthetic enzymes in leaves of sugarcane (*Saccharum spp*.). *Australian Journal of Plant Physiology* 23: 719-726.

Edwards E.J., Smith S.A. 2010. Phylogenetic analyses reveal the shady history of C_4 grasses. *Proceedings of the National Academy of Sciences* 107: 2532-2537.

Edwards E.J. 2012. New grass phylogeny resolves deep evolutionary relationships and discovers C_4 origins: Grass Phylogeny Working Group II. *New Phytologist* 193: 302-312.

Efeoğlu B., Ekmekçi Y., Çiçek N. 2009. Physiological responses of three maize cultivars to drought stress and recovery. *South African Journal of Botany* 75: 34-42.

Ehleringer J.R., Bjorkman O. 1977. Quantum yields for CO_2 uptake in C_3 and C_4 plants. *Plant Physiology* 59: 86-90.

Ehleringer J.R., Pearcy R.W. 1983. Variation in quantum yield for CO_2 uptake among C_3 and C_4 plants. *Plant Physiology* 73: 555-559.

Ehleringer J.R., Cerling T.E., Helliker B.R. 1997. C_4 photosynthesis, atmospheric CO_2, and climate. *Oecologia* 112: 285-299.

Ehleringer J.R. 1978. Implications of quantum yield differences on the distributions of C_3 and C4 grasses. *Oecologia* 31: 255-267.

Ehleringer J.R., Monson R.K. 1993. Evolutionary and ecological aspects of photosynthetic pathway variation. *Annual Review of Ecology and Systematics* 24: 411-439.

Ellis R.P. Vogel J.C. and Fuls A. 1980. Photosynthetic pathways and the geographical distribution of grasses in South West Africa/Namibia. *South African Journal of Science* 76: 307-312.

Fairbanks D.H.K., Thompson N.W., Vink D.E., Newby T.S., ven den Burg H.M,. Everard D.A. 2000. The South African land-cover characteristics database: a synopsis of the landscape. *South African Journal of Science* 96: 69-82.

Farquhar G.D., Sharkey T.D. 1982. Stomatal conductance and photosynthesis. *Annual Review of Plant Physiology* 33: 317-345.

Flexas J., Medrano H. 2002. Drought-inhibition of photosynthesis in C_3 plants: Stomatal and non-stomatal limitations revisited. *Annals of Botany* 89: 183-189.

Flexas J., Bota J., Cifre J., Escalona M.J., Galmés J., Gulias J., Lefi E.L., Martínez-Canellas S.F., Moreno M.T., Ribas-Carbó M., Riera D., Sampol B., Medrano H. 2004 Understanding down-regulation of photosynthesis under water stress: future prospects and searching for physiological tools for irrigation management. *Annals of Applied Biology* 144: 273-283.

Flexas J., Bota J., Galmés J., Medrano H., Ribas-Carbó M. 2006. Keeping a positive carbon balance under adverse conditions: responses of photosynthesis and respiration to water stress. *Physiological Plantarum* 127: 343-352.

Foyer C.H., Shigeoka S. 1998. Understanding oxidative stress and antioxidant functions to enhance photosynthesis. *Plant Physiology* 155: 93-100.

Fravolini A., Williams D.G., Thompson T.L. 2002. Carbon isotope discrimination and bundle sheath leakiness in three C_4 subtypes grown under variable nitrogen, water and atmospheric CO_2 supply. *Journal of Experimental Botany* 53: 2261-2269.

Furbank R.T., Hatch M.D. 1987. Mechanism of C_4 photosynthesis: the size and composition of the inorganic carbon pool in bundle sheath cells. *Plant Physiology* 85: 958-964

Furbank R.T. 1998. C_4 Pathway. In: Raghavendra A.S., ed. *Photosynthesis; a Comprehensive Treatise*. Cambridge University Press, Cambridge, UK. p. 123–135.

Furbank R.T. 2011. Evolution of the C_4 photosynthetic mechanism: are there really three C_4 acid decarboxylation types? *Journal of Experimental Botany* 62: 3102-3108.

Ghannoum O., von Caemmerer S., Conroy J.P. 2001. Carbon and water economy of Australian NAD-ME and NADP-ME C_4 grasses. *Australian Journal of Plant Physiology* 28: 213-223.

Ghannoum O., von Caemmerer S., Conroy J.P. 2002. The effect of drought on plant water use efficiency of nine NAD-ME and nine NADP-ME Australian C_4 grasses. *Functional Plant Biology* 29: 1337-1348.

Ghannoum O., Conroy J.P., Driscoll S.P., Paul M.J., Foyer C.H., Lawlor D.W. 2003. Nonstomatal limitations are responsible for drought-induced photosynthetic inhibition in four C_4 grasses. *New Phytologist* 159: 599-608.

Ghannoum O. 2009. C_4 photosynthesis and water stress. *Annals of Botany.* 103: 635-644.

Gibbs Russell G.E., Watson L., Koekemoer M., Smook L., Barker N.P., Anderson H.M., Dallwitz M.J. 1991. *Grasses of Southern Africa*. National Botanical Gardens / Botanical Research Institute. South Africa.

Girma F.S., Krieg D.R. 1992. Osmotic Adjustment in *Sorghum*: 1. Mechanisms of Diurnal Osmotic Potential Changes. *Plant Physiology* 99: 577-582.

Gonzalez L., Rogers M.J.R. 2003. Plant water status. In: Reigosa Roger M.J., ed. *Handbook of Plant Ecophysiology Techniques*. Kluwer Academic Publishers. New York, USA. p 185-191.

SANBI. 2014. Grazing and Burning Guidelines: Managing Grasslands for Biodiversity and Livestock Production. Compiled by Lechmere-Oertel, R.G. South African National Biodiversity Institute, Pretoria. 42 pages.

Griffiths H., Weller G., Toy L.F.M., Dennis R.J. 2012. You're so vein: bundle sheath physiology, phylogeny and evolution in C_3 and C_4 plants. *Plant, Cell and Environment* 36: 249-261.

Hare P.D., Cress W.A., van Staden J. 1998. Dissecting the roles of osmolyte accumulation during stress. *Plant, Cell and Environment* 21: 535-553.

Hatch M.D., Kagawa T., Craig S. 1975. Subdivision of C_4 pathway species based on differing C_4 acid decarboxylating systems and ultrastructural features. *Australian Journal of Plant Physiology* 2: 111-128.

Hatch M.D., Agostino A., Jenkins C.L.D. 1996. Measurement of the leakage of CO_2 from bundle-sheath cells of leaves during C_4 photosynthesis. *Plant Physiology* 108: 173-181.

Hatch M.D., Slack C.R. 1970. Photosynthetic CO_2-fixation pathways. *Annual Review of Plant Physiology* 21: 141-162.

Hattersley P.W. 1983. The distribution of C_3 and C_4 grasses in Australia in relation to climate. *Oecologia* 57: 113-128.

Hattersley P.W. 1984. Characterization of C_4 type leaf anatomy in grasses (Poaceae). Mesophyll:bundle sheath area ratios. *Annals of Botany* 53: 163-179.

Hibberd J.M., Covshoff S. 2010. The regulation of gene expression required for C_4 photosynthesis. *Annual Review of Plant Biology* 61: 181-207.

Huber M, Caballero R. 2011. The early Eocene equable climate problem revisited. *Climate of the Past* 7: 603–33.

Ibrahim D.G., Gilbert M.E., Ripley B.S., Osborne C.P. 2008. Seasonal differences in photosynthesis between the C_3 and C_4 subspecies of *Alloteropsis semialata* are offset by frost and drought. *Plant, Cell and Environment* 31: 1038-1050.

IPCC, 2013: Annex I: Atlas of Global and Regional Climate Projections Supplementary Material RCP8.5 [van Oldenborgh, G.J., Collins M., Arblaster J., Christensen J.H., Marotzke J., Power S.B., Rummukainen M., Zhou T. (eds.)]. In: Climate Change 2013: The Physical Science Basis. Contribution of Working Group I to the Fifth Assessment Report of the Intergovernmental Panel on Climate Change [Stocker T.F., Qin D., Plattner G.-K., Tignor M., Allen S.K., Boschung J., Nauels A., Xia A.Y., Bex V., Midgley P.M. (eds.)].

Jones H.G., Corlett J.E. 1992. Current topics in drought physiology. *The Journal of Agricultural Science* 119: 291-296.

Jones M.M., Turner N.C. 1978. Osmotic adjustment in leaves of sorghum in response to water deficits. *Plant Physilogy* 61: 122-126.

Kalapos T., van den Boogaard R., Lambers H. 1996. Effect of soil drying on growth, biomass allocation and leaf gas exchange of two annual grass species. *Plant and Soil* 185: 137–149.

Kanai R. and Edwards G.E. 1999. The biochemistry of C_4 photosynthesis. In: Sage R.F., Monson, R.K., eds. *C_4 Plant Biology*. Academic Press, San Diego, CA, USA. p. 49-87.

Kellogg, E.A. 1997. Phylogenetics aspects of the evolution of C_4 photosynthesis. In: Sage R.F., Monson R.K., eds. *C_4 Plant Biology*. Academic Press, San Diego, CA, USA. P. 411–444.

Knapp A.K., 1984. Water relations and growth of three grasses during wet and drought years in a tallgrass prairie. *Oecologia* 65: 35-43.

Kocacinar F., Sage R.F. 2003. Photosynthetic pathway alters xylem structure and hydraulic function in herbaceous plants. *Plant, Cell and Environment* 26: 2015-2026.

Kusaka M., Ohta M., Fukimura T. 2005. Contribution of inorganic components to osmotic adjustment and leaf folding for drought tolerance in pearl millet. *Physiologia Plantarum* 125: 474-489.

Lacuesta M., Dever L.V., Miñoz-Rueda A., Lea P.J. 1997. A study of photorespiratory ammonia production in the C_4 plant *Amaranthus edulis*, using mutants with altered photosynthetic capacities. *Physiologia Plantarum* 99: 447–455.

Lawlor D.W., Fock D.H. 1978. Photosynthesis, respiration, and carbon assimilation in water-stressed maize at two oxygen concentrations. *Journal of Experimental Botany* 29: 579-593.

Lawlor D.W., Khanna-Chopra R. 1984. Regulation of photosynthesis during water stress. In: Sybesma C., ed. *Advances in photosynthetic research, vol. IV*. The Hague: Martinus Nijhoff/Dr W. Junk Publishers, 379-382.

Lawlor D.W. 2001. *Photosynthesis Third Edition*, BIOS Scientific Publishers Limited Oxford, UK.

Lawlor D.W. 2002. Limitation to photosynthesis in water-stressed leaves: stomata vs. metabolism and the role of ATP. *Annals of Botany* 89: 871-885.

Lawlor D.W., Cornic G. 2002. Photosynthetic carbon assimilation and associated metabolism in relation to water deficits in higher plants. *Plant, Cell and Environment* 25: 275-294.

Lawlor D.W., Tezara W. 2009. Causes of decreased photosynthetic rate and metabolic capacity in water-deficient leaf cells: a critical evaluation of mechanisms and integration of processes. *Annals of Botany* 103: 561-579.

Lawlor D.W. 2013. Genetic engineering to improve plant performance under drought: physiological evaluation of achievements, limitations, and possibilities. *Journal of Experimental Botany* 64: 83 – 108.

Leakey A.D.B., Bernacchi C.J., Dohleman F.G., Ort D.R., Long S.P. 2004. Will photosynthesis of maize (*Zea mays*) in the US Corn Belt increase in future [CO_2] rich atmospheres? An analysis of diurnal courses of CO_2 uptake under free-air concentration enrichment (FACE). *Global Change Biology* 10: 951-962.

Leakey A.D.B., Uribelarrea M., Ainsworth E.A, Naidu S.L., Rogers A., Ort D.R., Long S.P. 2006. Photosynthesis, productivity, and yield of maize are not affected by open-air elevation of CO_2 concentration in the absence of drought. *Plant Physiology* 140: 779-790.

LeCain D.R., Morgan J.A., Mosier A.R., Nelson J.A. 2003. Soil and plant water relations determine photosynthetic responses of C_3 and C_4 grasses in a semi-arid ecosystem under elevated CO_2. *Annals of Botany* 92: 41–52.

Leegood R.C. 2000. Transport during C_4 photosynthesis. In: Leegood R.C., Sharkey T.D., von Caemmerer S., eds. *Photosynthesis: physiology and metabolism.* Kluwer. Dordrecht. p. 459-469.

Lloyd J., Farquhar G.D. 1994. ^{13}C discrimination during CO_2 assimilation by the terrestrial biosphere. *Oecologia* 99: 201-215.

Long S.P. 1999. Ecology of C_4 photosynthesis. In: Sage R.F., Monson, R.K., eds. *C_4 Plant Biology* Academic Press, San Diego, CA, USA. p. 215-242.

Lu C., Zhang J. 1999. Effects of water stress on Photosystem II photochemistry and its thermostability in wheat plants. *Journal of Experimental Botany* 50: 1199-1206.

Markelz R.J.C., Strellner R.S., Leakey A.D.B. 2011. Impairment of C_4 photosynthesis by drought is exacerbated by limiting nitrogen and ameliorated by elevated [CO_2] in maize. *Journal of Experimental Botany* 62: 3235-3246.

Maroco J.P, Pereira J.S., Chaves M. 2000. Growth, photosynthesis and water use efficiency of two C_4 Sahelian grasses subjected to water deficits. *Journal of Arid Environments* 45: 119-137.

Marques da Silva J., Arrabaça M.C. 2004. Photosynthesis in the water-stressed C_4 grass *Setaria sphacelata* is mainly limited by stomata with both rapidly and slowly imposed water deficits. *Physiological Plantarum* 121: 409-420.

Martin T.M. 2008. Photosynthetic and evolutionary determinants of the response of selected C_3 and C_4 (NADP-ME) grasses to fire. MSc Thesis. Rhodes University, Grahamstown, RSA.

Massad R.S., Tuzet A., Bethenod O. 2007. The effect of temperature on C_4-type leaf photosynthesis parameters. *Plant, Cell and Environment* 30: 1191-1204.

Maxwell K., Johnson G.N. 2000. Chlorophyll fluorescence - a practical guide. *Journal of Experimental Botany* 51: 659-668.

McDowell N., Pockman W.T., Allen C.D., Breshears D.D., Cobb N., Kolb T., Plaut J., Sperry J., West A., Williams D.G., Yepez E.A. 2008. Mechanisms of plant survival and mortality during drought: why do some plants survive while others succumb to drought? *New Phytologist* 178: 719–739.

Melis A. 1999. Photosystem-II damage and repair cycle in chloroplasts: what modulates the rate of photodamage in vivo? *Trends in Plant Science* 4: 130-135.

Meyer S., Hung S.P.N., Trémolières A., de Kouchkovsky Y. 1992. Energy coupling, membrane lipids and structure of thylakoids of lupin plants submitted to water stress. *Photosynthesis Research* 32: 95-107

Michelena V.A., Boyer J.S. 1982. Complete turgor maintenance at low water potentials in the elongating region of maize leaves. *Plant Physiology* 69: 1145-1149.

Molinari H.B.C., Marur C.J., Daros E., Campos M.K.F., Carvalho J.F.R.P., Bespalhok Filho J.C., Pereira L.F.P., Vieira L.G.E. 2007. Evaluation of the stress-inducible production of proline in transgenic sugarcane (*Saccharum* spp.): osmotic adjustment, chlorophyll fluorescence and oxidative stress. *Physiologia Plantarum* 130: 218-229.

Mucina L., Rutherford M.C. 2006. *The vegetation of South Africa, Lesotho and Swaziland.* South African National Biodiversity Institute (SANBI) Pretoria, South Africa.

Naidu S.L., Long S.P. 2004. Potential mechanisms of low-temperature tolerance of C_4 photosynthesis in *Miscanthus* x *giganteus*: an in vivo analysis. *Planta* 220: 145-155.

Nayyar H. 2003. Variation in osmoregulation in differentially drought-sensitive wheat genotypes involves calcium. *Biologia Plantarum* 47: 541-547.

Ogbaga C.C,. Stepien P., Johnson G.N. 2014. Sorghum (*Sorghum bicolor*) varieties adopt strongly contrasting strategies in response to drought. *Physiologia Plantarum* 152: 389-401.

Ogle K. 2003. Implications of interveinal distance for quantum yield in C_4 grasses: a modelling and meta-analysis. *Oecologia* 136: 532-542.

Ohnishi J., Flügge U.I., Heldt H.W., Kanai R. 1990. Involvement of Na^+ in active uptake of pyruvate in mesophyll chloroplasts of some C_4 plants. *Plant Physiology* 94: 950-959.

Oparka K.J., Prior D.A.M. 1992. Direct evidence for pressure-generated closure of plasmodesmata. *The plant Journal* 2: 741-750.

Osborne C.P., Freckleton R.P. 2009. Ecological selection pressures for C_4 photosynthesis in the grasses. *Proceedings of the Royal Society: Biological Sciences* 276: 1753-1760.

Pearcy R.W., Ehleringer J.1984. Comparative ecophysiology of C_3 and C_4 plants. *Plant, Cell and Environment* 7: 1-13.

Rawsthorne S. 1992. C3–C4 intermediate photosynthesis: linking physiology to gene expression. *Plant Journal* 2: 267–274.

Ripley B.S., Gilbert M.E., Ibrahim D.G., Osborne C.P. 2007. Drought constraints on C_4 photosynthesis: stomatal and metabolic limitations in C_3 and C_4 subspecies of *Alloteropsis semialata*. *Journal of Experimental Botany* 58: 1351-1363.

Ripley B.S., Abraham T.I., Osborne C.P. 2008. Nitrogen-limitation causes differential partitioning of growth in C_3 and C_4 subspecies of *Alloteropsis semialata*. *Journal of Experimental Botany* 59: 1705–1714.

Ripley B.S., Frole K.M., Gilbert M.E. 2010. Differences in drought sensitivities and photosynthetic limitations between co-occurring C_3 and C_4 (NADP-ME) Panicoid grasses. *Annals of Botany* 105: 493–503.

Roberts A.G., Oparka K.J. 2003. Plasmodesmata and the control of symplastic transport. *Plant, Cell and Environment* 26: 103-124.

Robinson-Beers K., Evert R.F. 1990. Ultrastructure of and plasmodesmatal frequency in mature leaves of sugarcane. *Planta* 184: 291-306.

Rong-hua L., Pei-guo G., Baum M., Grando S., Ceccarelli S. 2006. Evaluation of chlorophyll content and fluorescence parameters as indicators of drought tolerance in barley. *Agricultural Sciences in China* 5: 751-757.

Saccardy K., Cornic G., Brulfert J., Reyss A. 1996. Effect of drought stress on net CO_2 uptake by *Zea* leaves. *Planta* 199: 589-595.

Saccardy K., Pineau B., Roche O., Cornic G. 1998. Photochemical efficiency of Photosystem II and xanthophyll cycle components in *Zea mays* leaves exposed to water stress and high light. *Photosynthesis Research* 56: 57-66.

Sade N., Gebremedhin A., Moshelion M. 2012. Risk-taking plants: Anisohydric behavior as a stress-resistance trait. *Plant Signalling & Behaviour* 7: 767-770.

Sage R.F., Pearcy R.W. 1987. The nitrogen use efficiency of C_3 and C_4 plants. *Plant Physiology* 84: 959-963.

Sage R.F., Monson R.K. 1999. *C_4 Plant Biology*. Academic Press, San Diego, CA, USA.

Sage R.F., Wedin, D.A., Li M.R. 1999. The biogeography of C_4 photosynthesis: patterns and controlling factors. In: Sage R.F., Monson, R.K., eds. *C_4 Plant Biology*. Academic Press, San Diego, CA, USA. p. 313-373.

Sage R.F. 2004. The evolution of C_4 photosynthesis. *New Phytologist* 161: 341-370.

Sage R.F., McKown A.D. 2006. Is C_4 photosynthesis less phenotypically plastic than C_3 photosynthesis? *Journal of Experimental Botany* 57: 303-317.

Sage R.F., Christin P.A., Edwards E.J. 2011. The C_4 plant lineages of planet Earth. 62: 3155-3169.

Sage R.F., Sage T.L., Kocacinar F. 2012. Photorespiration and the evolution of C_4 photosynthesis. *Annual Review of Plant Biology* 63: 19-47.

Saliendra N.Z., Meinzer F.C., Perry M., Thorn M. 1996. Associations between partitioning of carboxylase activity and bundle sheath leakiness to CO_2, carbon isotope discrimination, photosynthesis and growth in sugarcane. *Journal of Experimental Botany* 47: 907-914.

Samarakoon A.B., Gifford R.M. 1996. Elevated CO_2 effects on water use and growth of maize in wet and drying soil. *Australian Journal of Plant Physiology* 23: 53–62.

Sarmiento G. 1992. A conceptual model relating environmental factors and vegetation formations in the lowlands of tropical South America. In: Furley P.A., Proctor J., Ratter J.A., eds. *Nature and Dynamics of Forest-Savanna Boundaries*. Chapman & Hall, London. p. 583-601.

Schölander P.F., Hammel H.T., Bradstreet E.D., Hemmingsen E.A. 1965. Sap pressure in vascular plants. *Science* 148: 339-345.

Scholes R.J., Archer S.R. 1997. Tree-grass interactions in savannas. *Annual Review of Ecology and Systematics* 28: 517-544.

Schulte P.J., Hinckley T.M. 1985. A comparison of pressure-volume curve data-analysis techniques. *Journal of Experimental Botany* 36: 1590-1602.

Schulze E.D., Ellis R., Schulze W., Trimborn P., Ziegler H. 1996. Diversity, metabolic types and $\delta^{13}C$ carbon isotope ratios in the grass flora of Namibia in relation to growth form, precipitation and habitat conditions. *Oecologia* 106: 352-369.

Seneweera S.P., Ghannoum O., Conroy J.P. 1998. High vapour pressure deficit and low soil water availability enhance shoot growth responses of a C_4 grass (*Panicum coloratum* cv. Bambatsi) to CO_2 enrichment. *Functional Plant Biology* 25: 287–292.

Seneweera S.P., Ghannoum O., Conroy J.P. 2001. Root and shoot factors contribute to the effect of drought on photosynthesis and growth of the C_4 grass *Panicum coloratum* at elevated CO_2 partial pressure. *Functional Plant Biology* 28: 451–460.

Sharma P., Jha A.B., Dubey R.S., Pessarakli M. 2012. Reactive oxygen species, oxidative damage and antioxidative defense mechanism in plants under stressful conditions. *Journal of Botany* 2012: 1-26.

Shongwe M.E., van Oldenborgh G.J., van den Hurk B.J.J.M., de Boer B., Coelho C.A.S., van Aalst M.K. 2009. Projected changes in mean and extreme precipitation in Africa under global warming. Part I: Southern Africa. *Journal of Climate* 22: 3819-3837.

Siebke K., Ghannoum O., Conroy J.P., Badger M.R., von Caemmerer S. 2003. Photosynthetic oxygen exchange in C_4 grasses: the role of oxygen as electron acceptor. *Plant, Cell and Environment* 26: 1963–1972.

Smith S.A., Donoghue M.J. 2008. Rates of molecular evolution are linked to life history in flowering plants. *Science* 322: 86–89.

Sowiński P., Bilska A., Barańska K., Fronk J., Kobus P. 2007. Plasmodesmata density in vascular bundles in leaves of C_4 grasses grown at different light conditions in respect to photosynthesis and photosynthate export efficiency. *Environmental and Experimental Botany* 61: 74–84.

Sowiński P., Szczepanik J., Minchin P.E.H. 2008. On the mechanism of C_4 photosynthesis intermediate exchange between Kranz mesophyll and bundle sheath cells in grasses. *Journal of Experimental Botany* 59: 1137–1147.

Still C.J., Berry J.A., Collatz G.J., DeFries R.S. 2003. Global distribution of C_3 and C_4 vegetation: Carbon cycle implications. *Global Biogeochemical Cycles* 17: 1006.

Taub D.R. 2000. Climate and the U.S. distribution of C_4 grass subfamilies and decarboxylation variants of C_4 photosynthesis. *American Journal of Botany* 87: 1211-1215.

Taylor S.H., Ripley B.S., Woodwarrd F.I., Osborne C.P. 2011. Drought limitation of photosynthesis differs between C_3 and C_4 grass species in a comparative experiment. *Plant, Cell and Environment* 34: 65-75.

Teeri J.A., Stowe L.G. 1976. Climatic patterns and the distribution of C_4 grasses in North America. *Oecologia* 23: 1-12.

Tezara W., Mitchell V.J., Driscoll S.D., Lawlor D.W. 1999. Water stress inhibits plant photosynthesis by decreasing coupling factor and ATP. *Nature* 401: 914-917.

Thorpe M.R., Minchin P.E.H. 1996. Mechanisms of long- and short-distance transport from sources to sinks. In. Zamski E., Schaffer A.A., eds. *Photoassimilate Distribution in Plants and Crops Source-sink Relationships.* Marcel Dekker Inc., New York, USA. p. 261–278.

Tieszen L.L., Senyimba M.M., Imbamba S.K., Troughton J.H. 1979. The distribution of C_3 and C_4 grasses and carbon isotope discrimination along an altitudinal and moisture gradient in Kenya. *Oecologia* 37: 337-350.

Tikkanen M., Mekala NR., Aro E.M. 2014. Photosystem II photoinhibition-repair cycle protects Photosystem I from irreversible damage. *Biochimica et Biophysica Acta (BBA) – Bioenergetics* 1837: 210-215.

Visser V., Woodward F.I., Freckleton R.P., Osborne C.P. 2012. Ecological determinants of phylogenetic structure of C_4 grass communities in South Africa. *Journal of Biogeography* 39: 232-246.

Visser V., Clayton W.D., Simpson D.A., Freckleton R.P., Osborne C.P. 2014. Mechanisms driving an unusual latitudinal diversity gradient for grasses. *Global Ecology and Biogeography* 23: 61-75.

van Oudtshoorn F. 2012. *Guide to grasses of Southern Africa*. Briza Publications. Pretoria, South Africa.

Vogel J.C., Fuls A., Ellis R.P. 1978. The geographical distribution of Kranz grasses in South Africa. *South African Journal of Science* 74: 209-217.

Vogel J.C., Fuls A., Danin A. 1986. Geographical and environmental distribution of C_3 and C_4 grasses in the Sinai, Negev, and Judean deserts. *Oecologia* 70: 258-265.

von Caemmerer S., Farquhar G.D. 1981. Some relationships between the biochemistry of photosynthesis and the gas exchange of leaves. *Planta* 153: 376-387.

von Caemmerer S. 2000. *Biochemical Models of Leaf Photosynthesis*. CSIRO Publishing. Canberra, Australia.

von Caemmerer S., Furbank R.T. 2003. The C_4 pathway: an efficient CO_2 pump. *Photosynthesis Research* 77: 191-207.

Voznesenskaya E.V., Chuong S.D.X., Koteyeva N.K., Edwards G.E., Franceschi V,R. 1996. Functional compartmentation of C_4 photosynthesis in the triple-layered chlorenchyma of *Aristida* (Poaceae). *Functional Plant Biology* 32: 67-77.

Wall G.W., Brooks T.J., Adam N.R., Cousins A., Kimball B.A., Pinter Jr P.J. 2001. Elevated atmospheric CO_2 improved *Sorghum* plant water status by ameliorating the adverse effects of drought. *New Phytologist* 152: 231–248.

Ward J.K., Tissue D.T., Thomas R.B., Strain B.R. 1999. Comparative response of model C_3 and C_4 plants to drought in low and elevated CO_2. *Global Change Biology* 5: 857-867.

Ward D.A. 1987. The temperature acclimation of photosynthetic responses to CO_2 in *Zea mays* and its relationship to the activities of photosynthetic enzymes and the CO_2-concentrating mechanism of C_4 photosynthesis. *Plant, Cell and Environment* 10: 407-411.

Webb C.O. 2000. Exploring the phylogenetic structure of ecological communities: an example for rain forest trees. *American Naturalist* 156: 145–155.

Williams D.G., Black R.A. 1994. Drought responses of native and introduced Hawaiian grass. *Oecologia* 97: 512-519

Williams D.G., Gempko V., Fravolini A., Leavitt S.W., Wall G.W., Kimball B.A. 2001. Carbon isotope discrimination by *Sorghum bicolor* under CO_2 enrichment and drought. *New Phytologist* 150: 285–293.

Wilson J.R., Hattersley P.W. 1983. *In vitro* digestion of bundle sheath cells in rumen fluid and its relation to the suberized lamella and C_4 photosynthetic type in *Panicum* species. *Grass and Forage Science* 38: 219-23.

Zachos J.C., Dickens G.R., Zeebe R.E. 2008. An early Cenozoic perspective on greenhouse warming and carbon-cycle dynamics. *Nature* 451: 279–83.

Zhang J.X., Nguyen H.T., Blum A. 1999. Genetic analysis of osmotic adjustment in crop plants. *Journal of Experimental Botany* 50: 291-302.